PROSTATE CANCER: INSIGHTS INTO TUMOR IMMUNOSUPPRESSION

by
Zoila Areli Lopez Bujanda M.S.

A dissertation submitted to Johns Hopkins University in conformity with the requirements for the degree of Doctor of Philosophy

Baltimore, Maryland
October 2020

Abstract

Prostate cancer (PCa) is a leading cause of cancer-related death in men worldwide, with an estimated 33,000 deaths projected in the U.S. in 2020. Although primary (localized) tumors can be cured by surgery or radiation, approximately 40% of patients eventually develop recurrent disease. While initially responsive to androgen-deprivation therapy (ADT), many patients with recurrent PCa eventually progress to a more advanced disease state known as metastatic castration-resistant PCa for which treatment options are less effective. Despite the clinical successes of treating various types of cancers with immune checkpoint blockade (ICB), responses in PCa patients remain limited. This is perhaps unsurprising given the low expression of co-inhibitory molecules, low mutational burden, and the immunosuppressive tumor microenvironment (TME) found in this disease. As described in the first chapter of this dissertation, tumor-associated antigens expressed by prostate tumor cells induce an immune response in patients with PCa, a notion that has been exploited previously by the FDA-approved Sipuleucel-T vaccine. In chapter 2 of this dissertation, we describe the robust tolerance to a model antigen that is established by the TME. We found that continuous expression of a model antigen leads to increased infiltration of regulatory T cells (T_{regs}) and polymorphonuclear myeloid-derived suppressor cells (PMN-MDSCs) to the TME of ADT-treated PCa tumors. In chapter 3, we investigated the tumor intrinsic mechanisms that lead to the recruitment and

accumulation of PMN-MDSCs. Our results suggest that loss of androgen-receptor mediated suppression of interleukine-8 (IL-8) expression and its subsequent upregulation as a potential mechanism that mediates the infiltration of PMN-MDSCs in ADT-treated PCa tumors. In chapter 4, we evaluated the pre-clinical significance of targeting PMN-MDSCs migration in an animal model. These studies show that mitigating the recruitment of PMN-MDSCs in combination with ICB and ADT increased polyfunctional CD8 T cells in tumor draining lymph nodes and spleens, and significantly delayed the onset of castration-resistance. This dissertation contributes to the understanding of PCa immunogenicity, the establishment of tolerance to CD8 antigen-specific T cell responses in the context of an immunosuppressive TME, and how PCa cells themselves orchestrate the recruitment of PMN-MDSCs to the TME.

Primary Reader and PhD Advisor: Charles G. Drake, MD, PhD

Secondary Reader: Tamara Lotan, MD

Head of Thesis Committee: Kenneth Pienta, MD

Thesis Committee: Alan Scott, PhD

Thesis Committee: Vasan Yegnasubramanian, MD

Thesis Committee: Tamara Lotan, MD

Preface

The following work was a test to resilience and perseverance. The contributions displayed here result from a Molecular Biologist leaving her comfort zone to adventure into Immunology – a subject that I came to know and love during my time as a PhD student. Quoting J.K. Rowling "it is impossible to live without failing at something, unless you live so cautiously that you might as well not have lived at all." I am thankful for every failure I encountered as part of my graduate training. It is thanks to those experiences that I have grown as a person and as a scientist.

Acknowledgements

First and foremost, I must thank my mentor Dr. Charles Drake (Chuck) who has been my sponsor and friend through my graduate training. Chuck is, simply put, a well-rounded physician scientist who is truly committed to improving patient care. His enthusiasm towards translating our discoveries from the bench to the bedside is contagious and it serves to sustain one during the long hours troubleshooting experiments that could otherwise lead to frustration. As a mentor, he has been nothing but incredibly supportive. He has trusted me to tackle scientific problems on my own and always kept himself available to discuss my experimental approaches. He has helped me to learn how to stand behind my results and to believe in the quality of my work. Knowing that I am interested in a career in academia, he encouraged me to present my work at various scientific meetings. I can truly say he has not only helped me become a better scientist but also a better speaker and communicator with his invaluable advice and of course his list of "dos & don'ts" that followed every scientific talk and manuscript preparation.

I must also thank the Sukumar lab which has been my scientific family at Johns Hopkins. I would not be at this stage without the constant support of this family that started a decade back while I was a visiting master's student. Both Sara Sukumar and MaryJo Fackler believed in me and encouraged me to learn college level English so that I could one day do my PhD in the United States. On top of a strong technical training, there I learned very insightful idioms that would

help keep me on course while pursuing my PhD: “slow and steady wins the race”, “don’t cry over spilled milk”, “every cloud has a silver lining”, and “don’t throw the baby out with the bathwater”. As I look back on my PhD journey, I know how fortunate I am to have met these two incredible role models for women in science.

I would also like to acknowledge the wonderful faculty at the pathobiology program that provides an incredible support system for all the students. I would especially like to thank Tamara Lotan and James Eshleman for being excellent clinical mentors from whom I learned how cancer pathology and molecular diagnosis guide cancer treatment – a mindset I will continue to keep in mind as I engage in future translational work. I am grateful for my committee members Kenneth Pienta, Alan Scott, Vasan Yegnasubramanian, and Tamara Lotan for their direction and support during our discussions, as well as for keeping me on track so that I could reach all milestones in my graduate career. Thanks to my professors at the Pathobiology program Sara Sukumar, Ed Gabrielson, and Angelo De Marzo and to my program director Lee Martin for their guidance through my PhD studies and especially while deciding whether to follow my mentor on his transition from Johns Hopkins to Columbia University. I especially would like to thank my sponsors Sara Sukumar, Ed Gabrielson, and Chuck Drake for their recommended books to develop good habits and improve my writing skills such as “the 7 habits of highly effective people”, “on writing well”, “the elements of style”, and “style toward clarity and grace.” Your guidance and advice have given me the confidence to apply for a postdoctoral F32 fellowship during my last year of PhD training and hopefully will lead to my first NIH funded grant proposal. Many thanks to my favorite chief graduate student Dr. Michael Urbanowski who I often turned to for advice, and to Stacey Morgan, the program coordinator, for all her assistance during my years as a graduate student. Additionally, I am grateful for a training grant from the Sidney Kimmel Comprehensive Cancer Center as well as grant from the U.S. Department of Defense (DOD) that helped support me financially during my tenure as a PhD student. I would like to acknowledge the incoming class of 2013 for being the best study group to have existed. You made problem-set solving engaging and exciting. I feel so lucky to have had you as my study buddies.

I am thankful for the people at the Bloomberg~Kimmel Institute for Cancer Immunotherapy at Johns Hopkins Medical Institutions and the Columbia Center for Translational Immunology (CCTI) at Columbia University Medical Center. Thanks for all the times we shared between free meals and happy hours discussing interesting data and bouncing ideas regarding future experiments. I feel privileged for having the opportunity to engage in thought experiments with all of you. These collaborative environments made great science possible and their

willingness to donate emergency reagents and help up when something ran out was simply invaluable.

I would also like to thank all the people I had the pleasure to collaborate with during my tenure as a PhD candidate both at Johns Hopkins (Michael Haffner, Ben Larman, Karen Sfanos, Todd Armstrong, and Leisha Emens) as well as at Columbia University (Cory Abate-Shen, Michael Shen, Clementine Le Magnen, Angela Christiano, Tamas Gonda, Ran Reshef, and Pawel Muranski). I would especially like to thank Michael Haffner for helping me move my project forward and facilitating communication with our collaborators at Johns Hopkins Medical Institutions. My thanks to our collaborators at Bristol-Myers Squibb (BMS), Alan Korman and Mark Selby for providing not only key reagents for the success of my project but also their critical review of the data. I am grateful to all the people at the Drake lab, especially Matthew Chaimowitz (Matt) who I helped train and it fills me with great pride to see him develop scientifically through the years. Matt, together with a PhD student in the lab Nividita Chowdhury (Nivi), with whom it has been extraordinary to work, thank you for all the occasions that you have helped with my experiments. Thanks to my undergraduate student for the summer, Nicholas Venturini, who was always super enthusiastic about working in the lab and has now moved on to medical school at Mount Sinai. You brought a refreshing vibe to our group and I truly learn a lot from my mentoring experience with you. I am positive you will go on to do great things.

I am grateful to all the friends that accompanied me through the PhD journey. My roommates Gustavo Valdivia, Marco Cornia, and Garrick Orchard with whom I shared amazing memories decompressing at home or going to our local bar – Otto bar. My soccer buddies with whom I played several tournaments. Especially to the “mini-pandy”, I look forward to the day I get to see you all again. My friends at CCTI Nato Teteloshvili, Paula Alonso, Rodney Macedo Gonzales, and Jorge Postigo Fernandez for having my back. Many thanks to my dear friends Preethi Korangath and Vanessa Merino who have always been there for me to talk through the frustrations of working away from my home country and my family, I am tremendously happy to see you thriving not only at work but also at home with your families. To my buddies from the Hopkins days Yuki Muroyama, Tom Nirschl, Ali Ghasemzadeh, Brian Francica, Christina Kochel, Wendy Mao, and Debebe Theodros, I was tremendously lucky to have you as lab members and friends in this journey.

I would also like to thank my family in Mexico for their constant support and inspiration. Thank you to my mother Zoila Bujanda Peraza and father Rigoberto Lopez Estudillo, without whom I would not have pursued a career in biological sciences. Special thanks to my sisters Edna and Ana, who accompanied me

during the beginning of my graduate studies while they came to stay with me for a semester abroad – I treasure the time we expended together. Many thanks to my in-laws, Linda Bleadingheiser and Jon Kerner who have welcomed me into their family and have gone out of their way to help in any way they can. I am very thankful for the multiple occasions that you have helped me navigating a difficult situation or editing a document.

Finally, I must also thank my husband (Zach) who arrived into my life during one of the most hectic times on this journey – the lead up to my comprehensive examination. Little did I know that this 'funny' guy would light up my life in ways I was not aware I needed. Thank you dear for been a wonderful friend, helping me study every step of the way, a generous boyfriend, who many times would bring me coffee or food whenever I found myself trapped in a long experiment, and an amazing spouse, who has always been therefore me. For your constant love and support, I will always be grateful.

To all above, and those beyond this page.

Thank you.

Zoila Areli Lopez-Bujanda
2020.10.22

– Page intentionally left blank –

Dedication

To my family

My support system and constant source of inspiration who encouraged me to keep going every step of the way – especially during the tough times.

"Caminante, son tus huellas el camino y nada más; Caminante, no hay camino se hace camino al andar[1]". Juan Manuel Serrat

[1] "Walker your footsteps are the road and nothing else; Walker, there is no path, the path is made by walking".

– Page intentionally left blank –

Contents

List of Tables

List of Figures

Introduction

> "(In the U.S.) More will die from cancer over the next two years than died in combat in all the wars the United States has ever fought, combined."
>
> Dr. Siddhartha Mukherjee (2010) – Assistant professor and oncologist at Columbia University, and the author of The Emperor of All Maladies: A Biography of Cancer.

Prostate cancer (PCa) is the second most common cause of cancer mortality in men in the United States, accounting for 1 in 5 new diagnoses of cancer and ranking second in mortality among all cancers in men.[1] The standard primary treatment for patients with localized PCa includes surgery and/or radiation therapy, followed by androgen-deprivation therapy (ADT: chemical or surgical castration) if disease returns. Alternatively, patients may be monitored closely if the cancer is thought to be of sufficiently low risk[2] and treated only upon signs of progression. In general, the earliest sign of recurrence after primary therapy comes in the form of 'biochemical recurrence' (BCR), an asymptomatic rise in prostate specific antigen (PSA) without any radiographic evidence of metastases.[3] Serial quantification of PSA provides a window of opportunity to treat patients 2–3 years before their metastatic disease becomes evident by imaging methods.[4]

PCa that presents in the metastatic state is generally treated with ADT, but most patients eventually become refractory to this treatment, developing castration-resistant disease, i.e. metastatic castration-resistant PCa (mCRPC). While there are a number FDA approved therapeutic agents for mCRPC (docetaxel, cabazitaxel, abiraterone, enzalutamide, radium-223, and sipuleucel-T) that have shown an impact on overall survival (OS), currently there is no treatment that can cure mCRPC.[5] Immunotherapy based on the blockade of immune checkpoints plays a role in the treatment of most advanced cancers,[6] but PCa is currently a notable exception.[7] In this introduction, we describe the adaptive immune response to tumor cells in PCa, and what is known about the mechanisms of tolerance and immune escape for these tumors. Next, we discuss the immunosuppressive tumor microenvironment (TME) in PCa, as well as new evidence for tumor-cell mediated myeloid infiltration through the PI3K / PTEN / AKT signaling pathway and, an alternative mechanism for immune evasion that may be regulated by an ER stress response. Finally, we discuss several interventions to break immunological tolerance induced by the mechanisms above.

The Adaptive Immune Response in Prostate Cancer

It is generally understood that the turnover of necrotic tumor cells within the tumor microenvironment leads to the activation of an adaptive immune response.[8] In this 'immunogenic cell death' cellular contents are released into the extracellular space after necrosis, where they can be internalized, processed and presented on major histocompatibility complexes (MHC) I and II by antigen presenting cells (APCs). Upon stimulation by a pathogen associated molecular pattern (PAMPs) or damage

associated molecular pattern (DAMPs), APCs migrate to the lymph node to activate T lymphocytes of the adaptive immune system. Both arms of adaptive immune system (T and B cell mediated) are important in controlling tumor growth. CD4 helper T (T_H) cells can be defined into several functionally different subsets on the basis of the combinations of cytokines they secrete.[9] Of these, interferon gamma (IFNγ) producing T_H1 cells contribute to the anti-tumor response by inducing high affinity IgG-driven B cell responses and by enhancing CD8 T cell activation. CD8 cytotoxic T lymphocytes (CTLs) are essential components of the adaptive anti-tumor immune response due to their ability to selectively and specifically induce apoptosis in tumor cells upon the interaction between their T cell receptor (TCR) and its ligand – an immunogenic tumor-associated antigen (TAA). When an activated CD8 CTL engages with its cognate ligand, presented on an MHCI molecule, it can drive non-immunogenic cell death, apoptosis, by secreting granzyme B and pore-forming proteins known as perforins.[10]

During the course of tumor progression, tumor cells undergo a process termed immunoediting that consists of three phases: elimination (i.e., cancer immunosurveillance), equilibrium, and escape.[11] Mutated proteins specific to tumor cells, also known as neoantigens, are the likely drivers of an effective anti-tumor immune response for the *elimination* of malignant cells and prevention of tumor outgrowth; however, this phase is followed by a latency period (*equilibrium*) in which, although many of the original malignant cells are destroyed, the emergence of new genetic variants is thought to help maintain growth until the

conditions in the TME allow for these cells to eventually *escape* immunosurveillance and establish as tumors.

Not surprisingly, the presence of a significant population of tumor specific T cells has been found important for the generation of anti-tumor immunity.[12] However, the density of tumor specific CD8 T cells found in patients with PCa is relatively low; while in other cancer types, such as head & neck squamous cell carcinoma, the infiltration of CD8 T cells is more robust (Fig. I.1). Currently, it is unknown why PCa has a low intra-tumoral CD8 T cell infiltration, although it is likely that the low tumor mutational burden in PCa plays a role.

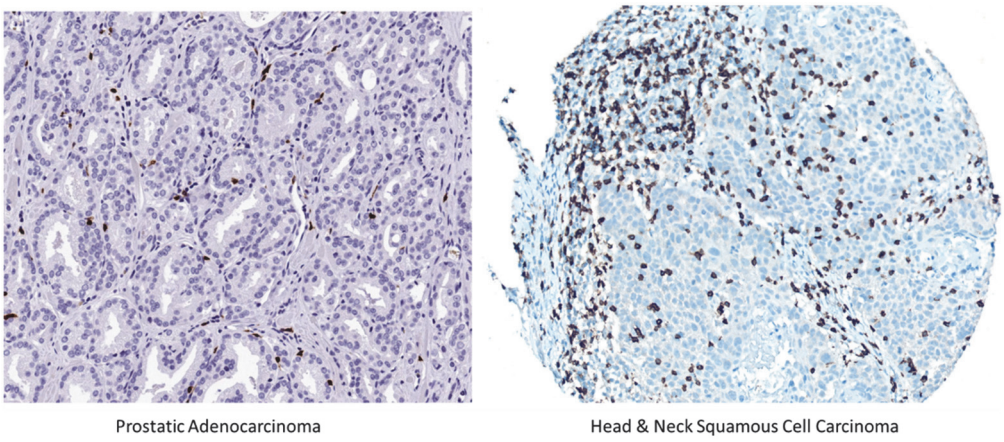

Figure I.1 | Sparse CD8 T Cell Infiltration in Prostate Cancer. Immunohistochemical staining of tumor infiltrating $CD8^+$ T cells in Prostatic Adenocarcinoma (left) and Head & Neck Squamous Cell Carcinoma (right) tissues.[13] Courtesy of Dr. Angelo De Marzo.

Tolerance

On the other side of T-cell activation, is T-cell 'tolerance', a broad term which encompasses several mechanisms.[14] These two processes counteract each other to regulate the effective elimination of foreign antigens (i.e. pathogens) while maintaining immune tolerance to self-antigens (i.e., healthy tissues). T cell activation or lack thereof determines T cell fate in both the thymus and the periphery. Mechanisms of 'central tolerance' in the thymus allow for selection of successful T cell clones based on their ability to interact with MHC class I or II on the surface of thymic epithelial cells (TECs) in the thymic cortex.[15] This process of *positive selection* leads to maturation and upregulation of CCR7 for migration to the thymic medulla.[16] There, T cells encounter tissue-specific antigens presented by medullary TECs via expression of AIRE.[17] If binding is too strong, T cells are deleted in an effort to prevent autoimmunity (*negative selection*).[18] T cells with intermediate binding become tolerized to potential self-antigens (*natural regulatory T cells*); while T cells with low binding can either recognize non-self (i.e., foreign or mutated) antigens or be further tolerized in the periphery. Although many autoreactive T cells are eliminated in the thymus, the majority of self-reactive T cells survive *negative selection* and are exported into the periphery.[19]

In the periphery, naïve T cells require three different signals for proper activation of their immune function: (i) TCR/antigen-MHC interaction, (ii) co-stimulation (e.g., CD28) and (iii) cytokines. TCR stimulation of T cells in the absence of appropriate co-stimulatory signals leads to *anergy*.[20-22] This low-level signaling pattern causes T cells to be functionally inert when encountering antigen

even in the presence of co-stimulation.[23] Immunological *ignorance* refers to an important mechanism of peripheral tolerance in which T cells are physically inhibited from coming into contact with their cognate antigens.[19,24] Tissues that are immunologically 'ignored' include the testes, ovaries, retina and possibly the non-inflamed prostate gland. In the context of cancer, the tumor microenvironment can also restrict the ability of T cells to interact with tumor cells.[25] In addition, T cells can also enter a state of *exhaustion* upon continuous TCR-specific stimulation.[26] This phenotype is characterized by the expression of multiple co-inhibitory molecules or immune checkpoints, reduced proliferation capacity, and loss of cytokine production and effector function.[27,28] Lastly, when the appropriate conditions are met (i.e., TGFβ, retinoic acid, and IL-2), conventional naïve CD4 T cells can be induced to express the transcription factor FOXP3 and become regulatory T cells (T_{regs}) in the periphery[29] to complement the existing natural T_{regs} already in tissues.

Immune Escape

In order for a tumor to establish successfully, tumor cells must escape immune recognition. Indeed, tumor cells from the prostate, breast, and lung tissues have been reported to downregulate the antigen processing machinery as mechanism of immune evasion.[30-34] In addition, molecules secreted by either tumor cells themselves or the tumor microenvironment have been shown to impair the proper recruitment, maturation and function of immune cells and ultimately hamper anti-tumor immunity.[35-37] The discovery of co-inhibitory molecules or immune checkpoints (i.e., CTLA-4 and PD-1 / PD-L1),[38-40] however, stands above other

mechanisms in terms of clinical relevance.[41-43] The integration of activating and inhibitory signals from the co-stimulatory and co-inhibitory molecules expressed on the surface of T cells at the time of TCR engagement determine whether T cells are activated or are rendered *tolerant*.[44] This process helps to modulate immune responses and prevent autoimmunity, but it also contributes to tumor progression. Indeed, ample evidence suggest that antigen-specific T cells remain in *tolerized* states during tumor immune escape, and that CTLA-4 / B7-1/2 and PD-1 / PD-L1 are two of the major interactions driving immune evasion in cancers.[45] Although many co-inhibitory molecules have been discovered (e.g., LAG-3, BTLA, VISTA, and CD160), here we will focus on the co-inhibitory molecules that are FDA-approved targets for cancer treatment.

Cytotoxic Lymphocyte Antigen-4

Cytotoxic T-lymphocyte-associated protein 4 (CTLA-4) was the first co-inhibitory molecule to be discovered.[38] CTLA-4 is closely related to the co-stimulatory molecule CD28,[46] and inhibits T cell activation by competing with the co-stimulatory molecule CD28 for binding to B7.1 and B7.2 ligands on APCs.[47-49] CTLA-4 has been shown to enable suppression of effector T cells by T_{regs},[50] and to play an important role in the prevention of autoimmune diseases.[51,52] CTLA-4 blockade facilitates *de novo* T cell priming events[53] and thus enhances antigen-specific T cell responses.[54] Indeed, in the context of tumors, inhibiting CTLA-4 / CD28 interactions has led to an increase in T cell infiltration to the TME in animal models[55] and patients.[56] Furthermore, CTLA-4 blockade with a depleting monoclonal antibody has been shown to delay tumor progression in several pre-

clinical tumor models, including PCa.[55,57,58] While CTLA-4 blockade has failed to meet the studies' primary end-point for the treatment of mCRPC in two randomized phase III studies,[54,59] recently reported long-term data from one of those studies did show a statistically significant increase in OS in PCa patients receiving anti-CTLA-4.[60]

Programmed Death-1

Programmed Death-1 receptor (PD-1) was the second co-inhibitory molecule to be discovered.[39] PD-1 inhibits T cell function upon engaging with its ligands PD-L1 and PD-L2 on tumor cells or APCs.[61-64] Upon engagement, the immunoreceptor tyrosine switch motif (ITSM) on the intracytoplasmic tail of PD-1 binds to the Src homology region 2 domain of the phosphatase SHP-2 (step 1),[65] and only then immunoreceptor tyrosine-based inhibitory motif (ITIM) binds the second SHP-2 (step 2) leading to a conformational switch that in turn displays the catalytic domain of SHP2 and inhibits TCR signaling.[66] Germline loss of PD-1 may lead to high levels of serum immunoglobulins,[67] mild lupus-like autoimmunity,[68] or cardiomyopathy.[69] In the context of tumors, PD-L1 on tumor infiltrating myeloid cells,[70] or possibly on tumor cells,[71] mediates *adaptive immune resistance* by binding to PD-1 on the attacking T cells.[72,73] Indeed, PD-L1 is expressed by tumor cells in various tumor types, including PCa,[71] and is upregulated by several of the cytokines secreted as a consequence of T cell activation – such as interferon gamma (IFNγ).[74,75] Thus, PD-1 or PD-L1 blockade can lead to *exhausted* T cells re-acquiring their effector function.[76]

In PCa, PD-L1 expression is associated with a more aggressive phenotype[77] and it is observed in 8% of cases in primary tumors and approximately 30% of mCRPC lesions (Fig. I.2).[71] The reasonable prevalence of PD-L1 expression in mCRPC suggests that targeting the PD-1 / PD-L1 pathway may have therapeutic implications in PCa treatment. While several clinical trials with anti-PD-1 monotherapy have some activity in mCRPC,[78] that activity is less significant than that observed in other tumor types.[79,80]

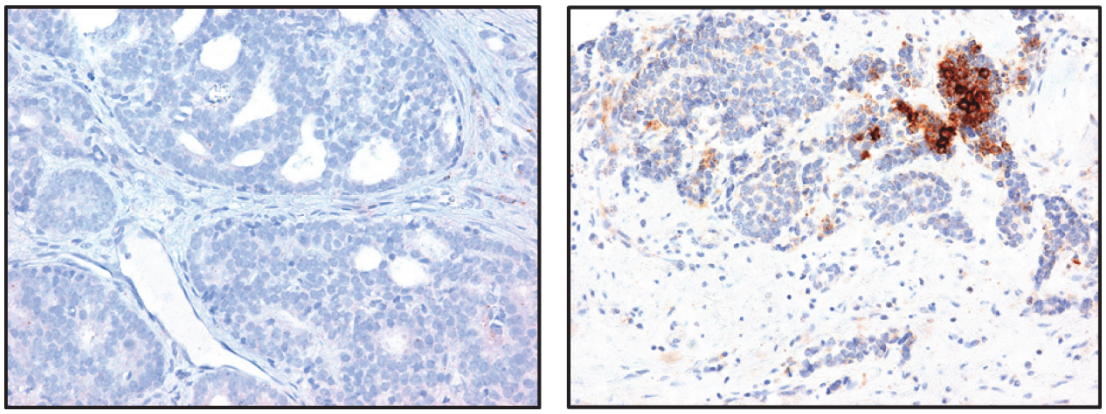

Figure I.2 | PD-L1 Expression in Prostate Cancer. Immunohistochemical staining of PD-L1 in primary prostate tumors (left) and a mCRPC lesion (right). Courtesy of Dr. Michael Haffner.

Immunosuppressive Tumor Microenvironment in Prostate Cancer

In general, the prognosis of cancer patients depends on tumor intrinsic histopathological characteristics (tumor grade) and on the extent of disease (stage) as defined by spread to draining lymph nodes (N), and/or evidence of distant metastases (M). Most recently, however, the importance of the composition of the immune compartment at the tumor site has become evident,[81] with some tumor types being characterized by a lack of T cell infiltration and presence of suppressive myeloid populations ('cold' tumors), while others are characterized for

their high T cell density ('hot' tumors).[82] These two immune phenotypes may be a reflection of possible disturbances in the cancer-immunity cycle (Fig. I.3). Through this cycle, anti-tumor immunity is generated in series of stepwise events. First, tumor neoantigens are captured (step 1), processed (step 2) and presented by APCs in the presence of co-stimulation and cytokines (step 3). Then, activated CD8 CTLs traffic to (step 4) and infiltrate the TME (step 5), where they recognize tumor neoantigens loaded on MHCI (step 6), and induce tumor cell death (step 7).[83] If neoantigens are presented by APCs in a tolerogenic context, T cell priming may then lead to the induction and expansion of T_{regs}. Additional factors in the TME may also hinder T cell infiltration or suppress their cytotoxic activity.

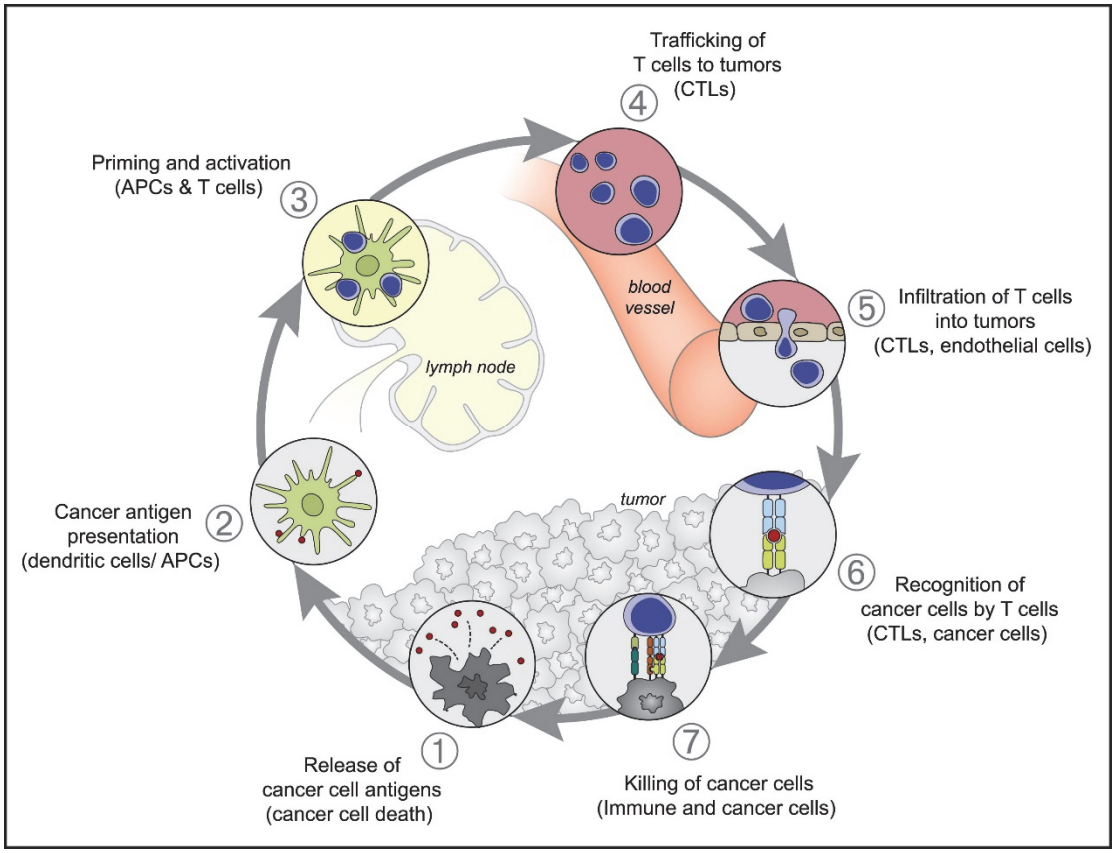

Figure I.3 | The Cancer-Immunity Cycle. The seven steps of the cancer immune cycle are described above. Abbreviations are as follows: APCs, antigen presenting cells; CTLs, cytotoxic T lymphocytes.[83]

Myeloid-derived Cells in the Tumor Microenvironment

Myeloid cells may orchestrate various aspects of cancer progression including: 1) establishing an immunosuppressive TME; 2) promoting tumor cell growth; 3) promoting angiogenesis; 4) establishing a metastatic niche and 5) facilitating metastasis. We will focus on the myeloid-derived cells that have been described to play a role in PCa progression.

Dendritic Cells

Bone marrow derived dendritic cells (BMDCs) are a heterogeneous group of APCs that can be classified into two basic subtypes: plasmacytoid DCs (pDCs), which accumulate in blood and lymphoid tissue, and classical DCs (cDCs), which infiltrate lymphoid and non-lymphoid tissues.[84] In humans, BMDCs are defined as cells that are negative for the lineage markers: CD3, CD19, CD20, CD56 and CD14, express class II MHC (HLA-DR$^+$), and are low or intermediate for CD11c (ITGAX).[85] While pDCs can be characterized by their production of interferon alpha (IFNα), cDCs express either CD1c (BDCA1) or CD141 (BDCA3).[85] cDCs expressing CD141 are a noteworthy subset of cDCs superior at cross-presenting soluble antigen.[86] In rodents, this subset of cross-presenting cDCs can be further sub-classified into two populations depending on their expression of surface markers and their localization: CD8α in lymphoid tissue and CD103 in non-lymphoid tissue.[87] Both types of cDCs differentiate from CD11c$^+$ precursors.[85]

Regardless of their subtype, cDCs in non-lymphoid tissues process captured antigen and, after activation and up-regulation of CCR7 and L-selectin, migrate to T cell zones in lymph nodes where they present antigen to induce either T cell response or tolerance. Cross-presenting cDCs are the most efficient antigen presenting cells and have the potential to activate both CD4 Th cells and CD8 CTLs.[88] In the presence of cancer, a subset of immature dendritic cells migrates to the tumor draining lymph node where they may stimulate the expansion of naturally occurring T_{regs} by secreting transforming growth factor beta (TGF-β).[89] Interleukin 10 (IL-10) and other factors in the TME that hinder dendritic cell maturation[90,91] and consequently facilitate antigen presentation in a suppressive context. Moreover, disrupting the ability of cDCs to present antigen to T cells may facilitate tumor immune evasion, as will be discussed later. In addition, CTLA-4 on T_{regs} may interact with the normally co-stimulatory molecules B7.1 and B7.2 on a subset of BMDCs (called suppressive DCs), inducing them to express indoleamine 2,3-dioxygenase (IDO), which further contributes to the immunosuppressive microenvironment (Fig. I.4).[92] This occurs when IDO catabolizes tryptophan, an essential amino acid for T cell function, in the TME.[93] As will be discussed below, a number of IDO inhibitors were developed for cancer immunotherapy.

Myeloid-Derived Suppressor Cells (MDSCs)

During an inflammatory response, bone marrow derived monocytes migrate into the tissues and replenish the resident pool of macrophages (Mϕ) and dendritic cells.[94] In cancer, this steady supply of mature leucocytes may be perturbed by factors promoting myelopoiesis - leading to an accumulation of immature myeloid

cells. Additional factors prevent these cells from differentiating into mature cells of the myeloid lineage (Mϕ, dendritic cells, and mature neutrophils) and promote their pathologic function.[95] Accordingly, monocytes from peripheral blood of PCa patients do not develop into mature dendritic cells as efficiently as those derived from healthy donor blood samples,[96] although a number of studies have shown that prolonged *ex-vivo* culture of monocytes from cancer patients can result in fully functional cDCs for cancer vaccines.[88]

Two main types of MDSCs have been identified: polymorphonuclear (PMN-MDSCs) and monocytic (M-MDSCs). PMN-MDSCs are phenotypically similar to neutrophils whilst M-MDSCs are similar to monocytes. In humans, PMN-MDSCs are defined as $CD11b^{+}$ ($ITGAM^{+}$) $CD14^{-}$ $CD15^{+}$ or $CD11b^{+}$ $CD14^{-}$ $CD66b^{+}$ (in some studies, $CD33^{dim}$ is used instead of $CD11b^{+}$).[97] In mice these cells are $CD11b^{+}$ $Ly6G^{+}$ $Ly6C^{low}$.[97] M-MDSCs are defined as $CD11b^{+}$ $CD14^{+}$ $HLA\text{-}DR^{-/low}$ $CD15^{-}$ in humans and $CD11b^{+}$ $Ly6G^{-}$ $Ly6C^{hi}$ in mice.[97] These two types of MDSCs utilize different mechanisms of immunosuppression.[98] Briefly, M-MDSCs produce high amounts of nitric oxide (NO; mediated by the *Nos2* gene), decrease T cell nutrient availability (L-arginine, L-cysteine, and tryptophan) in the microenvironment, and induce T_{reg} differentiation through the production of IL-10 and TGF-β.[99] PMN-MDSCs produce reactive oxygen and nitrogen species (ROS & RNS) that facilitate CXCR4–mediated tumor dissemination,[100] lead to the down-regulation of antigen presentation in cDCs,[101] impede CD8 T cell infiltration,[102] and induce antigen-specific CD8 T cell tolerance.[103] In addition, both types of MDSCs decrease CD4 and CD8 T cell homing to lymph nodes through the cleavage of L-

selectin from the plasma membranes of T cells.[104] Supporting a potential role for PMN-MDSC in PCa, protein nitration (i.e. 3-nitro-tyrosine formation) was found to be associated with PCa but not benign prostatic hyperplasia.[105]

Macrophages

Inflammatory monocytes that enter into tissues from the bloodstream have been suggested as the major source of macrophages (Mϕ) in the TME, i.e. tumor-associated Mϕ (TAMs).[106] However, the contribution of *in situ* expansion of tissue-resident Mϕ to TAMs in PCa remains an open question. Inflammatory monocytes are defined as $CD14^{hi}$ $CD16^{-}$ $CX3CR1^{low}$ $CCR2^{hi}$ in humans and $Ly6C^{hi}$ $CX3CR1^{low}$ $CCR2^{hi}$ in mice. The phenotype of these cells changes upon tumor infiltration; they mature into $CD14^{low}$ $CD16^{+}$ $CX3CR1^{+}$ $CCR2^{low}$ cells in humans and $Ly6C^{low}$ $CX3CR1^{+}$ $CCR2^{low}$ Mϕ in mice.[107,108] Mature Mϕ are subsequently polarized into distinct phenotypes depending on the cytokines present in the TME. *In vitro*, Mϕ can readily be polarized towards two distinct phenotypes (M1 and M2); but *in vivo*, these cells show a wide spectrum of polarization between those canonical states.[109] Mature Mϕ can be identified by the markers CD68 in humans and F4/80 (ADGRE1) in mice.[110] In mice, MHC-II^{hi} Mϕ have been shown to express M1 associated genes (*IL1b*, *IL12b*, and *Ptgs2*) and to produce NO more efficiently when stimulated with interferon gamma (INFγ) or LPS than MHC-II^{low} Mϕ –which are characterized by the expression of M2 associated genes (*IL10*, *Arg1*, *IL4Ra*, and *Mrc1*).[111] In general, M1 or classically activated Mϕ are considered anti-tumorigenic, while M2 or alternatively activated Mϕ are considered pro-tumorigenic. TAMs may promote tumor growth by increasing tumor angiogenesis,

through the expression of angiogenic growth factors and matrix metalloproteinases,[108] and by inducing T_{reg} differentiation via IL-10 production in the TME.[109] Interestingly, the phenotype of TAMs may flux between the M1 and M2 phenotype according to the cytokines present in the TME during tumor progression[108] (Fig. I.4).

Myeloid-derived Cells in Prostate Cancer Initiation and Progression

Myeloid-derived Cells in Cancer Initiation / Establishment of the TME

Chronic inflammation may play a role in PCa initiation.[112] Although the precise initiators of inflammation are unknown, potential etiologies include infectious agents, chronic noninfectious inflammatory diseases and/or other environmental factors.[113] Indeed, inflammation on biopsy cores of benign prostate tissue is associated with the presence of PCa.[114] Supporting a potential role for an inflammatory insult in tumorigenic inflammation, a human prostatic isolate of *Escherichia coli* accelerated PCa initiation in *Nkx3.1* mutant mice[115] and progression in a spontaneous murine model of PCa (Hi-Myc).[116]

Upon insult, inflammatory Mϕ ($Ly6C^{hi}$ $CX3CR1^{low}$ $CCR2^{hi}$) accumulate in damaged tissue where paracrine signaling directs their maturation.[108] Once in the TME, TAMs themselves become a major source of inflammatory mediators such as cytokines, chemokines and growth factors.[108] Among these mediators, interleukin-6 (IL-6) is of particular interest in PCa.[117] IL-6 binds to either its membrane receptor (IL6R) or its soluble receptor (sIL6R) to induce the formation of a functional complex that induces the homodimerization of interleukin 6 signal

transducer (IL6ST), also known as gp130, leading to the activation of the janus kinase (JAK) pathway.[118] JAK–mediated phosphorylation then leads to the activation of multiple signaling pathways, in particular: signal transducer and transcription activator 3 (STAT3), mitogen activated protein kinase (MAPK), and phosphoinositol-3 kinase / a serine/threonine kinase (PI3K / AKT)[119] (Fig. I.5).

The downstream effects of IL-6 signaling are cell type dependent. While IL-6 signaling has been suggested to promote cancer progression by regulating cell growth, differentiation and survival in prostate tumor cells,[118] IL-6 can also exert its pro-tumorigenic effects by modulating the TME. In this regard, IL-6 promotes monocyte differentiation toward M2-like Mϕ in culture,[120] and induces naïve T cells to differentiate into a subtype known as T_H17 that secretes high amounts of interleukin-17 (IL-17).[121,122] The accumulation of IL-17 in the TME leads to further up-regulation of IL-6, potentially generating an amplification loop.[123] In addition, paracrine IL-17 signaling may prime prostate tumor cells to produce factors that favor an M2-like phenotype within TAMs (Fig. I.4). Indeed, when media from murine prostate tumor cells cultured in the presence of IL-17 is used to culture Mϕ, IL-10 expression is increased.[124] Li and colleagues also reported that *in vitro* stimulation of a murine PCa cell line with IL-17 induces up-regulation of prostaglandin-endoperoxide synthase 2 (PTGS2), also known as COX-2.[124] This PTGS2 activity then leads to the conversion of arachidonic acid into Prostaglandin E2 (PGE2),[125] which in turn promotes the differentiation of monocytes into suppressive TAMs and prevents DC differentiation.[126] These data suggest that IL-6–mediated promotion of IL-17 secretion might play a pivotal role in the switch

between the M1 and M2 macrophage phenotypes during PCa initiation and progression.

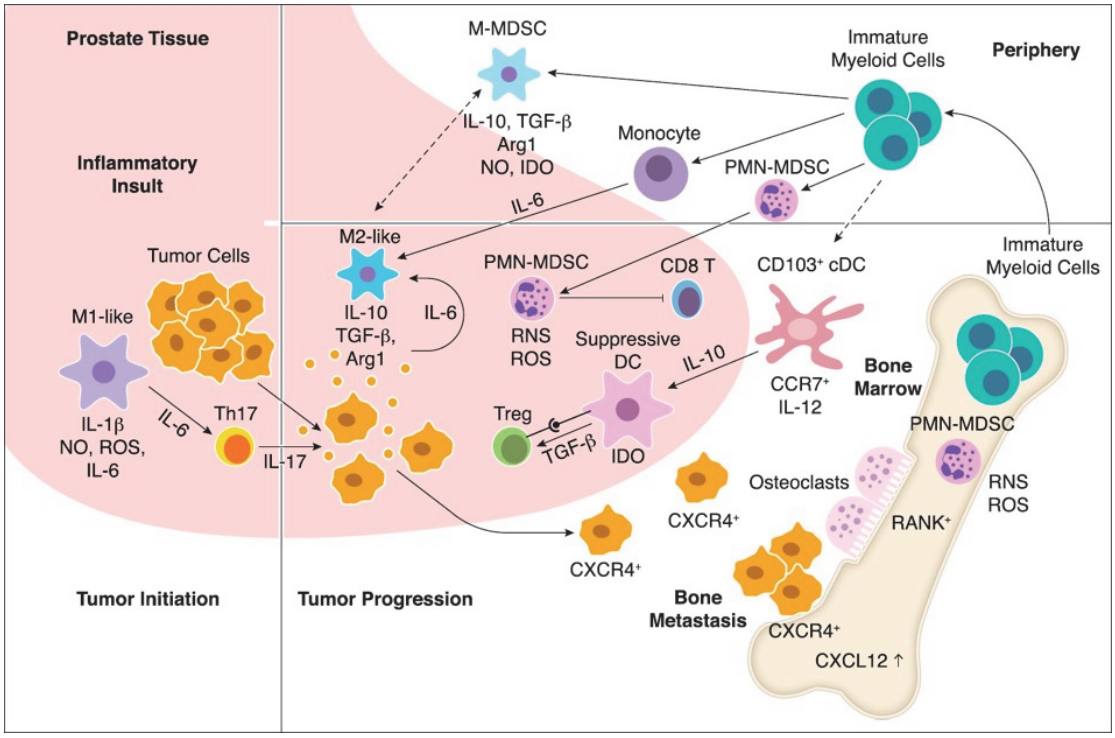

Figure I.4 | Contribution of Myeloid-derived Cells to Prostate Cancer Progression. M1-like Mϕ may contribute to tumor initiation after an inflammatory insult to the prostate gland,[112] likely by inducing accumulation of IL-17 and tumor-derived factors in the TME. Other myeloid-derived cells—M2-like Mϕ, MDSCs, and suppressive dendritic cells—likely infiltrate the TME early during tumor progression and suppress an antitumor response by inducing T_{regs} and preventing CD8 T cell infiltration and function. Bone resident Mϕ (osteoclasts) and PMN-MDSCs further contribute to tumor dissemination to bone by increasing osteoclastic bone resorption and regulating tumor cell homing (via CXCR4 expression), respectively. RNS, reactive nitrogen species; ROS, reactive oxygen species.

Myeloid-derived Cells in Cancer Progression

As shown in Figure I.4 above, there is a large body of evidence from clinical studies that suggests that myeloid cells (neutrophils, MDSCs and TAMs) contribute to cancer progression.[127] In PCa, the immunosuppressive TME has been shown to

hinder monocyte differentiation and DC maturation.[96] Accordingly, the percentage of M-MDSCs is significantly increased in the blood of PCa patients as compared to sex and age-matched controls.[128,129] Mechanistically, the ability of these cells to suppress T cell proliferation and to express high levels of IL-10 has been confirmed *in vitro*.[130] Although M-MDSCs levels return to normal after removal of the prostate gland,[129] elevated levels of M-MDSCs have been associated with a shorter median OS in mCRPC.[131]

Similarly, accumulation of PMN-MDSCs in the peripheral blood of PCa patients has been correlated with decreased OS, increased levels of CXCL8 and IL-6,[132] and PCa progression from localized to metastatic disease.[133] Accordingly, a retrospective analysis of patients with mCRPC that received personalized peptide vaccination showed that a PMN-MDSCs gene signature in peripheral blood mononuclear cells (PBMCs) post-vaccination correlated with poor prognosis.[134] Other studies showed that an elevated neutrophil to lymphocyte ratio (NLR) in the periphery correlates with a positive needle biopsy for PCa[135] and that NLR is a strong correlate of poorer OS in patients with mCRPC.[136] In addition, mCRPC patients with a low NLR at baseline showed a significantly longer OS after first and second-line chemotherapy.[128,137] At this point, it is difficult to discern whether the prognostic value of the NLR is due to the contribution of PMN-MDSCs in peripheral blood of PCa patients, or whether it reflects CXCL8 mediated neutrophil expansion. In this regard, a recently identified marker (OLR1) that distinguishes human neutrophils from PMN-MDSCs[138] may inform future studies

aimed at differentiating the contribution of neutrophil and PMN-MDSCs to PCa progression.

TAMs in the PCa TME are also associated with poor prognosis and outcome. An elevated density of $CD68^+$ TAMs infiltrating the prostate at the time of radical prostatectomy correlates with extracapsular extension (a marker of poor prognosis).[139] Similarly, $CD68^+$ TAMs infiltration in prostate needle biopsy specimens correlates with PCa progression as determined by PSA recurrence or PSA failure in patients treated with hormonal therapy as the first line of treatment.[140] In addition, an elevated density of $CD68^+$ TAMs in tissue from patients that underwent ADT prior to radical prostatectomy was found to be associated with an increased risk of biochemical recurrence.[141] In line with these observations, cell culture experiments have shown that IL-1β (a cytokine highly produced by Mϕ) in the TME may mediate androgen independence by inducing the degradation of the AR signaling complex.[142,143] In animal models, the reduction in tumor growth following depletion of Mϕ using clodronate-encapsulated liposomes or pharmacologic inhibitors of CSF1R signaling (GW2580 and PLX3397) support a role for TAMs in progression[144,145] and in biochemical recurrence in PCa.[143]

cDCs, which, in general, promote an adaptive CTL response, are associated with an improved prognosis in PCa patients.[146] In addition, elevated numbers of BMDCs in the peripheral blood of patients are associated with a less aggressive phenotype.[147] Accordingly, PCa patients who received a cDC-based vaccine and successfully mounted a specific T cell response against the vaccine

antigen showed a significantly increased OS as compared to those who received the vaccine but did not mount a specific T cell response.[148] These data highlight the potential importance of cDC maturation for an effective anti-tumor response and suggest that this process might be impeded in a subset of patients. Mechanistically, IL-10 inhibits BMDC differentiation from monocytes in culture[90,91] and may thus also inhibit the maturation of cDCs in the TME. It should be noted, however, that *ex-vivo* generation of BMDC is feasible in most PCa patients.

Myeloid-derived Cells and Cancer Cell Metastasis

Over time, prostate tumor cells accumulate genetic alterations that allow them to emigrate from the primary tumor and seed metastases at different anatomic sites.[149] These alterations may also allow them to recruit myeloid cells to the TME[150] and reprogram these cells in ways that may facilitate escape from the prostate gland, survival in the circulation, and the establishment of a pre-metastatic niche in distant sites.[151] Early evidence for the importance of TAMs in the metastatic process came from a breast cancer model where primary tumors developed similarly in macrophage-deficient mice but were unable to form pulmonary metastases.[152] Although there is currently no pre-clinical model that accurately recapitulates the metastatic processes involved in human PCa, M2-like Mϕ have been reported to infiltrate metastatic PCa lesions in rapid autopsy samples in higher concentrations than adjacent normal tissues.[120] In addition, clinical data support the accumulation of PMN-MDSCs and neutrophils in the peripheral blood of patients with mCRPC.[132,136]

Bone is the major metastatic site for human PCa[153] and is a rich reservoir of MDSCs in animal models.[99] Accordingly, prostate tumor cells may travel to this pre-metastatic niche following a chemokine gradient involving CXCR4[151] (Fig. I.4). This mechanism resembles a normal physiological process, in which immature myeloid cells in the bone marrow are maintained by CXCR4 / CXCL12-dependent chemokine signaling.[154] Indeed, increased CXCR4 expression on prostate tumor cells is associated with the presence of bone metastasis in PCa patients[155] and its role in bone homing was highlighted by pre-clinical models showing that CXCR4 blockade significantly reduced the total metastatic load in tumor-involved bone.[156] Interestingly, CXCR4 has been reported to be up-regulated by ROS–mediated phosphatase and tensin homolog (PTEN) loss[100] suggesting that the pre-metastatic niche might be driven to some degree by PMN-MDSC-derived ROS.

Another subset of myeloid-derived cells fundamental for the successful establishment of cancer metastasis in the bone are bone-resident Mϕ or osteoclasts. Osteoclasts are responsible for breaking down bone through a process of bone resorption that has the untoward effect of enabling tumor cell seeding[151] (Fig. I.4). This process is highly dependent on the receptor activator of NF-κB (RANK), recently renamed as TNFRSF11A, and its ligand RANKL or TNFSF11.[157] The RANK / RANKL pathway is a target of interest for the treatment of metastatic PCa; in addition to its role in osteoclast activity, the RANK / RANKL pathway can also be activated in tumor cells. Using a transgenic mouse model that express the SV40 large T antigen in prostate epithelium (TRAMP), Luo and

colleagues showed that metastasis to lymph node, liver, and lung was dependent on NF-κB signaling.[158]

A Potential Role for PI3K / PTEN / AKT Pathway Activation and ER Stress in the Suppressive TME

Recent pre-clinical data indicate that dysregulation of intrinsic pathways in tumor cells results in the production of inflammatory mediators and ultimately in immune infiltration.[159-161] In addition, pre-clinical models in other cancer types support the notion that these tumor-cell intrinsic pathways may promote resistance to ICB.[162] This may help to explain why only a small fraction of PCa patients responds to checkpoint blockade[163-166] and guide the search for new therapeutic agents to be used in combination with current immunotherapies.

PI3K / PTEN / AKT Pathway Activation and Recruitment of Myeloid Cells

The mutational landscape of mCRPC reveals that the most frequently altered genes include *AR* (62.7%), *TMPRSS2-ERG* and other *ETS* fusions (56.7%), *TP53* (53.3%), and *PTEN* (40.7%).[167] Beyond these more common mutations, somatic alterations in genes involved in cell survival pathways (*PI3K*, *Rb*, *RAF*, and *CDK*), genome maintenance (*BRCA2*, *BRCA1*, *ATM*), and cell fate (*WNT*) are also common in advanced disease.[167] Recent studies showed that T cell and dendritic cell infiltration may be mediated by PTEN loss and WNT / B-catenin activation in other tumor types.[161] These findings raise the possibility that the mutational signatures present in mCRPC could potentially underlay the suppressive microenvironment associated with disease.

As above, in PCa, PTEN loss, and subsequent PI3K / PTEN / AKT activation,[168,169] has been described by multiple groups. Activation of this pathway correlates with a more aggressive phenotype[170] and a decreased recurrence-free survival in patients with low-risk PCa (Gleason score 3+3 and 3+4).[171] In addition to PTEN loss due to genetic or epigenetic factors, PTEN activity can also be lost as a consequence of a highly oxidative TME without overt loss of the gene itself.[100] These data suggest that abundant ROS-producing cells, such as PMN-MDSCs, could play an indirect role in sustained PTEN down regulation (Fig. I.5).

Additional pre-clinical evidence supports the notion that myeloid-derived cells can be recruited through PI3K / PTEN / AKT signaling in prostate tumor cells (Fig. I.5). Using a conditional PTEN knockout mouse model, Garcia and colleagues showed that myeloid infiltration into the prostate gland is increased early during tumor development by epithelial PTEN loss.[172] In addition, *in vitro* experiments showed that myeloid recruitment may be mediated by CXCL8 / CXCR2 signaling in human PCa cell lines in which PTEN is lost.[173-175] It will be interesting to determine whether similar events occur in men with PCa, i.e. whether PTEN loss / PI3K activation correlates with the extent or function of an immunosuppressive microenvironment.

Additional Mechanisms for PI3K / PTEN / AKT Pathway Activation

One cytokine that may play a key role in linking PI3K / PTEN / AKT in tumor cells with myeloid recruitment is IL-6 (Fig. I.5). Paracrine IL-6 signaling has been shown to induce intraperitoneal accumulation of monocytes in IL-6 knockout mice treated intra-peritoneally with a fusion protein containing IL-6 fused to sIL6R.[176] This

signaling has been shown to activate the PI3K / PTEN / AKT signaling pathway in prostate tumor cells.[119] Together, these data suggest that paracrine IL-6 signaling could indirectly lead to PI3K / PTEN / AKT–mediated myeloid recruitment (Fig. I.5). However, other cytokines in the TME are also likely to contribute to the accumulation of myeloid-derived cells in prostate tumors.[159]

One process that may lay upstream of PI3K / PTEN / AKT activation and subsequent recruitment of MDSCs is prolonged ER stress – which ultimately leads to the unfolded protein response (UPR). This adaptive response increases tumor cell viability in the TME, and is characterized by increased levels of the endoplasmic reticulum chaperone protein: heat shock protein family A (Hsp70) member 5 (HSPA5), also known as GRP78.[177,178] The ER sensors: protein kinase RNA-like ER kinase (PERK), also known as EIF2AK3; inositol-requiring protein 1alpha (IRE-1α), also known as ERN1; and activating transcription factor 6 (ATF6) restore cell homeostasis in cancer cells in conditions of ER stress.[179,180] Activation of both PERK and IRE-1α involves their dimerization, oligomerization, and trans-autophosphorylation. Activated PERK leads to the inhibition of protein synthesis; while activated IRE-1α exposes its RNase domain which splices the mRNA of X-box binding protein 1 (XBP1) to generate a transcription factor (XBP1s) that upregulates a subset of chaperone proteins. ATF6 translocates from the ER to the Golgi apparatus during stress conditions and is processed into ATF6f –a transcription factor that controls the expression of selected UPR target genes. The UPR response is complex, and is well-discussed in a recent review.[181] Under resting conditions, HSPA5 binds to these ER sensors (PERK, IRE-1α, and ATF6)

and maintains them in an inactive state[182] thereby preventing an UPR response. A recent study in which persistent ER stress was modeled via multiple administrations of the toxin thapsigargin showed that ER stress induces the accumulation of MDSCs in the spleens of mice bearing subcutaneous colon tumors.[183] Although this study did not directly address a role for AKT activity in tumor cells, experiments by Fu and colleagues showed that *in vitro* stimulation of human prostate tumor cells with thapsigargin resulted in ER stress and AKT activation.[184] Furthermore, PI3K / PTEN / AKT activation was found to be abrogated by HSPA5 deletion in a PTEN conditional knockout mouse model.[184] Taken together, these data raise the intriguing possibility that, in PCa, myeloid recruitment following ER stress could possibly be regulated by PI3K / PTEN / AKT activation (Fig. I.5). These observations must be tempered, however, by the experimental models employed as it is not clear how well prolonged thapsigargin treatment models physiological stressors in the human prostate TME.

Although multiple mechanisms may be responsible for an ER stress response, one physiological mediator of increased ER stress in PCa could be saturated fatty acids (FA). Accumulation of saturated FA in the ER membrane activates the ER sensors IRE-1α and PERK by enhancing their dimerization via their transmembrane domains.[185] Although not directly tested in PCa specimens, PTEN inactivation in a human PCa cell line led to increased expression of FA synthase (FASN), a lipogenic enzyme that catalyzes the terminal steps in the synthesis of long chain saturated fatty acids.[186] In addition, *de novo* lipogenesis has been shown to promote membrane lipid saturation in prostate tumor cells[187]

and was found to be associated with an increased risk of PCa in a nested case-control study.[188] Together, these data suggest that saturated FA might induce ER stress and subsequent PI3K / PTEN / AKT pathway activation as a possible step in the recruitment of myeloid cells in PCa (Fig. I.5).

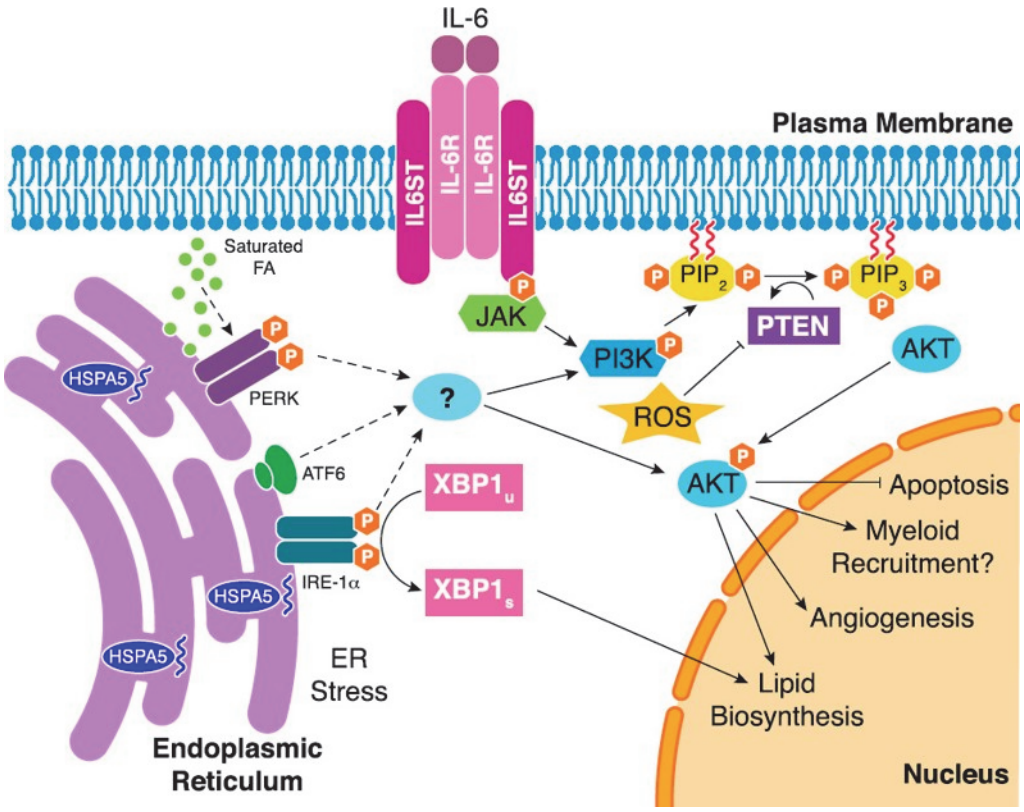

Figure I.5 | Effects of PI3K / PTEN / AKT Pathway Dysregulation in Prostate Tumor Cells. The noncanonical activation of AKT via IL-6 signaling, ROS accumulation, and ER stress response in PCa tumor cells is illustrated. Increased PI3K / PTEN / AKT pathway activation leads to prostate tumor cell survival (i.e., increased angiogenesis/lipid biosynthesis and decreased apoptosis) and the recruitment of myeloid cells. Binding of IL-6 to its receptor activates JAK, which leads to the phosphorylation of PI3K and, ultimately, to AKT signaling. Accumulation of ROS can also indirectly mediate AKT phosphorylation by down-regulating PTEN, which leads to unregulated PI3K activity. Finally, the ER stress response may also increase AKT signaling via the dissociation of HSPA5 from the ER sensors (PERK, IRE-1α, and ATF6), although the precise mechanism(s) by which this occurs is(are) currently unclear. In addition, XBP1s, generated by IRE-1α RNase activity, increases lipid biosynthesis (saturated FA), which may also

activate ER stress and maintain AKT signaling. HSPA5, heat shock protein family A member 5; IL-6R, IL-6 receptor; IL6ST, IL-6 signal transducer.

ER Stress in Myeloid Differentiation and Antigen Presentation

Recent studies showed that ER stress can be 'transmitted' from tumor cells to myeloid cells; in these experiments Mϕ cultured in conditioned medium from ER-stressed tumor cells evidenced an ER stress response themselves, with up-regulation of *Hspa5* and *Xbp1*s.[189] The exact mechanism by which this transmission is achieved is still a subject of investigation. It is possible, however, that TLR4 receptors on myeloid cells are activated as a consequence of immunogenic cancer cell death via the release of high mobility group protein B1 (HMGB1)[190] or lipids.[191] The notion that ER stress can be 'transmitted' from tumor cells to myeloid cells suggests that ER stress may not only be involved in myeloid cell recruitment, but also in hindering myeloid differentiation and contributing to immune evasion in the TME. Indeed, Gabrilovich and colleagues demonstrated that ER stress was increased in MDSCs isolated from both tumor-bearing mice and cancer patients with non–small cell lung cancer (NSCLC) and head and neck cancer (HNC).[192] Specifically, they showed clear up-regulation of XBP1s.[192] XBP1s has been reported to regulate cell proliferation in PCa cell lines,[193] but its role in MDSCs requires further investigation. Additionally, recent data from pre-clinical models involving induced ER stress in cancer cells stress suggest that XBP1s might regulate the immunosuppressive function of MDSCs by up-regulating *Arg1* and *Nos2*.[183] Since ER stress plays a pivotal role in human PCa, it is tempting to speculate that similar mechanisms might regulate the immunosuppressive phenotype of MDSCs in PCa.[180]

The immunologically suppressive role of ER stress extends to other cell types. For example, in intra-tumoral cDCs ER stress leads to down-regulation of their antigen cross-presentation capacity and subsequently to decreased priming of CTLs. This was demonstrated in animal models, where XBP1s up-regulation led to the accumulation of intracellular lipids in cDCs, as well as *in vitro* in BMDCs cultured with the ER stressor tunicamycin.[101] Lipid accumulation in cDCs may be mediated by the macrophage scavenger receptor 1 (Msr1) on the plasma membrane of dendritic cells[194] or by tumor-derived factors[195] that could induce ER stress in a HSPA5 dependent manner.[196] Cubillos-Ruiz and colleagues showed that cDCs accumulate lipids in a process that is mediated by triglyceride biosynthesis, rather than by lipid intake, and that is dependent on XBP1s.[101] Using a mouse model with XPB1 specifically knocked out in $CD11c^{+}$ cells, preventing ER stress in cDCs increased their function and enhanced their ability to prevent tumor progression as demonstrated by studies in which $XPB1^{-/-}$ cDCs were adoptively transferred to wild type mice challenged with ovarian tumors.[101] Thus, it is intriguing to further speculate that the dysregulated lipid environment in PCa may also mediate immunosuppression by altering the function of APCs such as cDC.[197]

Immunotherapy – Breaking Immunological Tolerance to Cancer

Immunotherapy with PD-1 / PD-L1 blockade plays a role in the treatment of many tumor types; as above PCa remains one of several exceptions. In PCa, the main challenge has been to overcome the so-called 'cold' tumor microenvironment given that the mechanisms underlying this phenotype remain unknown. As a general principle, more heavily mutated tumors show increased T cell infiltration.[198]

Although the mutational burden in mCRPC is generally low (median, 2.9 mutations/megabyte),[199] and only 3% to 8.3% of advanced PCa tumors have high tumor mutational burden (TMB),[199,200] tumors with microsatellite instability (MSI) have a greater number of tumor-associated antigens (TAAs) and thus be more likely to respond to immunotherapy approaches.[167,200-203] An alternative mechanism driving the establishment of 'cold' TMEs is the infiltration of suppressive cell populations, including T_{regs} and MDSCs, discussed above. A number of approaches have been taken to attempt to convert 'cold' tumors into 'hot' tumors and circumvent the development of tolerance in the setting of PCa immunotherapy, inhibition of negative regulators of immune activation (immune checkpoint blockade), induction of *de novo* anti-tumor immune response (vaccination and other neoantigen-driven approaches), and modulation of the myeloid compartment. Below, we describe these therapeutic avenues.

Immune Checkpoint Blockade (ICB)

The ability of the immune system to fight tumor cells has revolutionized cancer treatment in the last decade. Indeed, ICB, which targets co-inhibitory molecules on immune cells to promote anti-tumor immunity, has become the fourth pillar of cancer treatment along with standard therapies focused on targeting tumor cells themselves such as surgery, radiation, and chemotherapy.[204] As discussed above, co-inhibitory molecules play an important role in maintaining tolerance to self-antigens as well as controlling the magnitude of the immune response. While CTLA-4 is highly expressed on tumor infiltrating T_{regs},[205] the activity of PD-1 / PD-L1 blockade is likely more restricted to CD8 CTLs, as described above. Indeed,

anti-CTLA-4 has shown anti-tumor activity in two phase III clinical trials for mCRPC.[54,59] However, the observed effects were modest and suggest that CTLA-4 blockade alone is unlikely to be sufficient for robust clinical activity in PCa.[76] A reanalysis of data from one of those phase III clinical studies suggested that CTLA-4 blockade in combination with radiotherapy may be promising for the treatment of mCRPC with normal alkaline phosphatase, normal hemoglobin, and no visceral metastases.[164] Similarly, targeting CD8 CTLs in the tumor microenvironment mCRPC seems to be restricted to a subset of tumors expressing PD-L1[196] and/or presenting microsatellite instability.[206,207]

The mainstay treatment for mCRPC, androgen-deprivation therapy (ADT), induces a pro-inflammatory infiltrate[55,208] and temporarily abrogates immune tolerance to the prostate gland.[209] We and others showed that the combination of immune checkpoint blockade with ADT could provide an additive or perhaps even synergistic effect on the treatment of PCa.[76] Indeed, PD-1 blockade showed measurable radiographic response in 25% of PCa patients progressing on the second generation anti-androgen enzalutamide.[210] In line with these results, a recent phase II study suggests activity for the combination of PD-1 blockade and CTLA-4 blockade in patients with AR-V7-positive prostate cancer with DNA-repair deficiency (DRD).[211] This study enrolled 15 metastatic prostate cancer patients with AR-V7-expressing circulating tumor cells. Six of these patients had a positive DRD status as determined by targeted next-generation sequencing (three in BRCA2, two in ATM, one in ERCC4; none had microsatellite instability). Interestingly, PSA responses were observed in 33% of patients with a DRD^{+}

status, while none were observed on patients with a DRD^- status. Although these findings were not statistically significant. These encouraging results for CTLA-4 and PD-1 blockade are supported by an additional phase II study in men who had previously received ADT.[212] In this study, 25% of the 32 evaluated mCRPC patients receiving the combination therapy pre-chemotherapy had an objective response. Furthermore, an extended survival (51.2 months) was observed in 10% of mCRPC patients who received the combination therapy in the post-chemotherapy setting.

Cancer Vaccines and Other Neoantigen-driven Approaches

As discussed above, the immune system has the capacity to recognize and destroy tumor cells. Thus, cancer vaccination represents a viable strategy to generate a *de novo* anti-tumor immune response, or to boost an existing one. However, in established tumors, the immune system has been rendered immunologically tolerant – which means therapeutic cancer vaccines not only need to overcome the immunosuppressive microenvironment, but also need to be directed towards an immunogenic tumor-associated antigen (TAA). Thus, selecting an optimal TAA is a key aspect in developing a vaccine. Putative TAAs can either be selected as a consequence of tumor progression (*mutation associated neoantigens or MANAs*)[213,214] or be shared between tumor and healthy cells (*non-mutated neoantigens*). Non-mutated neoantigens are generally temporally expressed during development (e.g., MAGE, PAGE, NY-ESO-1), overexpressed by tumor cells (e.g., WT1), or expressed in a tissue-specific manner (e.g., PAP, PSMA, PSA).[215] Non-mutated TAAs have the advantage of being

readily recognized by T cell precursors due to incomplete thymic deletion or peripheral tolerance towards these self-antigens[216]. TAAs used in vaccines are commonly expressed by genetically modified cells, either from the patient or from a cell line, to protein pulsed and matured dendritic cells (*cell based vaccine*; e.g., Sipuleucel-T and GVAX) or a viral / bacterial vector (e.g., Prostvac-VF and ADXS031-142).

As discussed above, prostate tumors are characterized by a low mutational burden. However, non-mutated prostate-specific TAAs such as prostatic acid phosphatase (PAP) has proven to be useful targets for immunotherapy. Indeed, the only FDA approved therapeutic vaccine for the treatment of mCRPC, Sipuleucel-T, directs an immune response against the PAP target. In this approach, a patient's peripheral blood leukocytes are collected to generate monocyte-derived dendritic cells (moDCs) that recognize the PAP antigen on tumor cells once reinfused into the patient.[198,217] Similar approaches have shown to drive ex-vivo immune responses in patients with androgen independent disease when autologous moDCs are directed to target PSMA.[218] Additional non-mutated TAA targets such as prostate-specific antigen (PSA) have also been tested using different vaccine formulations in clinical trials with less promising results, including a recent negative phase III study.[76,219] In addition to single antigen targeting approaches, a whole cell vaccine combining LNCaP and PC3 PCa cell lines modified to secrete GM-CSF (GVAX) has also been investigated (Fig. I6). The potential advantage of this approached is the diversity of TAA targets provided by the vaccine; however, phase III clinical studies were terminated early.[198] Since

one of the mechanisms mediating the intrinsic resistance to vaccine therapies in PCa is immune tolerance, vaccines may need to be enhanced with combination approaches directed to modify the tumor microenvironment to be successful. Indeed, a phase I clinical trial evaluating GVAX in combination with anti-CTLA-4 showed encouraging anti-tumor activity in mCRPC.[220] Similarly, a PSA-targeting vaccine induced stable disease in about a third of patients when treated in combination with anti-PD-1 blockade.[221] Currently, a trial is ongoing that tests a PSMA targeted peptide vaccine administrated in combination with a TLR-3 agonist in PCa patients with progressive disease (NCT00694551).

Most recently, alternative approaches to activate cytotoxic T-cell responses independently of TCR signaling have been developed; namely, bispecific T-cell engagers (BiTEs) and chimeric antigen receptors (CARs). The first is a fusion of two monoclonal antibodies (single-chain fragment variable, scFvs) that simultaneously engage a TAA expressed in the surface of cancer cells and CD3ε T-cell receptor-associated molecule on the T-cell surface (Fig. I6).[222] The second, involves T cell transduction with a virus containing a chimeric antigen receptor composed of three components: 1) an extracellular domain also composed an scFV that recognizes the target TAA; 2) a transmembrane domain composed of membrane domain regions of various immune receptors such as CD3, CD8, CD28, or FcεRI; and 3) a cytoplasmic domain which is composed of one or more of intracellular regions involved in T-cell activation or co-stimulation such as CD8, CD28, CD137 or CD3ζ.[223] This type of therapy has shown significant clinical activity in liquid tumors such as leukemia where the targeted TAA (CD19) is

present in every cancer cell.[224-228] In solid tumors, an ideal target TAA would enable CAR-T cells to mount a cancer-specific immune response, thus sparing healthy tissue.[229]

Notably, a fully human (AMG 160) BiTE targeting PSMA in PCa cells and CD3 in T cells, demonstrated anti-tumor activity in xenograft models.[230] A phase I clinical study has shown the safety of this treatment approach;[231] however, the clinical activity in mCRPC remains to be reported (NCT03792841).[232] Similar BiTEs targeting PSCA have also shown some promise in pre-clinical work.[233] Preliminary results with CAR T cell directed to PSCA alone[234] or in combination with PSMA targeting CAR T cells,[235] suggest the potential of this new therapeutic strategy for PCa. Multiple clinical trials evaluating this class of agent are ongoing, as are studies with CAR T cells targeting other TAAs, such as epithelial cell adhesion molecules (NCT03873805, NCT03089203, NCT04053062, NCT03013712, and NCT02744287; Fig. I6).

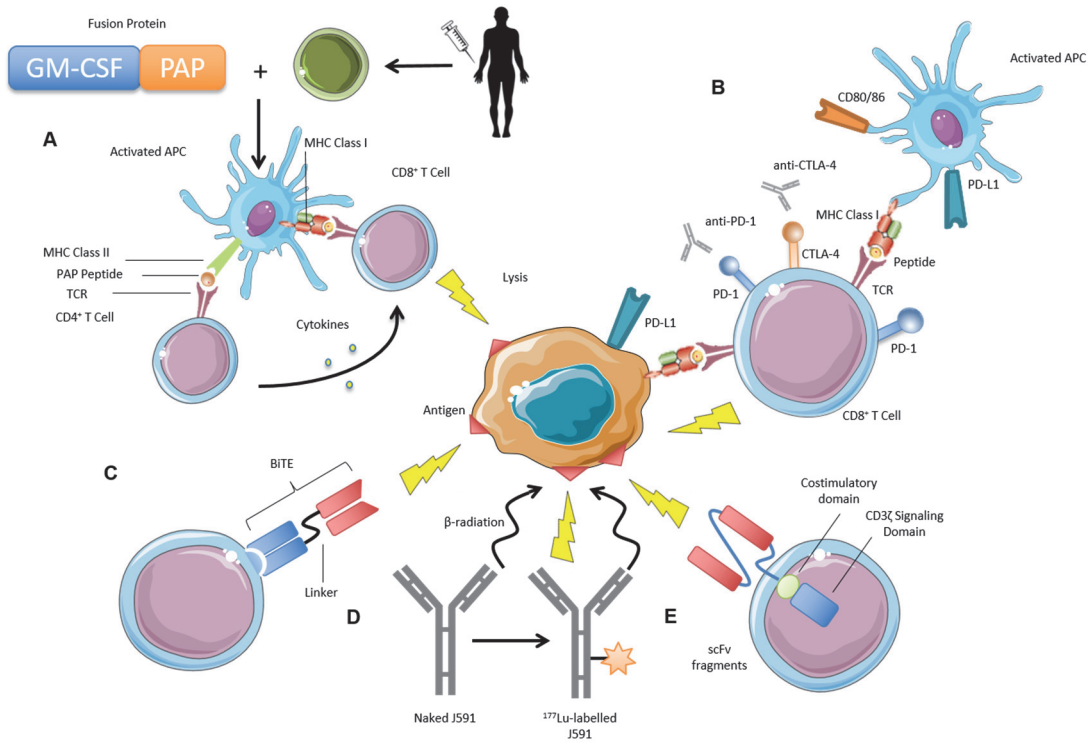

Figure I.6 | Immunotherapy Approaches in Prostate Cancer. A, Sipuleucel-T involves leukapheresis of immune cells followed by incubation with specific fusion protein (PA2024) which consists of prostatic acid phosphatase (PAP) coupled with granulocyte-macrophage colony stimulating factor (GM-CSF). Cells are then re-infused allowing for APC maturation and activation of $CD4^+$ and $CD8^+$ T cells to recognize and kill PAP presenting tumor cells. **B,** Checkpoint inhibitors are monoclonal antibodies which target immune checkpoints including programmed cell death 1 (PD-1) and cytotoxic T lymphocyte antigen 4 (CTLA-4) and prevent binding to PD-L1 and CD80 or CD86 respectively, which are expressed on tumor and other immune cells. This leads to an enhanced antitumor T-cell response. **C,** Bispecific antibodies are engineered antibodies that contain two binding sites, one for CD3 receptor found on T-cells and another for an antigen found on tumor cells. Several different constructs including Bi-specific T-cell engagers (BiTEs) are in clinical development. **D,** J591 is a humanized monoclonal antibody specific for prostate-specific membrane antigen (PSMA). The antibody can be labeled with lutetium-177, an isotope ideal for radiation therapy. The radioactive antibody targets PSMA presenting tumor cells and kills them with radiation. **E,** Chimeric antigen T-cell receptors (CAR-T) are receptors engineered to target antigens via an antibody derived single chain variable fragment, allowing the T-cell to function independent of the major histocompatibility complex. Pictured is a second-

generation CAR which contains a co-stimulatory domain and CD3ζ signaling domain.[198]

The combination of immunotherapy with treatments that lead to immunogenic cell death such as radiation therapy,[236] chemotherapy drugs such as taxanes,[237] or to high levels of T-cell infiltration such as androgen-deprivation therapy (ADT)[141,238-240] is likely to increase objective responses in PCa patients. Indeed, a phase II trial showed PAP-specific T cell responses were two fold higher in patients that received Sipuleucel-T before ADT in comparison to those that received it after ADT.[241] These data could have implications on the effect of ADT in modulating the tumor microenvironment, as well as in the sequence of immunotherapy administration for optimal clinical activity. Additional combination therapies targeting co-stimulatory molecules such as OX40, 4-1BB, CD30, CD40L, or ICOS may also increase the clinical responses achieved by these therapeutic interventions.

Therapeutic Modulation of the Myeloid Components in the Prostate Cancer Tumor Microenvironment

Although ICB has clear activity in multiple tumor types,[242] studies in PCa with such agents have generally been disappointing.[163-165] One possible explanation for this lack of activity could be related to the underlying myeloid components of the PCa microenvironment. Multiple interventions targeting myeloid cells and their effects on the TME have been recently reviewed,[243-245] and here we focus on novel targets relevant to the treatment of PCa.

One interesting agent in this regard is tasquinimod (Active Biotech AB, Sweden), a second-generation quinoline-3-carboxamide derivative.[246] Although its mechanism of action is still under investigation, tasquinimod was shown to target S100A9 – leading to the reduction of MDSCs in the TME in a breast cancer model.[247] In addition, tasquinimod was also reported to inhibit M2-like polarization and increase CTL infiltration when used in combination with a vaccine in a PCa model.[248] Recently, tasquinimod was found to not improve OS in men with mCRPC in a phase III study.[249,250] Still, the pre-clinical data suggest that tasquinimod could potentially be re-purposed in combination with immunotherapeutic approaches to PCa.

A novel approach to modulating the myeloid compartment in PCa is via targeting of the Hippo / YAP (Yes Associated Protein) pathway. In this tumor suppressor pathway, Hippo restricts organ size in mammals by antagonizing the oncoprotein YAP.[251] Consistent with a critical role for Hippo-YAP signaling in normal tissue homeostasis, the YAP oncoprotein is activated in a wide spectrum of human cancers.[252] In PCa, recent studies showed that the common TMPRSS2-ERG genomic fusion may lead to YAP activation.[253] In addition, YAP has recently been shown to bind the promoter of CXCL5 (a homologue of CXCL8) and up-regulate its expression in tumor cells to recruit MDSCs into the TME.[254] These data suggest that the YAP antagonist verteporfin (Novartis Pharmaceuticals, Switzerland)[252] and other related compounds could be of clinical use for the treatment of PCa. Indeed, a phase I clinical trial of verteporfin in patients with established bone metastases has been initiated (NCT02464761).

Another agent that targets the myeloid compartment is DS-8273a (Daiichi Sankyo Inc., Japan), a second-generation monoclonal antibody that targets death receptor 5 (DR5), also known as TNFRSF10B. Pre-clinical data from a lymphoma model and from DR5 knockout mice showed that DR5 promotes the accumulation of MDSCs, such that DR5 inhibition facilitates the expansion and function of CTLs.[192] These data suggest DR5 as a potential target for attenuating MDSCs infiltration into the TME. An earlier monoclonal antibody against DR5, CS-1008 (Daiichi Sankyo Inc., Japan), was demonstrated to be well-tolerated in a phase I trial and to induce stable disease in 8 out of 19 patients with metastatic colorectal cancer.[255] Taken together, these data support the clinical potential of targeting DR5. The safety and tolerability of DS-8273a is currently being evaluated in an open label clinical trial for patients with advanced solid tumors or lymphomas (NCT02076451) and, like the YAP inhibitor discussed above, DR5 inhibitors may eventually have utility in PCa.

Alternatively, the immunosuppressive microenvironment in PCa may be modulated by decreasing TAM recruitment to the tumor site. Since this recruitment is at least partially mediated by colony stimulation factor 1 receptor (CSF1R) signaling on inflammatory Mϕ, its inhibition has been proposed as a potential treatment for several tumor types, including PCa. In animal models of PCa, CSF1R blockade with small molecules was shown to delay tumor growth.[143,145] Accordingly, two tyrosine kinase inhibitors, PLX3397 (Plexxikon, Berkeley CA) and axitinib (Pfizer Inc, New York City NY), are now being tested in patients with advanced CRPC (NCT01499043) and in PCa patients undergoing androgen

ablation therapy (NCT01409200), respectively. In addition to small molecules, monoclonal antibodies can be used to target CSF1R – resulting in the subsequent inhibition of the recruitment of inflammatory Mϕ to the TME. Demonstrating clear enthusiasm for this approach, a total of four monoclonal antibodies against CSF1R are currently in clinical trials for the treatment of various tumor types: FPA008 (FivePrime, San Francisco CA –NCT02526017), IMC-CS4 (Eli Lilly, Indianapolis IN –NCT01346358 & NCT02265536), AMG 820 (Amgen, Thousand Oaks CA – NCT01444404 & NCT02713529), and RG7155 (Hoffmann-La Roche, Switzerland –NCT01494688, NCT02760797 & NCT02323191). Interestingly, RG7155 was shown to induce objective clinical responses in 74% of patients with extra-articular pigmented villonodular tenosynovitis (PVNTS)[256] and is now in clinical trials for several solid tumors in combination with chemotherapy (NCT01494688) and PD-L1 blockade, atezolizumab (Hoffmann-La Roche, Switzerland –NCT02323191). Although the majority of these clinical studies are not specifically recruiting PCa patients, the activity of IMC-CS4 is being evaluated in a phase I study for advanced breast cancer and CRPC (NCT02265536).

The phenotype of TAM could potentially be modulated by the neutralization of IL-6 / IL6R signaling. Current inhibitors of this pathway include monoclonal antibodies against IL-6, siltuximab (Janssen Pharmaceutica, Belgium), and IL6R, tocilizumab (Hoffmann-La Roche, Switzerland). Pre-clinical studies demonstrated a therapeutic effect of siltuximab in PCa;[257] this observation was supported in a multicenter phase II study that tested siltuximab in patients with CRPC that were pretreated with one prior chemotherapy.[258] Although none of the patients showed

a clinically defined response to the treatment, 23% achieved stable disease.[258] Less encouraging results were observed when siltuximab was given in combination with chemotherapy agents to patients with mCRPC,[259] suggesting that IL-6 / IL6R blockade may be more effective earlier during disease progression when the contribution of TAM to the development of CRPC is likely to take place. Tocilizumab is currently FDA-approved for the treatment of rheumatoid arthritis, and was found to induce and maintain complete remission of patients with giant cell arteritis[260]– a disease for which Mϕ are the major drivers.[261] The maximal tolerated dose of tocilizumab in hepatocellular carcinoma patients will be evaluated in a phase IB study that will be followed by the phase II design where the primary end point will be median progression free survival (NCT02997956). Although there are currently no trials underway, it is possible that tocilizumab could eventually be evaluated in PCa patients.

An effective CTL response against PCa may also hinge upon addressing the suppressive phenotype of not only MDSCs but also a subset of BMDCs in the TME. In this regard, IDO inhibition has been shown to decrease host-mediated immunosuppression and enhance antitumor immunity in multiple pre-clinical models.[262] As discussed above, IDO is the rate-limiting step in the catabolism of tryptophan[93] and is produced by MDSCs and suppressive DCs in the TME. Accordingly, IDO inhibition with 1-d-MT (a tryptophan racemic isoform: 1-methyl-l-tryptophan) was shown to improve response to CTLA-4 blockade in a pre-clinical model of melanoma[263] suggesting that IDO inhibition can reverse the immunosuppressive microenvironment in cancer. Three IDO inhibitors are

currently in clinical trials for the treatment of various solid tumors: indoximod (NewLink Genetics Corporation, Ames IA –NCT01560923 & NCT02077881), GDC-0919 (Genentech Inc, San Francisco CA –NCT02048709), and epacadostat (Incyte Corporation, Wilmington DE –NCT02752074 & NCT02327078). Recently, data from an ongoing phase I/II study presented at the *Society for Immunotherapy of Cancer* annual meeting suggest interesting anti-tumor activity in several tumor types when epacadostat is used in combination with PD-1 blockade, pembrolizumab (Merck, Kenilworth NJ –meeting abstract #142); this combination is currently being tested in a phase III trial for advanced melanoma (NCT02752074). Furthermore, epacadostat is being tested in combination with a second PD-1 blocking antibody, nivolumab (Bristol-Myers Squibb, New York City NY), in a phase I/II study for lymphomas and several solid tumors (NCT02327078). Although PCa patients are not being included in these studies, presumably due to the lack of activity of PD-1 and PD-L1 blockade as a single agent, it is possible that IDO inhibitors may reverse the immunosuppressive TME and prime T cells for checkpoint blockade in PCa. The ongoing phase II combining indoximod with Sipuleucel-T (Valeant Pharmaceuticals, Canada) for the treatment of mCRPC is likely to shed some light on the effect of modulating the immunosuppressive microenvironment in PCa (NCT01560923).

Elevated osteoclast activity is an important aspect of the pathophysiology of treatment-related complications in PCa. The inhibition of bone-resident Mϕ (osteoclasts) with the RANKL directed monoclonal antibody, denosumab (Amgen, Thousand Oaks CA), or with zoledronic acid (Novartis Pharmaceuticals,

Switzerland) effectively reduces the loss of bone mineral density associated with androgen deprivation therapy[264] and prolongs bone metastasis-free survival in CRPC patients.[153] In phase III trials, denosumab was found to be superior at preventing skeletal complications than treatment with zoledronic acid.[265] However, treatment with zoledronic acid was also shown to decrease the number of MDSCs in the spleens of tumor bearing mice and to increase the induction of an antigen-specific CTL response when combined with vaccination.[266] These data suggest zoledronic acid as a possible agent to reduce the accumulation of MDSCs in PCa and support its combination with a cancer vaccine for the treatment of PCa. Whether denosumab also decreases the number of MDSCs in PCa patients has yet to be examined.

In keeping with the data discussed above showing that CXCR4 / CXCL12 chemokine signaling may be involved in metastatic dissemination (Fig. I.4), inhibition of CXCR4 / CXCL12 signaling was shown to inhibit tumor growth and reduce metastasis in pre-clinical models of PCa.[267,268] Both the synthetic peptide CTCE-9908 (British Canadian BioScience Corporation, Canada), and AMD3100 (Sanofi-Aventis, France), bind to CXCR4 on tumor cells and prevent CXCL12 mediated recruitment to bone marrow. As previously discussed, CXCR4 is also expressed on monocytes and MDSCs in the bone marrow; but the contribution of these cells to an anti-CXCR4 treatment response has yet to be investigated. Clinical data show that CXCR4 blockade results in myeloid-derived cells leaving the bone marrow. Indeed, AMD3100 is FDA approved to increase hematopoietic stem cell recruitment to peripheral blood in the treatment of multiple myeloma.[269]

In addition, AMD3100 was shown to decrease the production of matrix metalloproteinases in the TME of a breast cancer tumor model,[270] and CTCE-9908 was shown to reduce angiogenesis (by inhibiting VEGF production) and recruitment of MDSCs into the TME of a PCa model.[267] CTCE-9908 was well-tolerated by patients with solid tumors in a phase I/II clinical trial.[271] Recently, another small molecule, X4P-001 (X4 Pharmaceuticals, Cambridge, MA) has been reported to block CXCR4 in peripheral blood of patients infected with HIV[272] and has now moved into a phase I/II study for the treatment of renal cell carcinoma in combination with the standard of care tyrosine kinase inhibitor, axitinib (Pfizer Inc, NY, NY –NCT02667886), and in combination with PD-1 blockade, nivolumab (Bristol-Myers Squibb, Princeton, NJ –NCT02923531). In addition, AMD3100 is now being evaluated in a phase I study for the treatment of mCRPC (NCT02478125) and preliminary reports from clinical studies using MDX-1338, an IgG4 antibody that binds CXCR4, showed encouraging clinical activity in the treatment of in hematological malignancies[273] and may be considered for the treatment of solid tumors like PCa in the future.

Rationale for and Summary of Experimental Findings

Is now fairly well accepted that cancers that are detected clinically must have evaded an antitumor immune response.[274] Whereas CD8 T cells are effective in mediating tumor cell lysis, their infiltration into prostate tumors is modest in relation to the infiltration of these tumors with myeloid-derived cells in human and mouse specimens.[141,159,172] Although TAAs expressed by prostate tumor cells are able to induce an immune response in patients with PCa, it seems likely that the

immunosuppressive microenvironment established by myeloid-derived cells (TAMs, PMN-MDSC/neutrophils, M-MDSC, and suppressive DCs) hinders the anti-tumor response in PCa. The involvement of myeloid-derived cells in PCa treatment failure is supported by clinical evidence.[141,275] Understanding the genetic alterations that lead to the dysregulation of intrinsic signaling pathways in prostate tumor cells and the mechanisms by which they regulate the infiltration of myeloid-derived cells may have a significant impact on PCa treatment. These genetic alterations may not only serve as biomarkers to aid in treatment selection, but also as targets to modulate the infiltration of myeloid-derived cells and the immunosuppressive microenvironment. Recent pre-clinical data suggest a link between PTEN loss, myeloid recruitment, and an immunosuppressive microenvironment in PCa. Disrupting the immunosuppressive microenvironment of PCa by inhibiting myeloid-derived cells, or their products, requires further exploration in the treatment of this malignancy. It is possible, however, that the efficacy of these treatments may be limited as a single agent and that combination regimens may be required. Interestingly, PCa is one of the few solid tumor types for which a therapeutic vaccine is currently FDA-approved.[276] Conversely, immune checkpoint blockade with anti-CTLA-4 has shown relatively limited success;[54,164,165] this may be partially explained by the pre-existence of an immunosuppressive TME.[275]

In the data that follow, we present studies that advance our understanding of mechanisms of the immunosuppression in PCa. Chapter 1 details the identification of a set of androgen-regulated genes expressed by the subpopulation

of epithelial cells surrounding the ductal lumen that survive chemical castration known as castration-resistant luminal epithelial cells (CRLECs). We successfully identified transglutaminase 4 (Tgm4) as a potential prostate-specific antigen in mouse and human databases. We showed that monocyte-derived dendritic cells (moDCs), pulsed with TGM4 whole protein induce pro-inflammatory CD4 and CD8 T cells, responded in autologous co-culture experiments with PBMCs of healthy donors. Furthermore, we found that breaking peripheral immune tolerance with a whole-cell vaccine, GVAX, results in the detection of TGM4 antibodies. Collectively, our findings suggest TGM4 as a prostate specific antigen that is conserved during the tumorigenic process and that could serve as a potential target for the development of a vaccine. Chapter 2, describes the robust peripheral tolerance to a model antigen in the context of a immunosuppressive TME. We found antigen-specific CD8 T cell recognition led to a reduction of effector cytokine production. This tolerance was robust and was not significantly mitigated by either the TLR-agonist Poly I:C or by ADT. Supporting persistent tolerance, we observed continued T_{reg} infiltration even late after ADT (at onset of castration-resistance), supporting a long-lived tolerogenic mechanism. Chapter 3 and 4 focus on identifying the mechanism that drives the recruitment of PMN-MDSCs into the TME of CRPC and the therapeutic implications of mitigating the IL-8 / CXCR2 pathway in combination with ICB. In chapter 3 we analyzed cancer cells isolated from castration-sensitive and castration-resistant prostate tumors, and discovered that castration resulted in significant secretion of Interleukin-8 (IL-8) and it's likely murine homolog Cxcl15. These chemokines drove subsequent intra-tumoral

infiltration with polymorphonuclear myeloid-derived suppressor cells (PMN-MDSCs), promoting tumor progression. PMN-MDSC infiltration was abrogated when IL-8 was deleted from PCa epithelial cells using CRISPR/Cas9, or when PMN-MDSC migration was blocked with antibodies against the IL-8 receptor CXCR2. In chapter 4 we showed that blocking PMN-MDSC infiltration in combination with anti-CTLA-4 delayed the onset of castration-resistance and increased the density of polyfunctional CD8 T cells in tumors. Taken together, our findings establish castration-mediated IL-8 secretion and subsequent PMN-MDSC infiltration as a key suppressive mechanism in the progression of PCa. Targeting of the IL-8 / CXCR2 axis around the time of ADT, in combination with ICB, represents a novel therapeutic approach to delay PCa progression to advanced disease.

Chapter I – An Immunogenic Prostate-Specific Tumor-Associated Antigen

"Women who developed an immune response to the self-protein MUC1 have a much lower risk for ovarian cancer."

Dr. Olivera J. Finn (2009) – a pioneer in cancer immunotherapy.

Professor at the Department of Immunology at the University of Pittsburgh.

1.1 Introduction

Multiple immunological approaches have been studied as therapeutic options for CRPC,[198] with limited success. In contrast to other tumor types, immunotherapy using immune checkpoint inhibitors (i.e., anti-PD-1 / PD-L1, anti-CTLA-4) has shown limited responses in mCRPC to date.[76] Conversely, the ability of the only therapeutic FDA-approved PCa vaccine (sipuleucel-T) to extend survival[276-278] suggests that immunotherapy has potential in mCRPC. Due to the non-vital nature of the prostate gland, effective adaptive responses against prostate-restricted TAAs such as PAP, PSA, PSCA, TARP, STEAP1, and PSMA are feasible therapeutic targets for PCa,[76,198,279-281] although their clinical relevance remains unknown. As described above, the identification of novel prostate-restricted TAAs that induce *de novo* anti-tumor immune responses could guide the development

of future immunotherapies. Here, we used a number of orthogonal approaches to identify transglutaminase 4 (TGM4) as a prostate-restricted TAA that is regulated in an androgen dependent manner. The potential immunogenicity of this protein was verified using *in vitro* studies, as well as samples from a neo-adjuvant clinical trial.[282]

1.2 Results

1.2.1 Castration-Resistant Luminal Epithelial Cells (CRLECs) Up-regulate Putative Prostate Antigens

Prior work showed that the murine prostate gland contains a population of Castration-Resistant Luminal Epithelial Cells (CRLECs) that is sufficient to regenerate prostatic architecture following consecutive rounds of androgen deprivation/repletion and which is the likely population of origin for PCa.[283] This population shares many features with castration-resistant prostate tumor cells.[284-286] To screen for potential prostate-restricted TAAs expressed by CRLECs, we quantified gene expression using a transgenic mouse model in which GFP expression is driven by the luminal-restricted *Hoxb13* promoter upon doxycycline administration. Using cells sorted from these animals, we quantified the transcriptional profile of CRLECs following an androgen deprivation/repletion cycle (Fig. 1.1A-D). We next defined a signature for androgen-responsive genes in our dataset as the intersection of genes differentially expressed when comparing untreated vs ADT-treated samples and ADT-treated vs ADT-treated followed by testosterone repletion (ADT+TR) samples. To derive this gene signature, we used an ADT Log2-fold-change below the 0.005 percentile and a p value below 0.01

(Table 1.1; Fig. 1.1E). We then correlated each sample pair in terms of their expression of this gene signature, to quantify the degree of similarity between untreated and androgen-repleted samples (Fig. 1.1F). Samples exposed to androgens showed a pairwise Pearson correlation of the androgen-responsive gene signature greater than 0.8 between samples from untreated animals and ADT-treated animals followed by testosterone repletion, confirming the genetic program re-established by testosterone treatment (Fig. 1.1F). Conversely, the androgen-responsive gene signature in either untreated or testosterone-repleted animals correlated poorly with the signature in androgen-deprived animals, further confirming the relative specificity of this signature (Fig. 1.1F). Consistent with prior data,[287-292] we found that ADT down-regulated the expression of several androgen-responsive genes including *Psca*, *Nkx3.1*, *Fkbp5*, and *Tmprss2* (Fig. 1.1E). The relative androgen dependence of these transcripts is shown in Figure 1.1D, with *Spink1*, *Msmb*, and *Tgm4* up-regulated 3,500fold, 1,900 fold, and 1,500 fold respectively by androgen repletion; while androgen repletion up-regulated the expression of *Psca* by 15 fold, *Nkx3.1* by 10 fold, *Fkbp5* by 5 fold, and *Tmprss2* by 2 fold. These results support a role for androgens in the regulation of *Spink1*, *Msmb*, and *Tgm4* genes as part of an androgen-responsive gene signature in CRLECs.

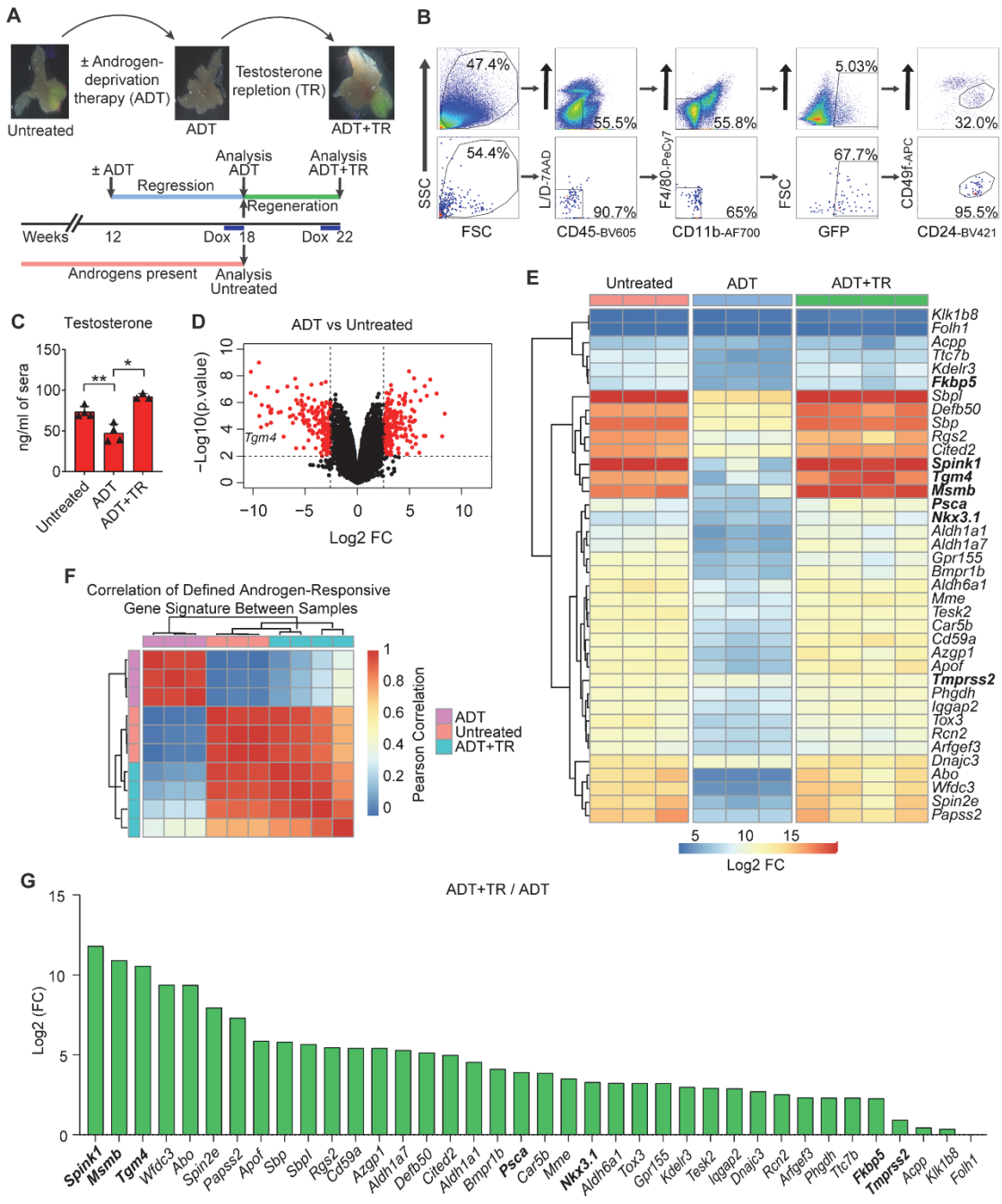

Figure 1.1 | Putative Prostate Antigens are Expressed by Murine Castration-Resistant Luminal Epithelial Cells in an Androgen Dependent Manner. A, Schematic representation of Androgen-induced prostate regression/regeneration in *Hoxb13-rtTA|TetO-H2BGFP* transgenic mice to model the cells-of-origin of PCa (CRLECs). Top, representative fluorescent images of GFP^{+} murine luminal epithelial cells to androgen-deprivation therapy (ADT) and testosterone repletion (TR) in murine prostates. Bottom, mice were treated with ADT (androgen

depletion), testosterone pellets (androgen repletion), and/or Doxycycline (DOX) as indicated in the diagram and described in the methods. **B,** top: sorting strategy used in the isolation of Castration-Resistant Luminal Epithelial Cells (CRLECs) based on their expression of GFP and their $CD45^{-}CD11b^{-}F4/80^{-}CD24^{+}CD49f^{int}$ phenotype; bottom: purity check of GFP^{+} sorted cells. **C,** *Hoxb13-rtTA*|*TetO-H2BGFP* transgenic mice were left either untreated, treated with ADT, or treated with ADT plus androgen/testosterone repletion (TR; n ≥ 3 per group). Serum testosterone concentrations were measured using the Holm-Sidak method as described in the methods. **D,** Volcano plot showing gene expression among all MTA 1.0 microarray transcripts expressed by GFP^{+} murine CRLECs from ADT vs Untreated groups. **E,** Differential expression profile of GFP^{+} CRLECs isolated from the prostates of mice left untreated, treated with ADT, or treated with ADT plus androgen/testosterone repletion (TR; n ≥ 3 per group). Heatmap showing androgen-responsive genes downregulated by ADT compared to both untreated and ADT+TR samples (n ≥ 3 per group). **F,** Heatmap showing pairwise Pearson correlation of androgen-responsive gene expression between CRLECs isolated from each mouse as described above. Androgen-responsive gene signature shown in **E**, with pairwise correlation between mice shown computed across all genes and annotated by treatment group. **G,** Log2 fold-change in expression of androgen-responsive genes in GFP^{+} CRLECs isolated from the prostates of mice treated with ADT in combination with androgen/testosterone repletion (TR) compared to ADT alone.

Table 1.1 | Androgen-Responsive Gene Signature.

Genes_Names	Untreated_Mean	ADT_Mean	ADT+TR_Mean
Spink1	974655.826	242.082839	866409.778
Msmb	185656.976	304.480284	586966.036
Tgm4	70377.3384	171.134126	258787.337
Wfdc3	17628.3521	25.6334721	17022.2898
Abo	21839.4161	18.5782581	12236.6201
Spin2e	24494.2699	64.7073191	16071.311
Papss2	47167.7556	155.938174	24754.0592
Apof	4356.16635	109.809521	6416.89651
Sbp	271100.203	4318.09719	241202.862
Sbpl	972667.149	17157.4001	870112.549
Rgs2	89658.3296	861.462986	38194.7043
Cd59a	2848.94752	171.7333	7394.37502
Azgp1	4258.78643	101.636022	4367.89512
Aldh1a7	1269.07094	48.7085793	1904.55733
Defb50	84900.5728	5400.16086	189625.374

Cited2	84223.3905	2620.51261	83842.1156
Aldh1a1	792.742768	40.7153434	958.740455
Bmpr1b	3581.6037	91.7754047	1593.68855
Psca	761.528032	108.213249	1626.43731
Car5b	4778.12871	224.429005	3270.96929
Mme	3666.21751	374.513263	4283.53898
Aldh6a1	7756.03357	459.040828	4331.99241
Tox3	4170.44803	172.964242	1625.86584
Gpr155	2168.92833	84.4151478	787.393368
Kdelr3	452.66376	45.630999	363.53375
Tesk2	5409.32676	407.292094	3098.13115
Iqgap2	2209.91219	289.03826	2145.4395
Dnajc3	11549.291	1830.1041	12030.3834
Rcn2	2090.81544	197.998451	1138.20148
Arfgef3	1607.08665	188.667659	948.79395
Phgdh	2591.53291	374.639533	1865.79207
Ttc7b	422.125059	39.7501941	197.90181

We next applied this signature to an independent, publicly available dataset in which epithelial lineage-marked YFP^+ tumor cells from the prostates of transgenic mice expressing YFP under the luminal-restricted *Nkx3.1* promoter were profiled (GSE39509).[293] These data also showed *Tgm4* to be among the most highly over-expressed genes in prostate tumors with a luminal origin (Fig. 1.2). Together, these findings support the notion that TGM4 is an androgen-responsive transcript expressed by prostate luminal epithelial cells, including CRLECs, in multiple datasets.

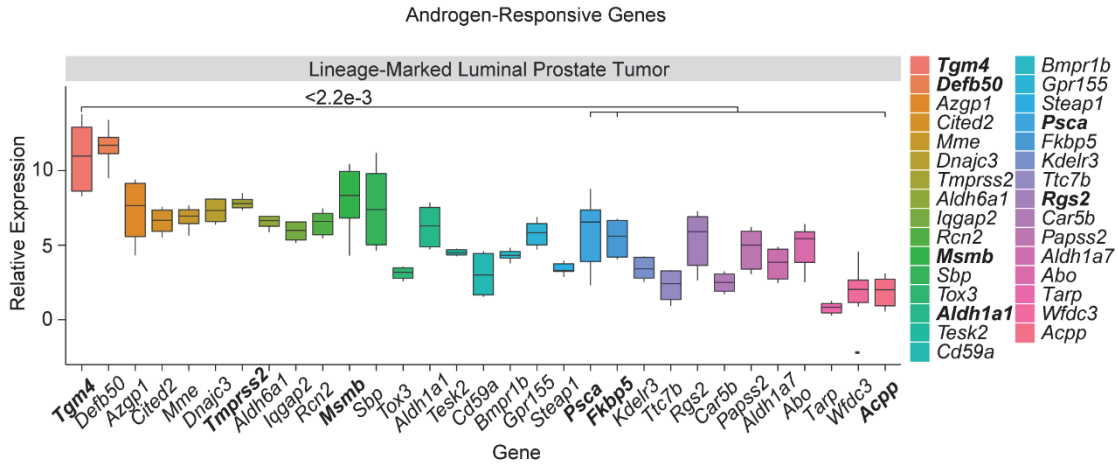

Figure 1.2 | *Tgm4* is Highly Expressed by Prostate Tumors Originated in Luminal Epithelial Cells. Relative expression of androgen-responsive genes, as well as *Tarp* and *Steap1*, in prostate tumors originated from luminal epithelial cells isolated from lineage-marked *Nkx3.1*$^{CreERT2/+}$; *Pten*$^{flox/flox}$; *R26R-YFP/+* transgenic mice (n ≥ 5; GSE39509).[293] Boxplots of Log10(FPKM) normalized gene expression are shown (n = 6). For b and d, selected genes for each comparison are defined as genes with ADT Log2-fold-change below the 0.005 percentile and p < 0.01, in addition to a set of known androgen-responsive genes from the literature (*Acpp*, *Klk1b8*, *Fkbp5*, *Nkx3.1*, *Tmprss2*, and *Folh1*). Wilcoxon test was used for statistical analysis between Tgm4 and each indicated gene; p values are displayed.

1.2.2 TGM4 Shows Prostate-Restricted Expression in Murine and Human Datasets

To avoid inducing immunologically off target effects, TAA's should have high expression on tumor tissue and minimal or undetectable expression on normal tissue(s). To evaluate which of the androgen-responsive genes are prostate tissue restricted, we interrogated two databases of gene expression from murine (RIKEN FANTOM5)[294] and human (GTEx)[295] normal tissues. We found low expression levels of *Defb50*, *Msmb*, *Sbp*, *Fkbp5*, *Spink1* and *Tgm4* in all murine extra-prostatic tissues evaluated (Fig. 1.3). Human data, however, showed significant *FKBP5* and *SPINK1* expression in lung, liver, skin, colon, kidney, and salivary gland

samples; these were greater than those for *TGM4* (Fig. 1.4). Of note, *DEFB50*, *MSMB*, and *SBP* were not included in the human database. The expression levels of the established prostate-restricted targets *FOLH1*/*PSMA*, *KLK3/PSA*, and *PSCA* were high in human prostate tissues, however, medium to low levels of expression were also observed in extra-prostatic tissues. Specifically, brain, lung, liver, and kidney tissues showed intermediate levels of *FOLH1*/*PSMA* expression. Detectable expression levels of *PSCA*, and *ACPP*/*PAP* were found in human skin, lung and kidney tissues; and both *PSCA* and *ACPP*/*PAP* expression were significantly higher than that of *TGM4* in these extra-prostatic tissues. Further, expression of *KLK3/PSA*, *PSCA*, *ACPP*/*PAP* and *FOLH1*/*PSMA* was present in human colon and salivary glands (Fig. 1.4), whereas *TGM4* was not detectable in these human tissues. Expression of additional prostate-restricted TAAs, including *TARP* and *STEAP1,* were also observed in both murine and human prostates, although at lower levels than *TGM4* (Fig. 1.3 & 1.4). While *STEAP1* expression was present in almost all the human tissues analyzed (lung, liver, skin, colon, kidney, and salivary gland), extra-prostatic *TARP* expression was only observed in lung, kidney, and salivary gland (Fig. 1.4). In summary, these data indicate that TGM4 is generally not expressed at the message level in non-prostate tissues, further supporting its investigation as a potential prostate-restricted TAA.

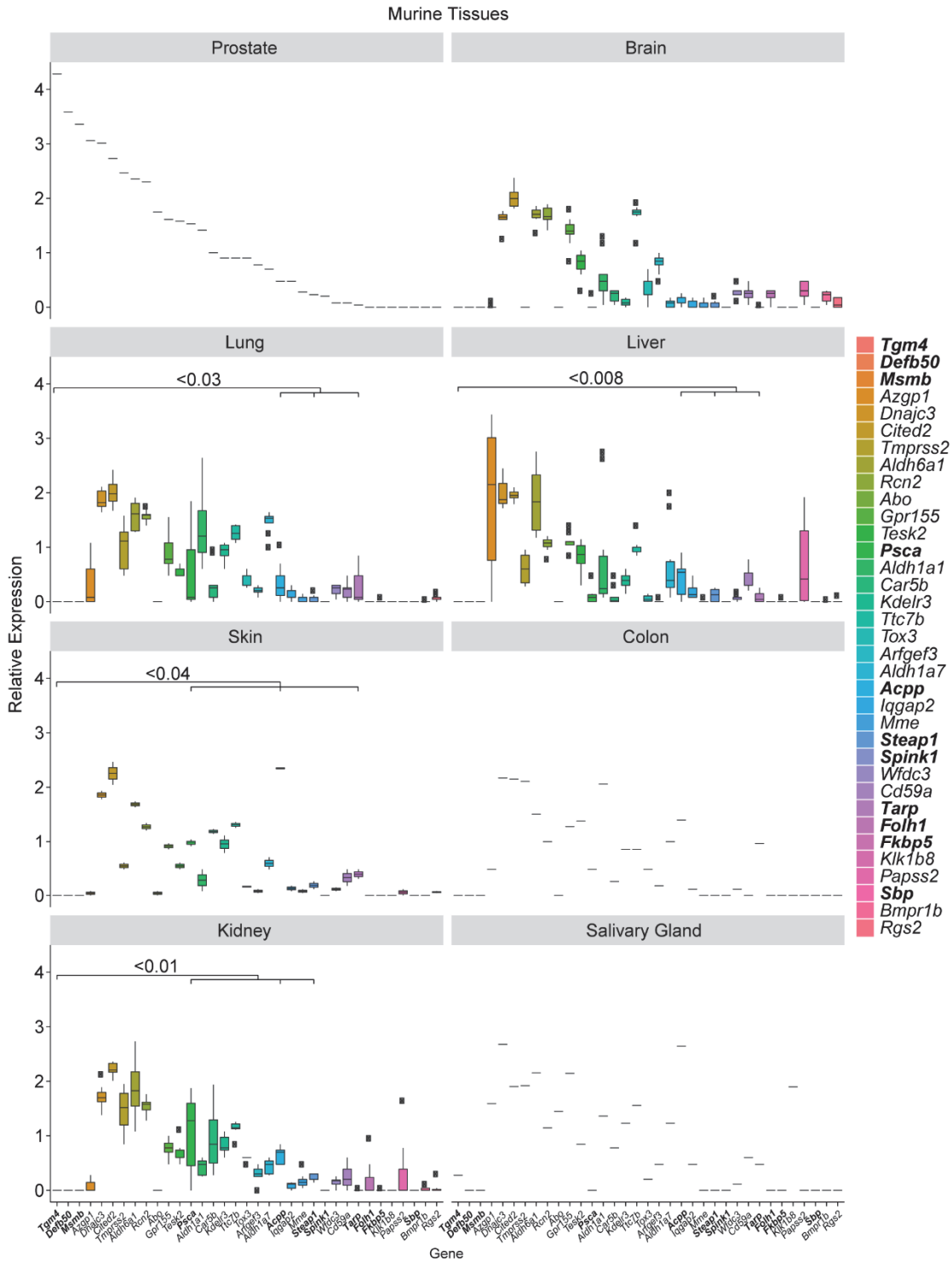

Figure 1.3 | Expression of Putative Prostate Antigens is Restricted to the Prostate in Mouse. Relative expression of androgen-responsive genes, as well as *Tarp* and *Steap1*, across normal murine tissues. Boxplots of Log10(TPM) normalized gene expression in prostate (n = 1), brain (n = 9), colon (n = 1), liver (n

= 10), lung (n = 9), skin (n = 2), and kidney (n = 7), and salivary gland (n = 1) from RIKEN FANTOM5 are shown, and genes are ordered by decreasing expression in murine prostate.

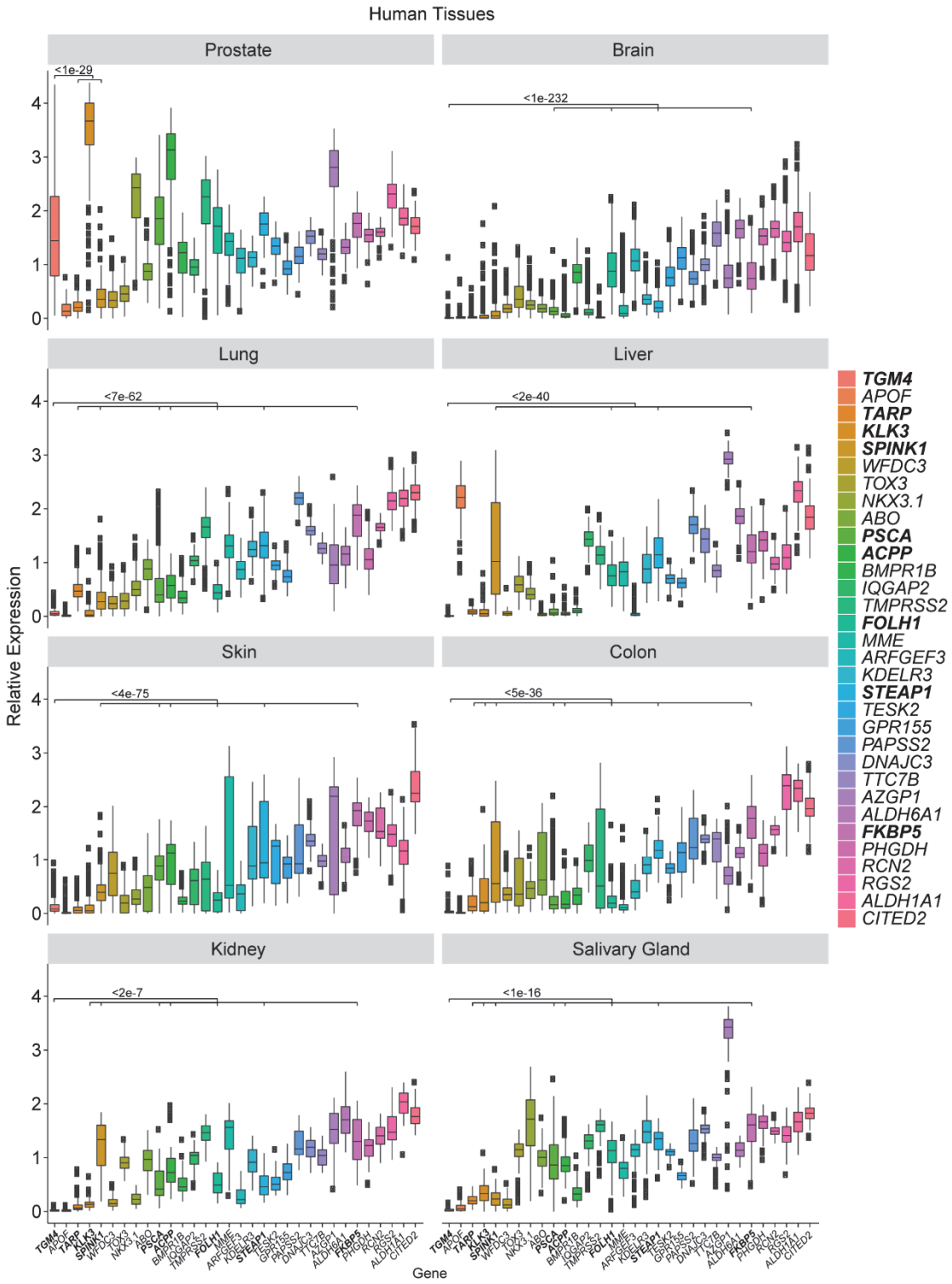

Figure 1.4 | Expression of Putative Prostate Antigens is Restricted to the Prostate in Humans. Relative expression of androgen-responsive genes, as well as *TARP* and *STEAP1*, across normal human tissues. Boxplots of Log10(TPM) normalized gene expression in prostate (n = 152), brain (n = 1671), colon (n = 507), liver (n = 175), lung (n = 427), skin (n = 1203), kidney (n = 45), and salivary gland (n = 97) from GTEx are shown. Wilcoxon test was used for statistical analysis between TGM4 and each indicated gene; p values are displayed.

1.2.3 TGM4 Expression Correlates with Prostate Cancer Recurrence

We next studied the levels of *TGM4* expression in primary PCa and other human cancer types included in The Cancer Genome Atlas (TCGA). Consistent with data from murine luminal epithelial prostate tumors (Fig. 1.2), the highest levels of *TGM4* expression were found in prostate adenocarcinomas (PRAD; Fig. 1.5A). We next tested whether *TGM4* expression in primary tumors is associated with disease progression in an independent dataset of prostate adenocarcinomas (GSE21032). This analysis of differential *TGM4* expression revealed that patients whose primary tumors had higher expression of TGM4 showed a significant decrease in time-to-PSA recurrence when compared to patients with low TGM4 expression in their primary tumors using an optimal cutpoint determined by maximizing the long-rank statistic (Fig. 1.5B-C). These data support the notion that TGM4 expression may correlate with poor prognosis in PCa.[296]

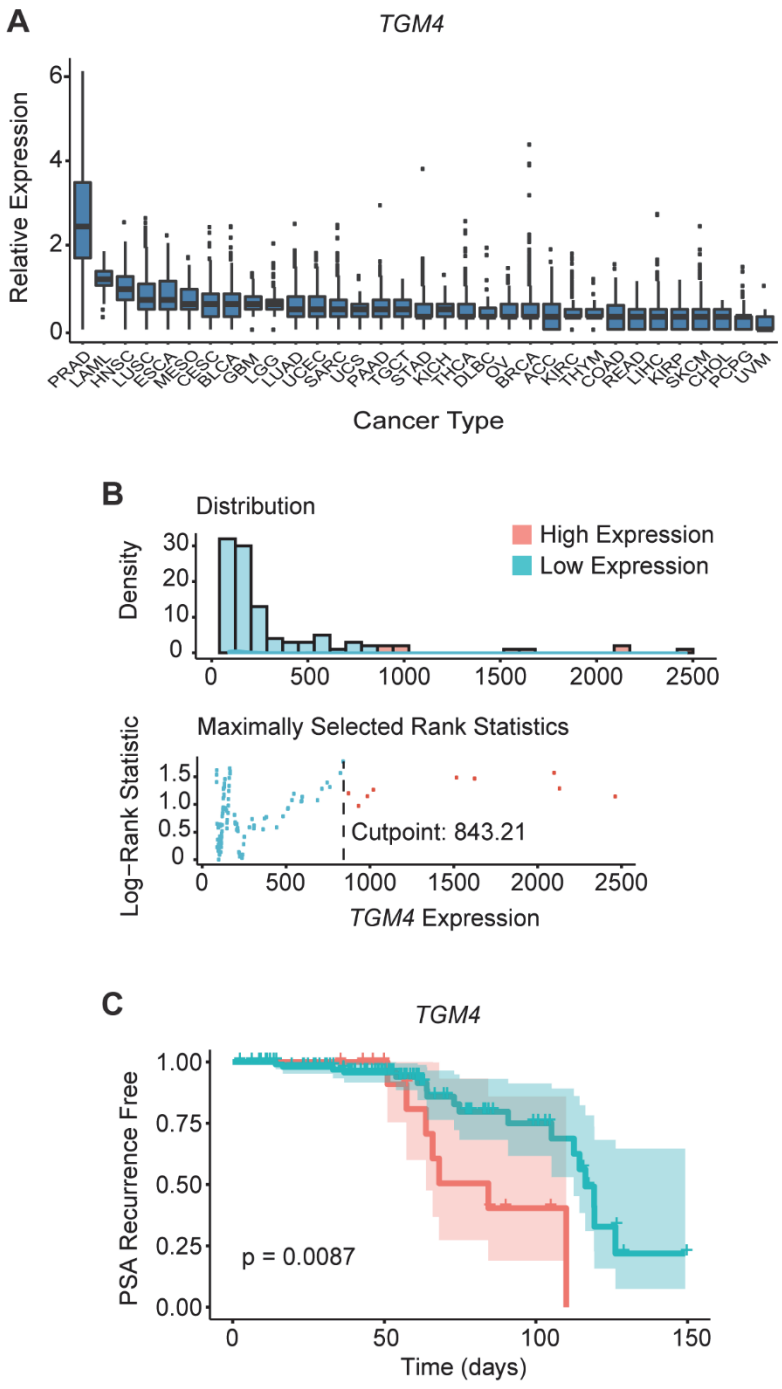

Figure 1.5 | TGM4 Expression is Maintained by Prostate Tumor Cells. A, Relative expression of *TGM4* across human cancer types in The Cancer Genome Atlas (TCGA) database, including 558 primary prostate adenocarcinomas (PRAD).[297] Boxplots of Log10(TPM) normalized gene expression are shown, with cancer types ordered by decreasing *TGM4* expression. **B,** Optimal cutpoint for *TGM4* expression. Top, Distribution of *TGM4* expression across primary prostate

adenocarcinomas (n = 218; GSE21032).[298] Bottom, the overall log-rank p-value for TGM4 expression is plotted. A vertical line drawn at the optimal cutpoint of 843.21. **C,** Kaplan-Meier curves comparing biochemical recurrence-free survival of patients with prostate adenocarcinomas, with log-rank p-value reported from multiple cox regression of biochemical recurrence-free against *TGM4* expression levels (high TGM4, n = 24; low TGM4 n = 107). Biochemical recurrence was determined as an increase in PSA serum levels ≥0.2 ng/ml on two occasions as described in the methods.

1.2.4 The Prostate-Restricted TAA TGM4 Induces an *In Vitro* CD8$^+$ T-Cell Response When Presented By Autologous Monocyte-derived DCs

To further determine whether TGM4 could serve as a potentially targetable TAA, we tested whether T cell responses to TGM4 could be induced *in vitro.* For these experiments, naïve T cells purified from the peripheral blood mononuclear cells (PBMCs) of healthy male donors (n = 10) were individually co-cultured with autologous monocyte-derived dendritic cells (moDCs) pulsed with either full-length protein TAAs (PAP, PSA, and TGM4) or a positive control comprised of an overlapping viral peptide-library (CEFT and pp65) in a 30-day culture system (Fig. 1.6A-B). To analyze responses, we used multiparametric flow cytometry to quantify antigen-driven expansion of CD8 T cells, and identified eight distinct populations using self-organizing maps for clustering analysis (FlowSOM; Fig. 1.6C-D). Of these, Pop6 appeared to represent central memory (CM) CD8 T cells and Pop4 naïve CD8 T cells (Fig 1.6D). Antigen-driven expansion of effector memory (EM) CD8 T cells was reflected by Pop5, which upregulated the self-renewing transcription factor TCF1 and the interleukin-7 receptor (CD127) (Fig. 1.6D). The expansion of both activated CM and EM CD8 T cells was confirmed

post-stimulation (Fig. 1.6E-F). Importantly, activated ($CD69^+$) $CD27^+CD28^+$ memory CD8 T cells expanded to a significantly greater degree in co-cultures with TAA-pulsed moDCs than with the positive control viral antigens (Fig. 1.6E-F). Accordingly, higher percentages of CM and EM expressed PD-1 and TIM3 when stimulated by TAA loaded moDCs, in this setting these molecules likely represent early activation markers rather than markers of exhaustion (Fig. 1.6G). Additional manual gating for the EM CD8 T-cell population expressing the pro-inflammatory transcription factor TBET (Pop 1; Fig. 1.6D) was performed (Fig. 1.6H). Here, we found that TGM4-pulsed moDCs drove the expansion of $TBET^+$ activated EM CD8 T cells to a significantly greater extent than PAP-pulsed and PSA-pulsed moDCs, but to a similar degree to the viral control antigens, CEFT and pp65 (Fig. 1.6I). These findings show that donor-derived naïve CD8 T cells expand and differentiate following TGM4 recognition and suggest that this prostate-restricted TAA could potentially be more immunogenic than either PAP or PSA.

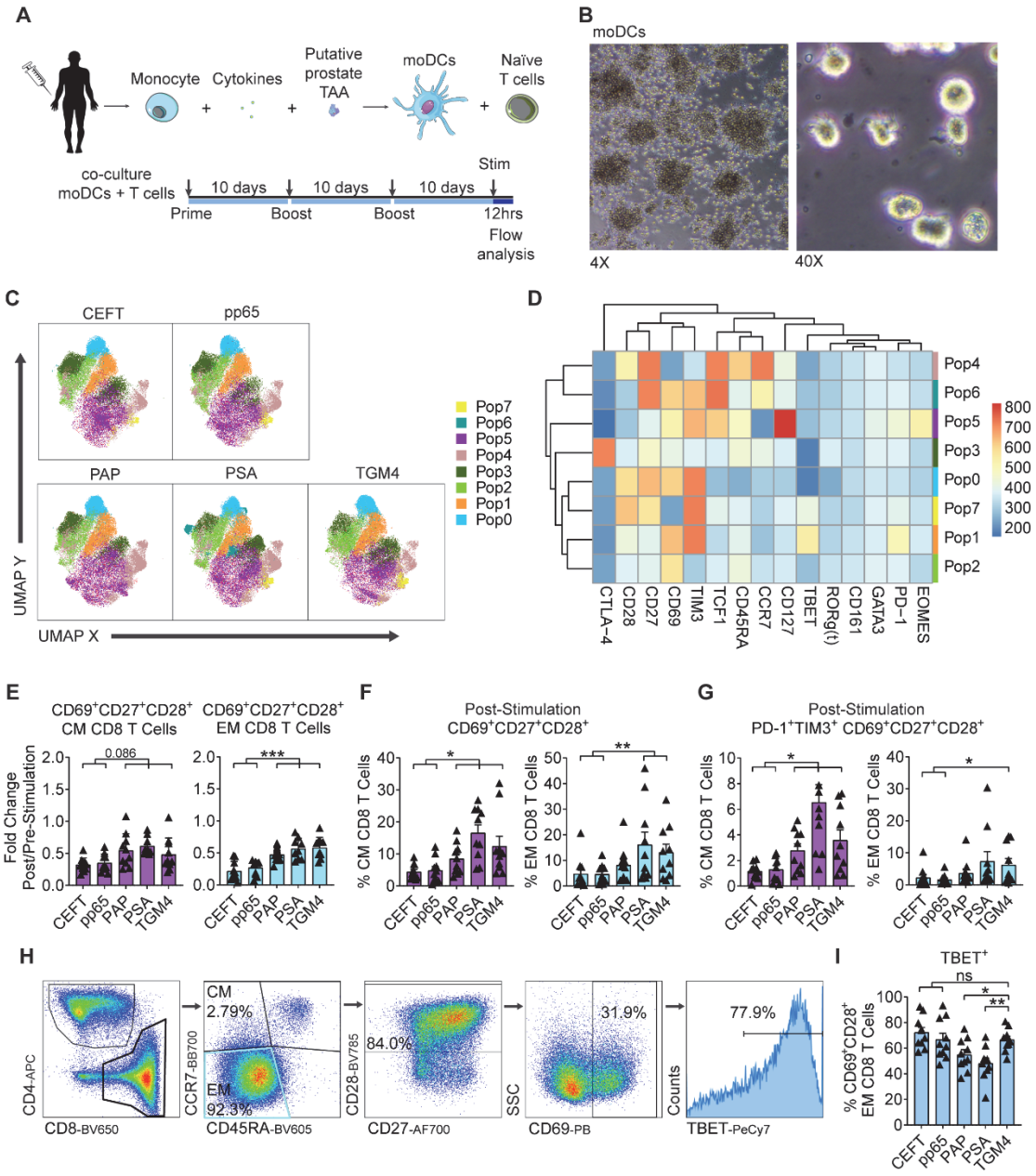

Figure 1.6 | TGM4 Induces CD8 T-Cell Activation and Expansion *In Vitro*. A, Schematic representation of the 30 days prime/boost co-culture of autologous monocyte-derive dendritic cells (moDCs) and naïve T cells. **B,** Representative images of differentiated moDCs. 4X (left) and 40X (right) magnification. **C,** Differential expression of functional markers on expanded populations of CD8 T cells following co-culture with autologous protein-pulsed moDCs. Heatmap showing unsupervised clusters determined with the FlowSOM algorithm as described in the methods. **D,** Expanded CD8 T-cell populations defined by FlowSOM in **C** were projected onto UMAP space as described in the methods.

Colors correspond to FlowSOM populations. **E,** Fold change on activated $CD69^+CD27^+CD28^+$ EM CD8 T cells (left) and CM T cells (right) following the last 12 hrs stimulation in expanded T cells. **F,** Activated $CD69^+CD27^+CD28^+$ cells as a percentage of EM CD8 T cells (left) and CM CD8 T cells (right) following *in vitro* expansion as in **E**. **G,** $PD1^+TIM3^+$ $CD69^+CD27^+CD28^+$ cells as a percentage of EM CD8 T cells (left) and CD8 T cells (right) following *in vitro* expansion as in **E**. **H,** Gating strategy used to manually analyze $TBET^+$ in activated $CD69^+CD28^+$ effector memory (EM) CD8 T cells defined as $CCR7^-CD45RA^-$ following co-culture with autologous protein-pulsed moDCs. **I,** $TBET^+$ cells as a percentage of activated $CD69^+CD28^+$ EM CD8 T cells in expanded T cells gated as in **c**. Unpaired t-tests performed, *p*-values ≤ 0.05 (*), 0.01 (**), and 0.001 (***); not statistical significance is represented as ns.

1.2.5 The Prostate-Restricted TAA TGM4 Induces an *In Vitro* $CD4^+$ T-Cell Response When Presented By Autologous Monocyte-derived DCs

We next performed similar analyses to those above for CD4 T cells. As shown in Figure 1.7A-B, FlowSOM clustering showed ten distinct populations of antigen-driven expanded CD4 T cells. Most of these clusters were observed in all antigen-driven expanded CD4 T cells (with the exception of Pop 5; Fig. 1.7A). Of these, Pop9 appears to represent CM CD4 T cells and Pop6 naïve CD4 T cells (Fig 1.7B). In terms of CM and EM CD4 T cells, we found that stimulation by TAA-pulsed moDCs increased the proportion and percentages of activated ($CD69^+$) $CD27^+CD28^+$ CM CD4 T cells to a significantly greater extent than did co-culture with the positive control viral antigens (Fig. 1.7D). Accordingly, higher percentages of CM and EM expressed the activation markers PD-1 and TIM3 when stimulated with TAAs (Fig. 1.7E). Additional manual gating for the EM CD4 T-cell population expressing the pro-inflammatory transcription factor TBET (Pop 0; Fig. 1.7B) was performed (Fig. 1.7F-G). Here, we observed TGM4-pulsed moDCs increased

expansion of TBET^{+} activated EM CD4 T cells to a greater degree than PAP-pulsed or PSA-pulsed moDCs, with levels similar to those from positive control viral antigens, CEFT and pp65 (Fig. 1.7H). These data support the notion that TGM4 can potentially drive pro-immunogenic CD4 T cell responses in addition to the CD8 responses shown above.

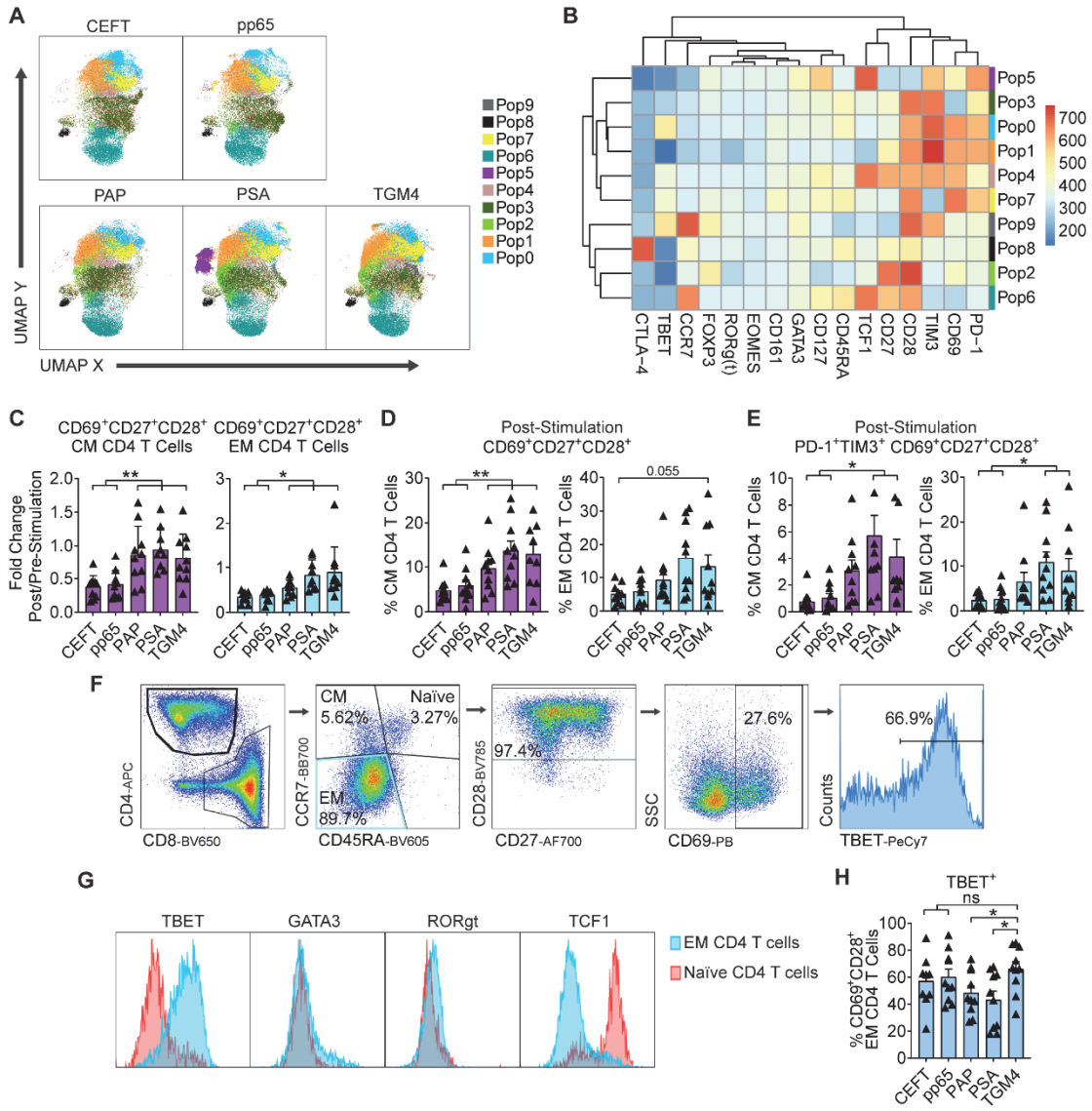

Figure 1.7 | TGM4 Induces CD4 T-Cell Activation and Expansion *In Vitro*. A, Differential expression of functional markers on expanded populations of CD4 T cells following co-culture with autologous protein-pulsed moDCs. Heatmap

showing unsupervised clusters determined with the FlowSOM algorithm as described in the methods. **B,** Expanded CD4 T cell populations defined by FlowSOM in **A** were projected onto UMAP space as described in the methods. Colors correspond to FlowSOM populations. **C,** Fold change on activated $CD69^+CD27^+CD28^+$ EM CD4 T cells (left) and CM CD4 T cells (right) following the last 12 hrs stimulation in expanded T cells. **D,** Activated $CD69^+CD27^+CD28^+$ cells as a percentage of EM CD4 T cells (left) and CM CD4 T cells (right) following *in vitro* expansion as in **C**. **E,** $PD1^+TIM3^+$ $CD69^+CD27^+CD28^+$ cells as a percentage of EM CD4 T cells (left) and CM CD4 T cells (right) following *in vitro* expansion as in **C**. **F,** Gating strategy used to manually analyze $TBET^+$ in activated $CD69^+CD28^+$ effector memory (EM) CD4 T cells defined as $CCR7^-CD45RA^-$ following co-culture with autologous protein-pulsed moDCs. **G,** Representative histograms of expression levels of functional transcription factors determined by flow cytometry in expanded EM and naïve CD4 T cells. **H,** $TBET^+$ cells as a percentage of activated $CD69^+CD28^+$ EM CD4 T cell in expanded T cells gated as in **F**. Unpaired t-tests performed, *p*-values ≤ 0.05 (*) and 0.01 (**); not statistical significance is represented as ns.

1.2.6 Prostate Cancer Patients Develop A Humoral Response to TGM4 After GVAX Treatment

Given the induced CD4 T-cell responses to TGM4 observed *in vitro* (Figure 1.7), we hypothesized that PCa patients might leverage CD4 T cell help to mount an IgG antibody response against this prostate-restricted TAA. To address this question we analyzed pre- and post-treatment sera from patients with localized prostate tumors treated with either ADT (n = 14) or ADT plus a cell-based PCa vaccine (GVAX+ADT; n = 13) in the neo-adjuvant setting[282] (Figure 1.8A). To profile antibody responses, we used Phage-ImmunoPrecipitation Sequencing (PhIP-Seq),[27] focusing on IgG antibody responses. For these assays, serum samples pre- and post-treatment were used to immunoprecipitate a T7 phage-displayed library expressing overlapping 90-aa peptides covering 29,371 human open reading frames (Fig. 1.8B).[299,300] Fewer than 8% of vaccinated patients

developed antibody responses to PSA or PSMA and antibodies against PAP were not detected in any patient studied (Fig. 1.8C-D). By contrast, approximately 30% of vaccinated patients developed an antibody response to TGM4. Further, antibody responses to TGM4 and other androgen-responsive TAAs correlated with PSA recurrence in this dataset (Fig. 1.8E-F). These results suggest that vaccine-induced responses to androgen-responsive TAAs may have clinical relevance in PCa patients.

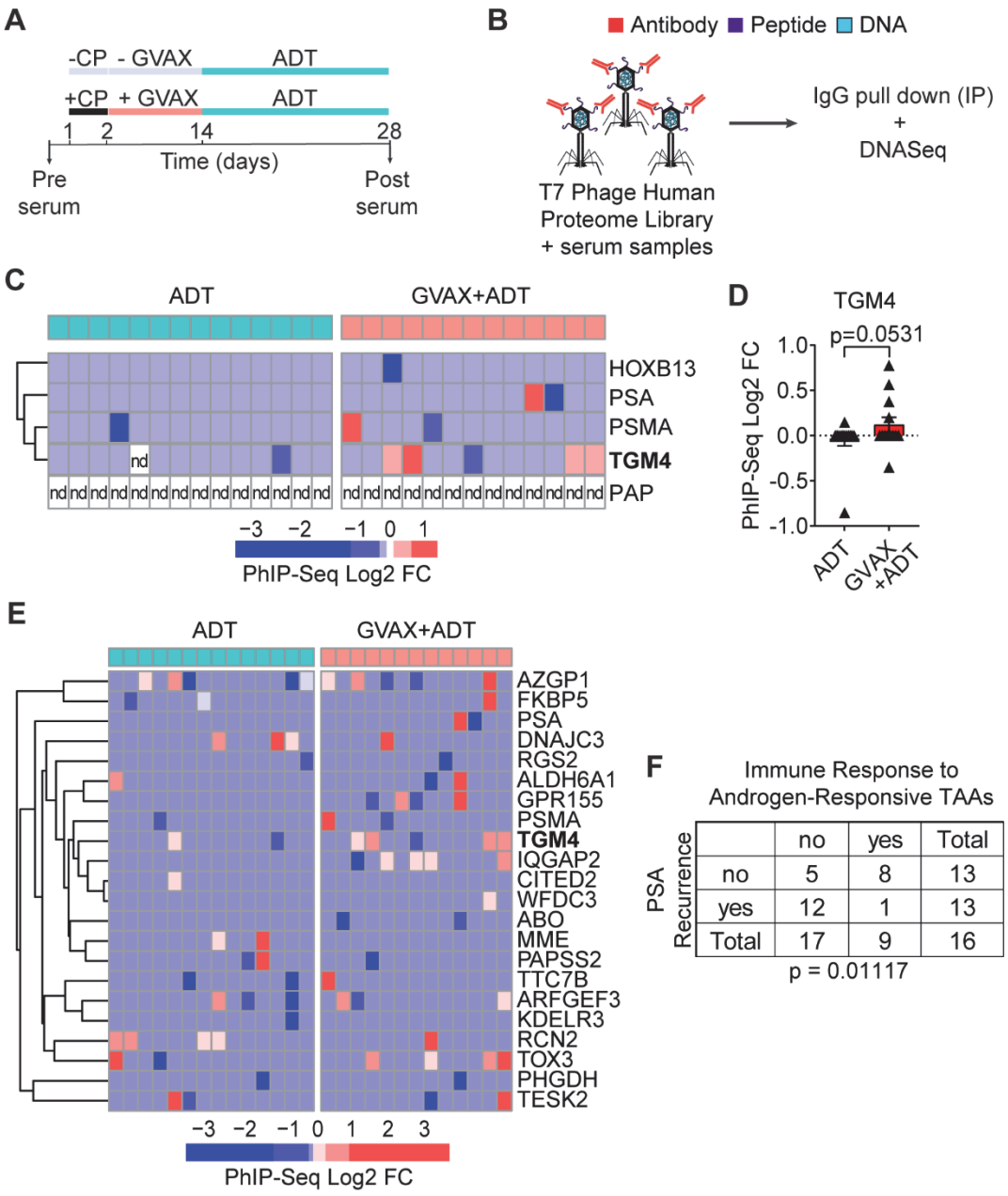

Figure 1.8 | GVAX Vaccination Induces Antibody Responses Against TGM4 In Prostate Cancer Patients. **A,** Schematic representation of the treatment paradigm of patients with prostate adenocarcinoma treated with ADT alone or cyclophosphamide (CP) followed by GVAX and ADT in a neo-adjuvant trial (NCT01696877). **B,** Schematic diagram of the Phage-ImmunoPrecipitation Sequencing (PhIP-Seq) assay. **C,** Heatmap of antibody binding to selected prostate-restricted tumor associated antigens (TAAs) determined as described in the methods. **D,** Antibody response to TGM4 across prostate adenocarcinoma patients treated as in **A**; nd stands for not detected. **E,** Heatmap of antibody

binding to androgen-responsive antigens determined as described in Fig. 2. **F,** Table summarizing responses for ADT only and GVAX followed by ADT treatment groups. Fisher's exact test shows significant over-representation of immune response to androgen-responsive TAAs in the set of patients without biochemical recurrence.

1.3 Discussion

The clinical activity of a PCa vaccine based on PAP-loaded autologous moDCs (Sipuleucel-T) highlights the potential of immunotherapy to enhance *de novo* anti-tumor immune responses to prostate-restricted TAAs. Despite the clinical utility of PAP as an immunological target, responses to this prostate-restricted TAA are heterogeneous.[241,301-304] Other prostate-restricted TAAs such as PSA, PSCA, and PSMA have also shown intriguing results in pre-clinical studies and are currently under investigation in clinical trials (NCT03089203, NCT04053062, NCT03873805, and NCT02744287).[234,305-307] However, the identification of novel prostate-restricted immunological targets remains an unmet need. Here we show that the putative cell-of-origin for PCa,[308] a subpopulation of epithelial cells surrounding the ductal lumen that survive after androgen deprivation - known as Castration-Resistant Luminal Epithelial Cells (CRLECs), express high levels of prostate specific TGM4 in an androgen dependent manner. Our findings are in agreement with a recent study that histologically located TGM4 at the protein level to luminal cells in the anterior and dorsal lobes of murine prostates,[309] as well as with previous *in vitro* studies suggesting *TGM4* may be responsive to androgens in a human PCa cell line.[287,310] Although *Tgm4* is expressed in benign prostate tissue, the non-vital nature of the prostate gland makes it a feasible target for immunotherapy in patients with recurrent disease after primary therapy with

radiation or surgery. In addition, we found that *Tgm4* expression is increased in prostate tumors originating from luminal epithelial cells. Furthermore, the relatively low levels of TGM4 expression observed in brain, colon, liver, lung, skin, kidney, and salivary gland tissues suggest that targeting TGM4 might be associated with fewer off-target immune-related adverse events (irAEs) than other potential TAA's.

Of note, there has been some controversy regarding TGM4 expression in prostate tumor lesions as compared to benign prostate tissue, with some studies reporting TGM4 expression in tumor lesions to be lower[311-313] or higher[296] than in benign prostate tissue. At the message level, *TGM4* expression has been reported to be reduced in prostate adenocarcinoma and metastatic PCa tissue compared to the benign tissue by qPCR[311] and northern hybridization;[312] however, further studies demonstrated that only one of four *TGM4* splice variants (4-L) is lost in PCa samples.[314] At the protein level, two independent immunohistochemistry analyses of prostate tissue microarray slides revealed that TGM4 expression was higher in benign prostatic tissue when a polyclonal antibody was used,[313] but higher in prostate adenocarcinomas when evaluated with a monoclonal antibody.[296] Thus, potential discrepancies could possibly be explained by the reagents used in each study. In line with a potential role for TGM4 in disease progression,[315,316] our results suggest that TGM4 expression is associated with decreased time to recurrence.

To understand whether TGM4 expression was able to induce an antigen-driven immune response, we evaluated the immunogenicity of TGM4 and several additional prostate-restricted TAAs in functional assays with pulsed moDCs

presenting one of the three human proteins (TGM4, PAP, or PSA) to autologous naïve T cells from healthy male donors. Using these tools, we found that pro-inflammatory activated TBET^{+} EM CD8 and CD4 T cells were expanded by TGM4-pulsed moDCs to a greater extent than PAP-pulsed and PSA-pulsed moDCs in healthy male donors. These studies were notable in that they support the notion that a TGM4 targeted vaccine could potentially induce T cell immunity.

We also found that an IgG antibody response to TGM4 was detected in a fraction of PCa patients treated with GVAX in a neoadjuvant trial. Those data further support the potential for antigen-driven CD4 T cell responses to TGM4, since CD4 T help is required for antibody class switching to IgG. This finding is in line with the modest improvement in time-to-PSA progression observed in this trial,[317] an improvement which was not associated with an increase in tumor-infiltrating CD8 T cells. Further supporting the immunogenicity of TGM4, work from others showed that autoantibodies were found in 100% of *Aire*-deficient and 22% of non-obese diabetic male mice that spontaneously developed prostatitis, but not in females.[318] Interestingly, several other members of the transglutaminase family have also been identified as immune targets in inflammatory and autoimmune disorders.[319-321] *Aire*-deficient mice with antibodies targeting TGM4 lack production of TGM4, suggesting that TGM4-expressing cells may be destroyed by an autoimmune reaction.[318] Further, the development of antibodies targeting TGM4 was only observed post-puberty[318] which parallels the androgen-responsive regulation we observed and implies peripheral antigen recognition in the absence of central tolerance.

In summary, these studies support further evaluation of TGM4 as a prostate-restricted TAA. Given the immunosuppressive nature of the tumor microenvironment in PCa,[198,322-325] it is likely that vaccine induced responses against TGM4 may not be sufficient alone for an effective anti-tumor response. Instead, targeted vaccines may need to be administrated in combination with other therapies targeting the recruitment and accumulation of regulatory T cells and / or myeloid-derived suppressive cells. Future studies evaluating TGM4 as a putative target antigen in mCPRC are required to explore these issues.

Chapter II – Robust Antigen-Specific CD8 T Cell Tolerance to a Model Prostate Cancer Neoantigen

"Effector cells in the innate or adaptive systems should become tolerant to continuously expressed motifs, or even gradually increasing ones."

Dr. Paul Ehrlich (1909) – a pioneer of the concept of cancer immunosurveillance and one of the main founders of chemotherapy.

Nobel Prize in Physiology or Medicine (1908).

2.1 Introduction

As discussed above, antigens expressed only in the tumor, neoantigens, are by definition not susceptible to central tolerance. However, multiple peripheral tolerance mechanisms attenuate or otherwise prevent responses to antigens presented in a non-inflammatory context. Immunotherapy must overcome these peripheral tolerance mechanisms in order to mount an effective adaptive anti-tumor immune response.[274,326-329] Several studies have shown T cell tolerance in mice with prostate-specific expression of a model or viral antigen.[327,330-333] For example, using a model in which influenza hemagglutinin is over-expressed in the prostate gland and in autochthonous prostate tumors of transgenic

adenocarcinoma of mouse prostate (TRAMP) mice, we showed CD4 T cell tolerance that could be transiently mitigated by androgen-deprivation therapy (ADT).[327] Peripheral tolerance to this continuously expressed antigen was further supported by studies in double transgenic mice in which cytolytic activity of hemagglutinin-specific CD8 T cells was restored after adoptively transferring hemagglutinin-specific CD8 T cells from TRAMP tumor-bearing hosts into tumor-free hosts.[330] Additional models support T cell tolerance to prostate-restricted expression of ovalbumin in prostate gland of probasin ovalbumin expressing transgenic (POET-1) mice[331] and influenza virus in autochronous prostate tumors of TRAMP mice.[332] In each of these models, antigens were expressed using the androgen-driven rat probasin promoter where antigen levels can be abrogated through androgen deprivation. Thus, it is not known whether similar tolerance mechanisms exist to an antigen whose expression is independent of androgen signaling.

To understand peripheral tolerance to a bona-fide cancer antigen and to investigate whether immunotherapy interventions can break CD8 peripheral tolerance, we developed a murine PCa cell line (Myc-CaP/Neu) that expresses the rat Her-2/neu protein which is immunogenic in a breast cancer model.[334,335] In addition, rat Her-2/neu specific CD8 T cells from TCR transgenic mice are available, and these facilitate antigen-specific interrogation of T cell tolerance.[336] Using these tools, we found that the rat Her-2/neu protein was successfully processed and the immunodominant peptide ($RNEU_{420-429}$) was presented to

transgenic CD8 T cells. We further investigated whether peripheral tolerance was induced, and whether tolerance could be mitigated by TLR-agonists or ADT.

2.2 Results

2.2.1 Generation of Neu Expressing Myc-CaP Cells

To study antigen-specific CD8 T cell responses to androgen-deprivation therapy (ADT) sensitive PCa, we introduced a model tumor antigen for which an antigen-specific T cell expressing a transgenic TCR has been generated.[336] The model was based on the Myc-CaP cell line,[337] which was derived from a transgenic PCa model driven by prostate-specific overexpression of the *MYC* oncogene[338] – a gene commonly up-regulated in invasive PCa patients.[339] Myc-CaP cells originate from the immunocompetent FVB/N strain. To model a bona-fide cancer antigen, Myc-CaP cells were transduced with a lentivirus encoding the rat Her-2/neu (pWPXL-Neu; Fig. 2.1A-B). This construct included the immunodominant epitope previously shown to bind to the class I MHC molecule H-2D^{q}.[340] Transduced tumor cells were sorted to > 99% purity (Fig. 2.1C) and rat Her-2/neu (RNEU) expression was confirmed by immunofluorescence (Fig. 2.1D).

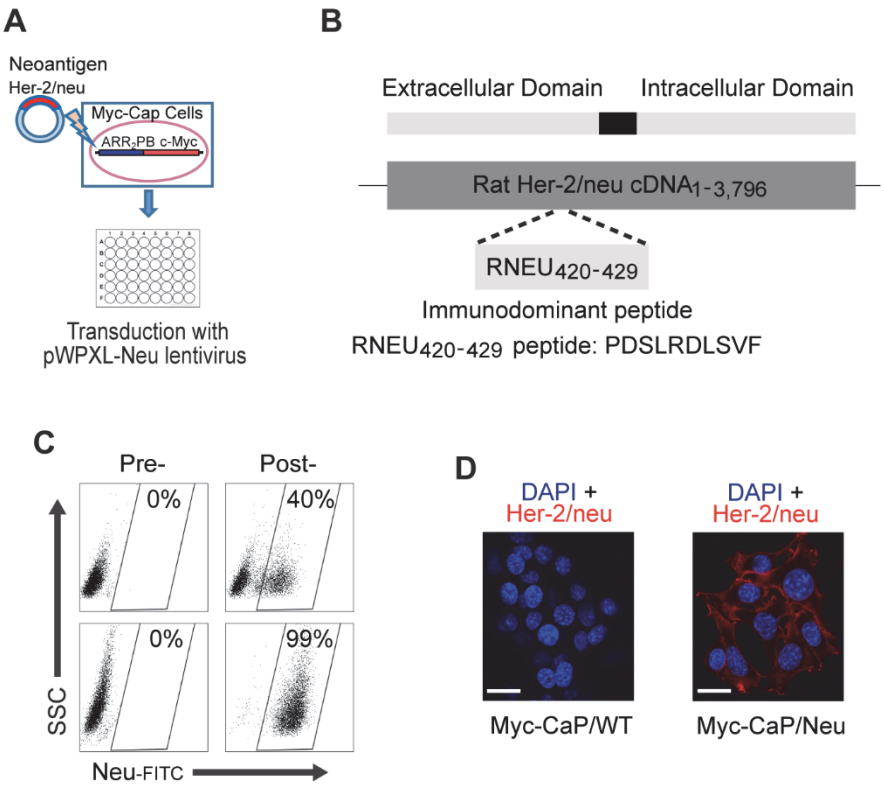

Figure 2.1 | Generation of the Myc-CaP/Neu Cell Line. **A,** Schematic for the transduction of the Her-2/neu neoantigen into the androgen responsive Myc-CaP cell line. **B,** The extracellular rat Her-2/neu (neu) cDNA fragment containing the immunodominant MHC-I epitope recognized by the FVB/N-derived T cell clone TCRVβ4 ($RNEU_{420-429}$ peptide: PDSLRDLSVF)[340] was ligated into the vector pWPXL. **C,** Sorting strategy to isolate Myc-CaP cells based on their expression of the rat neu antigen. Myc-CaP cells pre- and post- transduction with lentivirus containing $RNEU_{420-429}$ peptide (top,) and pre- and post- sorting for neu expressing cells (Myc-CaP/Neu; bottom). **D,** Fluorescent detection of Her-2/neu in formalin-fixed WT Myc-CaP and Myc-CaP/Neu tumor cells grown on poly-D-Lysine coated coverslips. Expression of the antigen on tumor cells was evaluated with CF640-labeled αHer-2/neu antibody (red); nuclei were counterstained with DAPI (blue). Scale bar = 100 μm.

2.2.2 RNEU-specific Cytotoxic CD8 T Cell Responses to Myc-CaP/Neu Tumor Cells

Granulocyte-macrophage colony-stimulating factor (GM-CSF) stimulates the recruitment of dendritic cells and augments tumor antigen presentation.[334,341] Thus, GM-CSF has been used as a component of therapeutic cancer vaccines to stimulate anti-tumor immunity in pre-clinical models[342] as well as in multiple clinical trials.[343,344] To determine whether CD8 T cells recognize $RNEU_{420-429}$ in Myc-CaP/Neu cells, we performed vaccination studies using a vaccine (GVAX) comprised of irradiated Myc-CaP/Neu cells co-administered with GM-CSF secreting bystanders. As a readout for Her-2/neu expression, CFSE-labeled RNEU-specific CD8 T cells from $Thy1.2^+$ donor mice were adoptively transferred 24 hours post-vaccination into $Thy1.1^+$ recipient FVB/NJ mice (Fig. 2.2A-B). Five days post-transfer, RNEU-specific CD8 T cells recovered from the inguinal lymph nodes (ILNs) and spleens of vaccinated recipient mice had undergone significant division (Fig. 2.2C). In contrast, RNEU-specific CD8 T cells recovered from ILNs and spleens of naïve recipients had not undergone significant division (Fig. 2.2C); these data support antigen expression and subsequent recognition. Intracellular staining for canonical effector cytokines (TNFα, IFNγ, GzB, and IL-2) confirmed T cell activation (Fig. 2.2D-E).

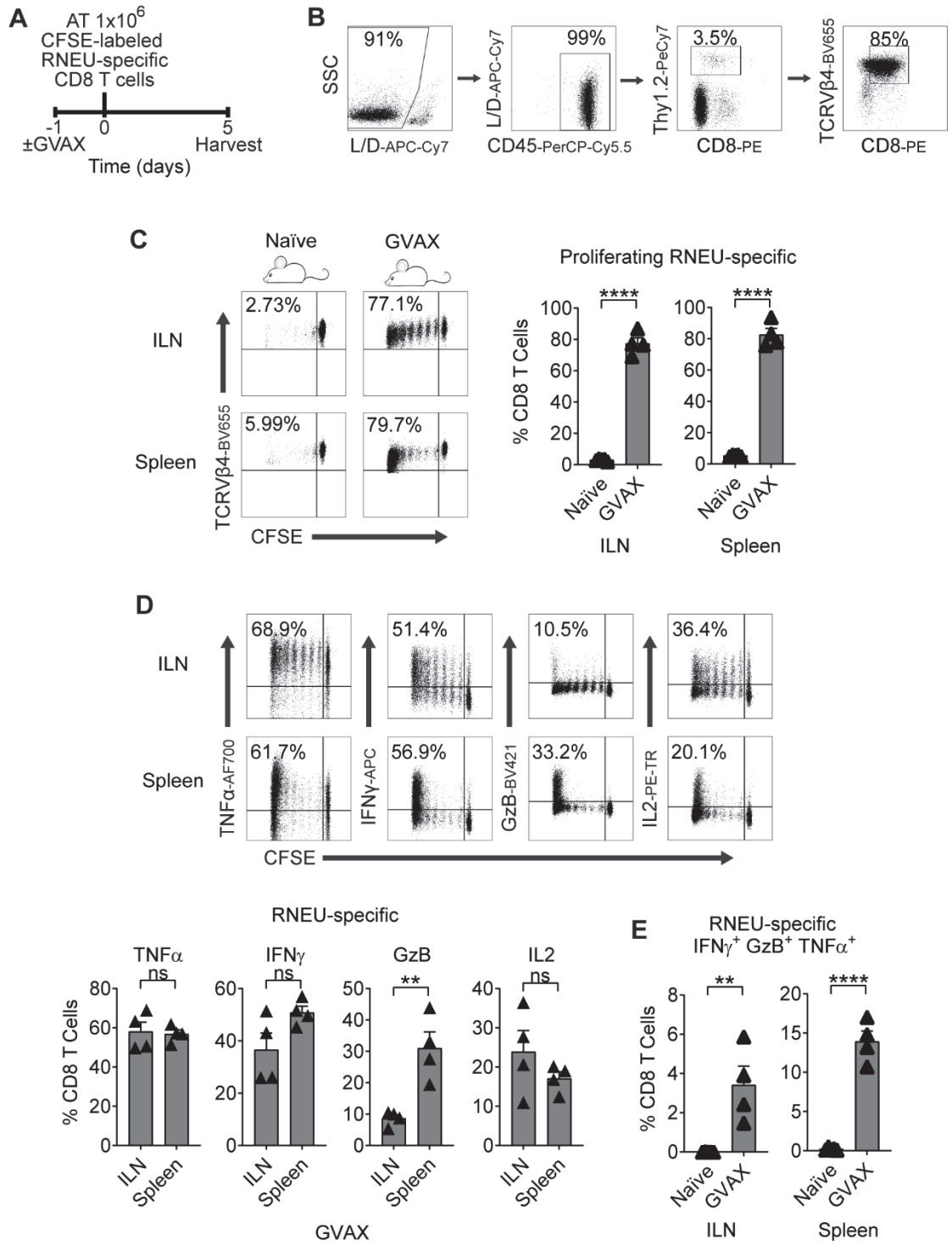

Figure 2.2 | GVAX Vaccination Induces a Systemic Cytotoxic CD8 T Cell Response to Rat-Neu Neoantigen. A, Treatment scheme for the neu-expressing (GM-CSF–secreting) vaccination (GVAX) group. One day after the vaccination, $1x10^6$ high-avidity CFSE-labeled Thy1.2$^+$ RNEU$_{420–429}$-specific CD8 T cells were

adoptively transferred (AT) into mice. On day 5, inguinal LNs (ILN) and spleens were harvested and analyzed by flow cytometry. **B,** Gating strategy to profile RNEU-specific CD8 T cells by flow cytometry. FVB/N-derived T cell clone TCRVβ4 were gated based on $CD45^+CD8^+Thy1.2^+$. **C,** Percentages of proliferating $TCRV\beta4^+$ CD8 T cells in indicated tissues (representative flow plots and quantification; n ≥ 4 per group, repeated x 2). **D,** Percentages of cytokine production by RNEU-specific $TCRV\beta4^+$ CD8 T cells (representative flow plots and quantification; n ≥ 4 per group, repeated x 2). **E,** Percentages of polyfunctional RNEU-specific $TCRV\beta4^+$ $IFN\gamma^+GzB^+TNF\alpha^+$ CD8 T cells in indicated tissues (n ≥ 4 per group, repeated x 2). Proliferating $TCRV\beta4^+$ CD8 T cells, and their cytokine production, were calculated as fraction of $TCRV\beta4^+$ CD8 T cells.

We next tested whether adoptively transferred Her-2/neu specific CD8 T cells could recognize well-established Her-2/neu-expressing tumors (Fig. 2.3A-C). As shown in Figure 2.3, implanted Myc-CaP/Neu tumors induced proliferation of adoptively transferred RNEU-specific CD8 T cells in tumor-draining lymph nodes (TDLNs) and spleens, while Myc-CaP/WT tumors did not (Fig. 2.3D). To evaluate the functional capacity of RNEU-specific CD8 T cells recovered from TDLNs and spleens, we performed intracellular staining for TNFα, IFNγ, GzB, and IL-2. In line with our previous observations (Fig. 2.2D), a fraction of RNEU-specific CD8 T cells isolated from Myc-CaP/Neu tumor-bearing recipients expressed these cytotoxic effector cytokines (Fig. 2.3E).

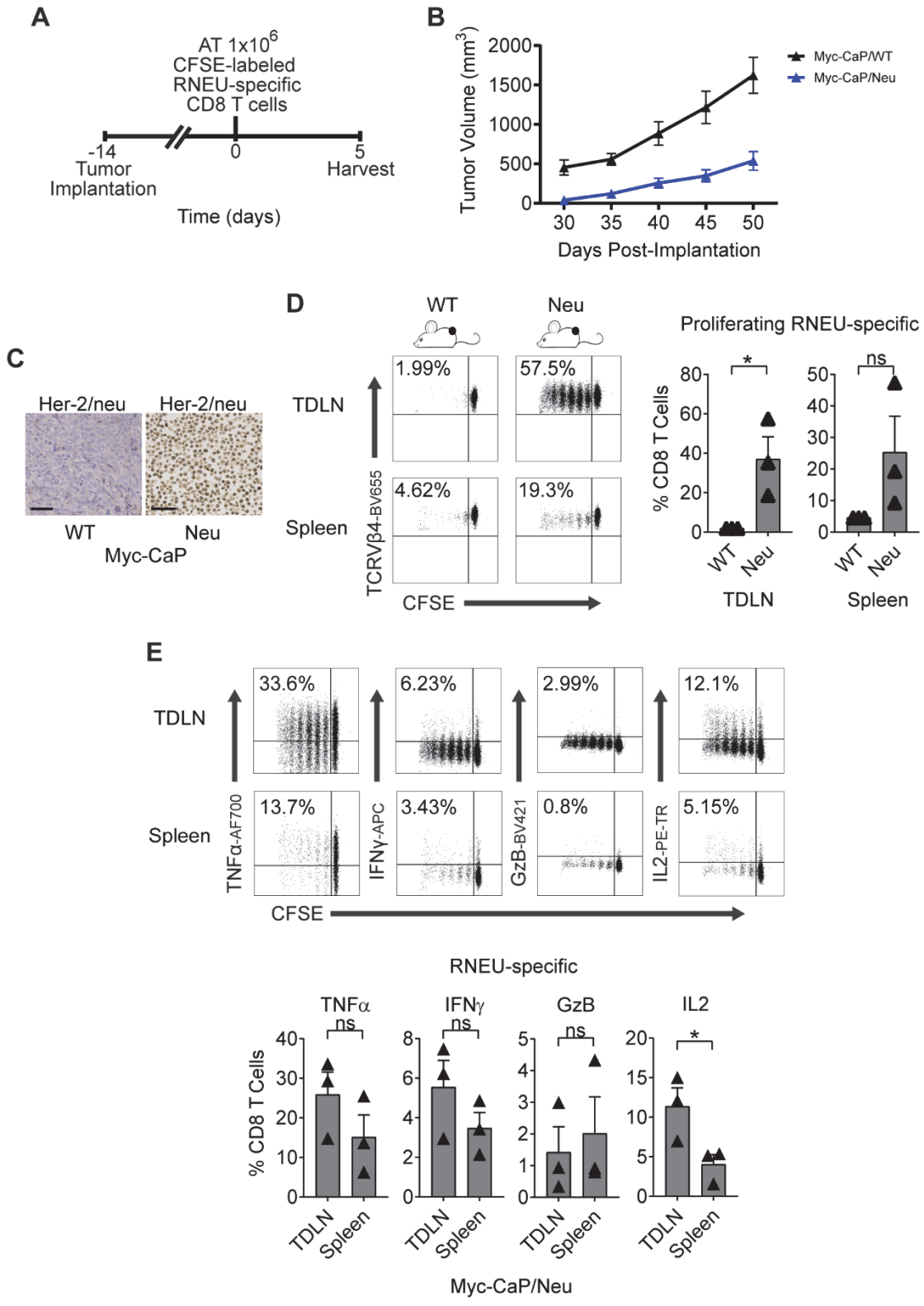

Figure 2.3 | Established Myc-CaP Tumors Maintain Her-2/neu Expression and Induce a Systemic Cytotoxic CD8 T Cell Response to Rat-Neu Neoantigen.

A, Treatment scheme for tumor implantation with either $1x10^6$ Myc-CaP/WT or Myc-CaP/Neu cells. Fourteen days after tumor implantation, $1x10^6$ high-avidity CFSE-labeled Thy1.2$^+$ $RNEU_{420–429}$-specific CD8 T cells were adoptively transferred (AT) into the mice. On day 5, tumor-draining lymph nodes (TDLNs) were harvested and analyzed by flow cytometry. **B,** Tumor growth curves of mice from Myc-CaP/WT and Myc-CaP/Neu tumor bearing mice. Average tumor volume (±s.e.m.) for each experimental group. **C,** Her-2/neu expression on indicated murine allografts (representative immunohistochemistry; repeated x 2). Scale bar = 50 μm. **D,** Percentages of proliferating TCRVβ4$^+$ CD8 T cells in indicated tissues (representative flow plots and quantification; n ≥ 3 per group, repeated x 2). **E,** Percentages of cytokine production by RNEU-specific TCRVβ4$^+$ CD8 T cells in indicated tissues (representative flow plots and quantification; n ≥ 3 per group, repeated x 2). Proliferating TCRVβ4$^+$ CD8 T cells, and their cytokine production, were calculated as fraction of TCRVβ4$^+$ CD8 T cells.

2.2.3 Established Tumors Suppress Antigen-Specific CD8 T Responses Induced by Vaccination

We next tested whether vaccination with Myc-CaP/Neu cells + GM-CSF producing bystander (GVAX) would affect tumor antigen-specific CD8 T cell responses in the setting of a suppressive TME (Fig. 2.4A-C). Here we found that RNEU-specific CD8 T cells recovered from vaccinated Myc-CaP/Neu tumor-bearing recipients divided less and exhibited a lower percentage of TNFα, IFNγ, and IL2 cytokine producing RNEU-derived CD8 T cells than those harvested from vaccinated, non-tumor bearing (naïve) recipients (Fig. 2.4D-E). These data suggest that recognition of the Her-2/neu peptide ($RNEU_{420-429}$: PDSLRDLSVF) is tolerogenic in the context of a suppressive TME, and that vaccination may not be sufficient to mitigate this tolerance.

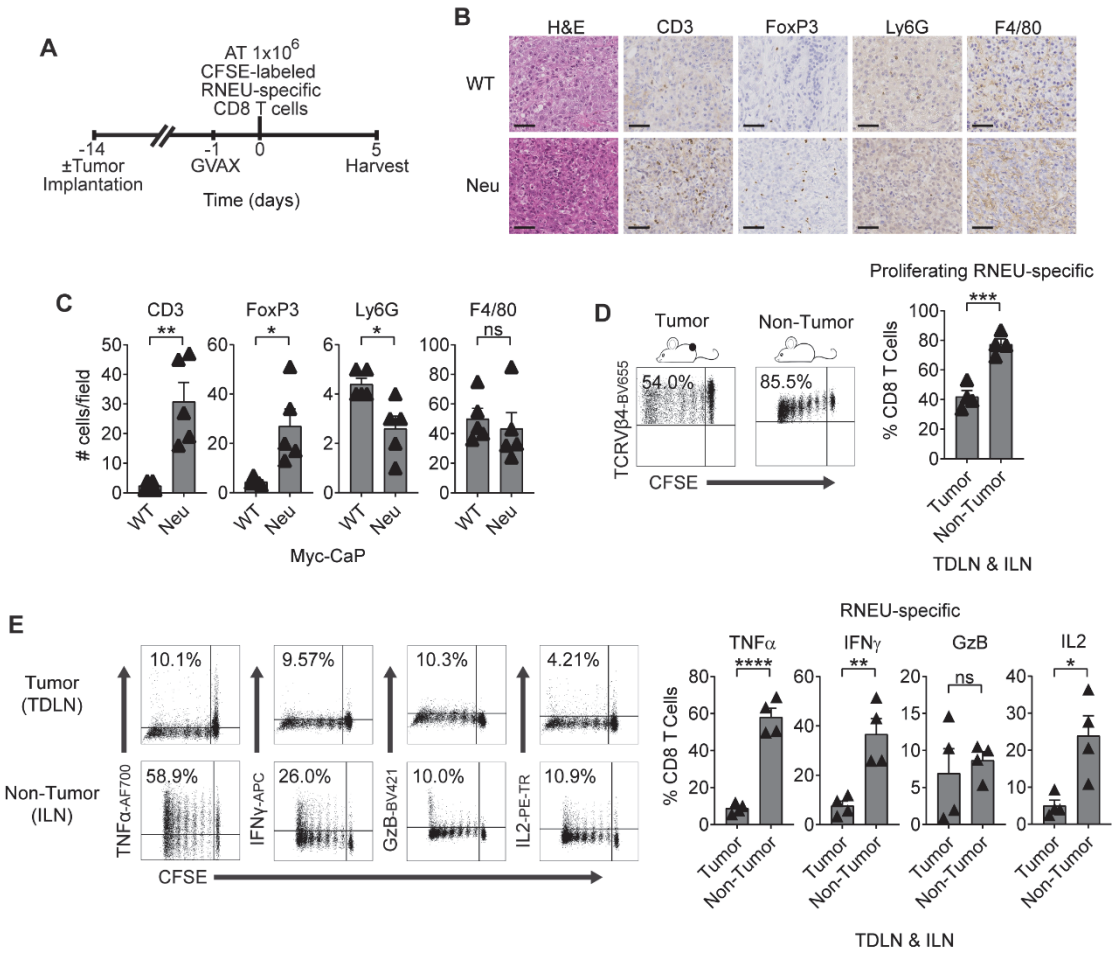

Figure 2.4 | Myc-CaP/Neu Tumors Attenuate The RNEU-specific CD8 T Cell Response Induced by Vaccination with Her-2/neu Expressing Cells. A, Treatment scheme for tumor implantation with $1x10^6$ Myc-CaP/Neu cells. One day after the neu-expressing (GM-CSF–secreting) vaccine (GVAX) was administrated, $1x10^6$ high-avidity CFSE-labeled Thy1.2$^+$ $RNEU_{420–429}$-specific CD8 T cells were adoptively transferred (AT) into the mice. On day 5, tumor-draining lymph nodes (TDLNs; tumor) and inguinal LNs (ILNs; non-tumor) were harvested and analyzed by flow cytometry. **B,** Tumor infiltrating lymphocytes (TIL; CD3), regulatory T cells (FoxP3), myeloid-derived suppressor cells (Ly6G), and Mϕ (F4/80) of indicated murine allografts (representative immunohistochemistry; repeated x 2). Scale bar = 50 µm. **C,** Counts of immune cells in tumor microenvironment (TME). **D,** Percentages of proliferating TCRVβ4$^+$ CD8 T cells in TDLNs and ILNs (representative flow plots and quantification; n ≥ 4 per group, repeated x 2). **E,** Percentages of cytokine production by RNEU-specific TCRVβ4$^+$ CD8 T cells in TDLNs and ILNs (representative flow plots and quantification; n ≥ 4 per group, repeated x 2). Proliferating TCRVβ4$^+$ CD8 T cells, and their cytokine production, were calculated as fraction of TCRVβ4$^+$ CD8 T cells. ILNs and TDLNs were

isolated from naïve and tumor bearing mice respectively. Whole-cell vaccination (GVAX) was prepared as described in materials and methods.

2.2.4 TLR Agonists Do Not Mitigate Antigen-Specific CD8 T Cell Tolerance to a Tumor Antigen

The TLR3 agonist Poly I:C is a synthetic polyinosinic-polycytidylic double-stranded RNA widely used as a vaccine adjuvant due to its ability to induce DC maturation and T_H1 polarization.[345,346] Thus, we tested whether Poly I:C would affect the induction of tolerance in dividing RNEU-specific CD8 T cells isolated from Myc-CaP/Neu tumor-bearing recipient mice (Fig. 2.5A). We found that IP treatment with Poly I:C 24 hours prior to the adoptive transfer of RNEU-specific CD8 T cells did not mitigate the induction of peripheral tolerance in TDLNs of Myc-CaP/Neu tumor-bearing recipient mice (Fig. 2.5B-D). As a positive control, we tested whether IP Poly I:C treatment was able to induce a cytotoxic effector response in RNEU-specific T cells harvested from the ILN of naïve recipients; indeed this was the case (Fig. 2.6). So, while Her-2 specific T cells may achieve cytolytic potential with Poly I:C, recognition of peripherally expressed tumor antigen in the context of the TME renders them tolerant.

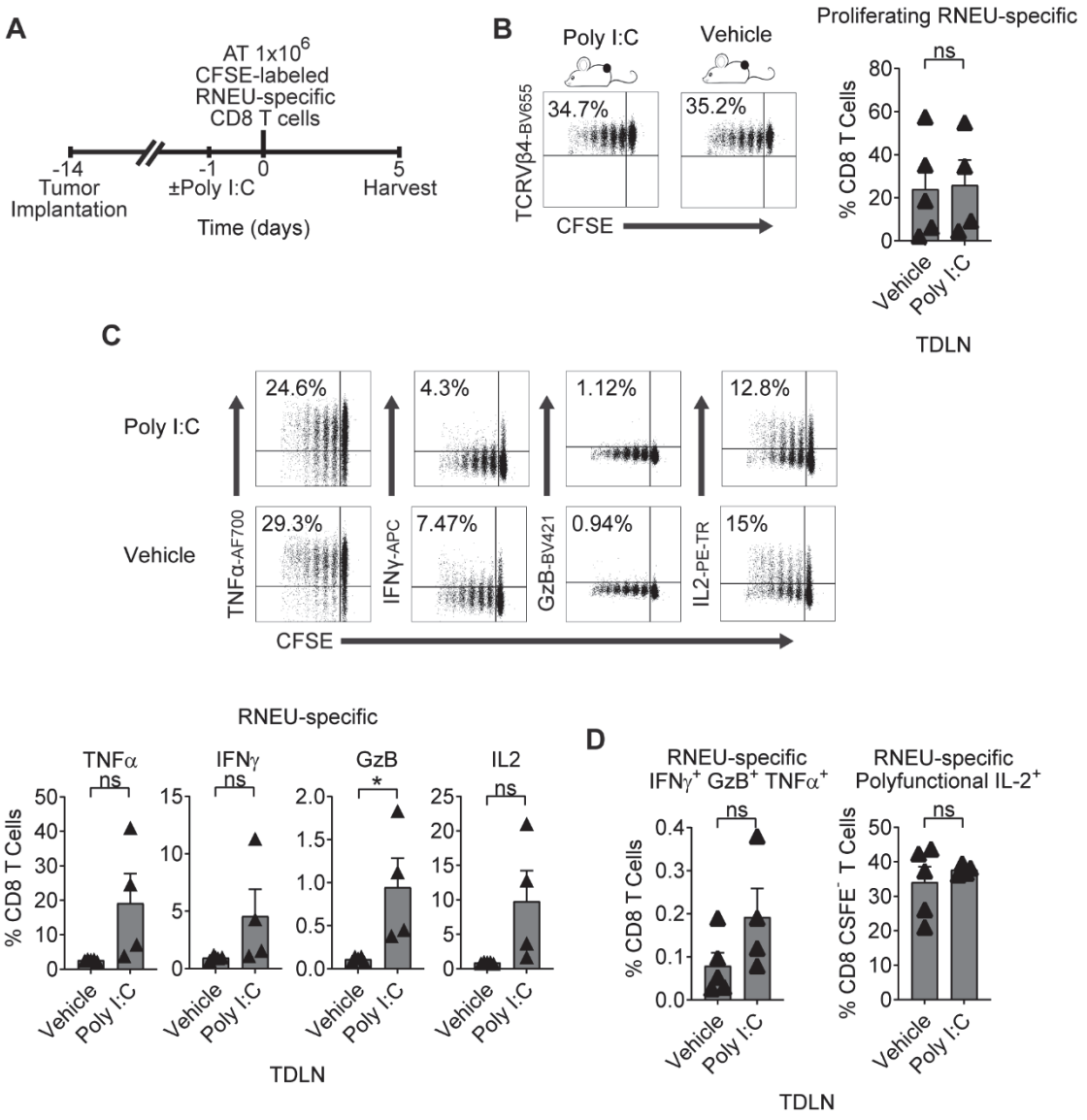

Figure 2.5 | Tumor-Induced RNEU-specific CD8 T Cell Tolerance is Maintained After Stimulation with a TLR3 Agonist. A, Treatment scheme for tumor implantation with 1x10^6 Myc-CaP/Neu cells. One day after Poly I:C IP administration, 1x10^6 high-avidity CFSE-labeled Thy1.2$^+$ RNEU$_{420–429}$-specific CD8 T cells were adoptively transferred (AT) into the mice. On day 5, tumor-draining lymph nodes (TDLNs) were harvested and analyzed by flow cytometry. **B,** Percentages of proliferating TCRVβ4$^+$ CD8 T cells in TDLNs (representative flow plots and quantification; n ≥ 4 per group, repeated x 2). **C,** Percentages of cytokine production by RNEU-specific TCRVβ4$^+$ CD8 T cells (representative flow plots and quantification; n ≥ 4 per group, repeated x 2). **D,** Percentages of polyfunctional TCRVβ4$^+$ CD8$^+$ IFNγ$^+$GzB$^+$TNFα$^+$ in TDLNs (n ≥ 4 per group,

repeated x 2). Proliferating TCRVβ4⁺ CD8 T cells, and their cytokine production, were calculated as fraction of TCRVβ4⁺ CD8 T cells.

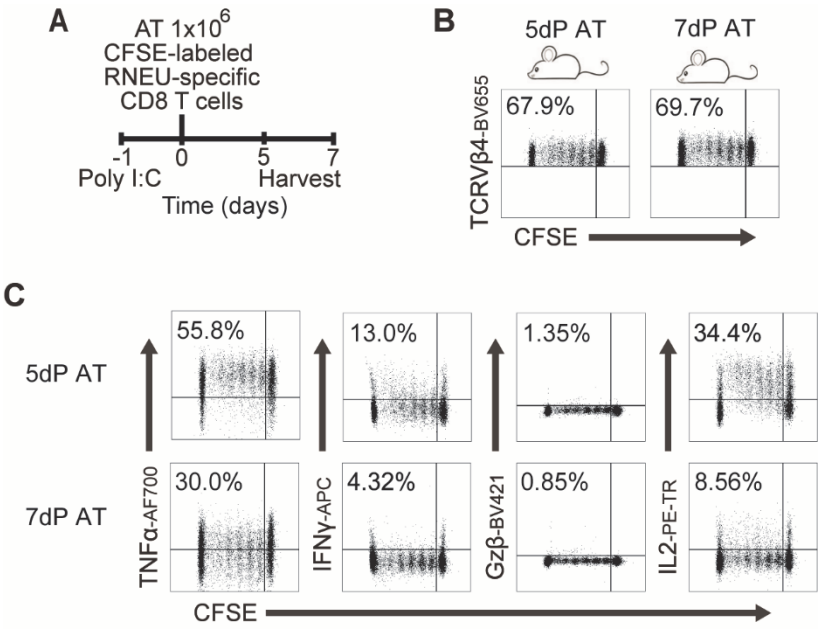

Figure 2.6 | TLR3 Agonist Induces a Systemic Cytotoxic CD8 T Cell Response to Rat-Neu Neoantigen. A) Treatment scheme for stimulation with TLR3 agonist. One day after Poly I:C IP administration, 1x10^6 high-avidity CFSE-labeled Thy1.2$^+$ RNEU$_{420–429}$-specific CD8 T cells were adoptively transferred (AT) into the mice. On day 5 and 7, inguinal LNs (ILN) were harvested and analyzed by flow cytometry. **B,** Percentages of proliferating TCRVβ4⁺ CD8 T cells in ILNs (unique flow plots; n = 1 per group). **C,** Percentages of proliferating TCRVβ4⁺ CD8 T cells in ILNs (unique flow plots; n = 1 per group).

2.2.4 Androgen-Deprivation Therapy (ADT) Does Not Mitigate Antigen-Specific CD8 T Cell Tolerance to a Tumor Antigen

Our prior work showed that ADT transiently mitigates CD4 T cell tolerance to a model antigen expressed under the androgen-regulated probasin promoter. To test whether a similar effect occurred, in the context of a tumor antigen whose expression is not driven by an androgen-regulated promoter, we implanted Myc-CaP/Neu tumors in WT recipients and then treated them with ADT prior to adoptive transfer of CFSE-labeled RNEU-specific CD8 T cells (Fig. 2.7A). Consistent with

prior data,[55] over time, ADT increased the infiltration of immune cells with the potential to suppress CD8 T cell responses – T_{regs}, PMN-MDSCs, and Mϕ (Fig. 2.7B-C). ADT (7 or 24 days) prior to adoptive transfer did not significantly increase the percentage of dividing RNEU-specific CD8 T cells relative to intact (vehicle; non-castrated) recipients (Fig. 2.7D), and did not increase cytokine secretion by RNEU-specific CD8 CTLs (Fig. 2.7E). These data support the robustness of CD8 T cell tolerance to this prostate-tumor restricted antigen and suggest that prior results using influenza hemagglutinin driven by the androgen-responsive probasin promoter as a model antigen may reflect mitigation of tolerance by transient antigen loss.[12]

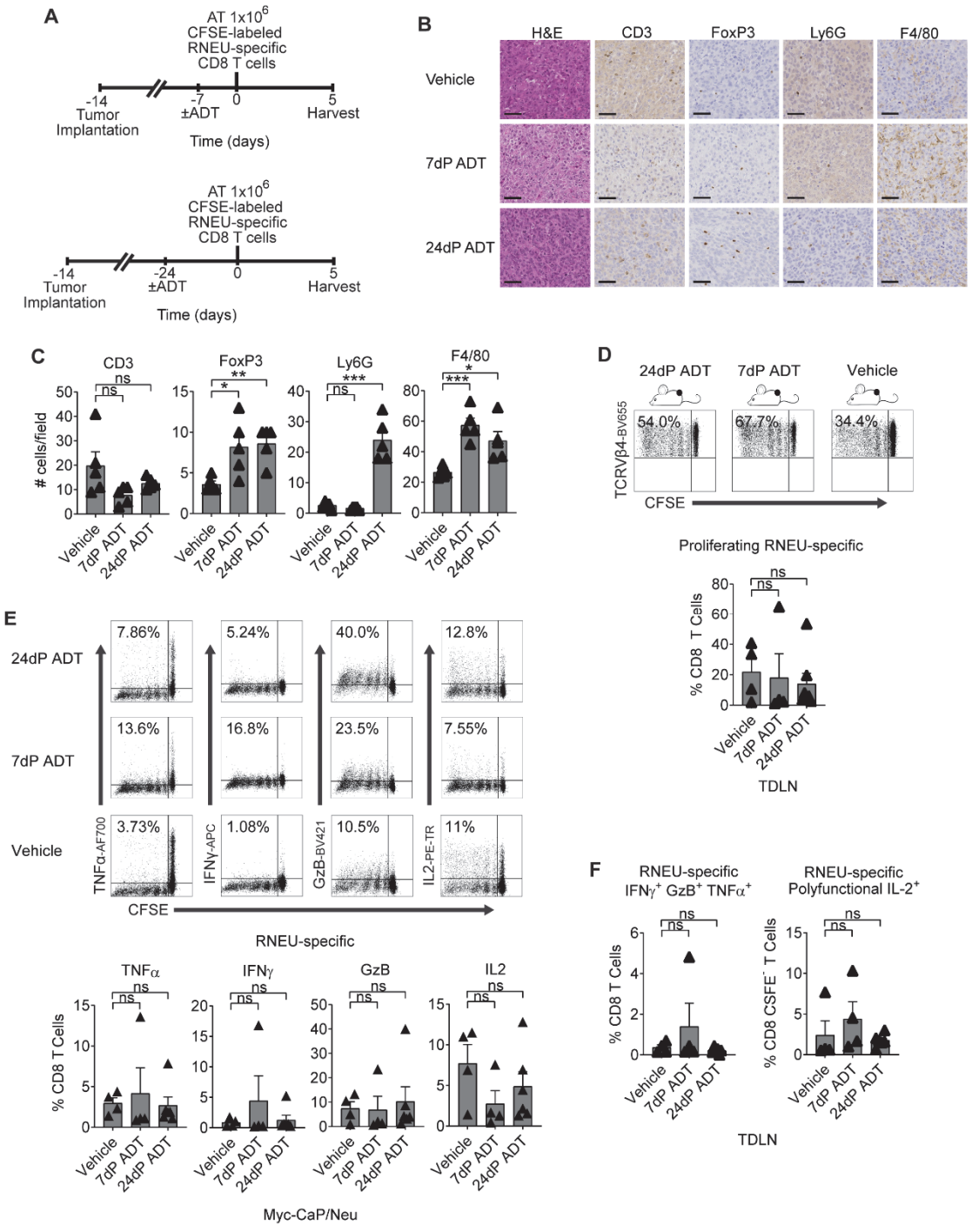

Figure 2.7 | Androgen-Deprivation Therapy (ADT) Does Not Significantly Attenuate Tumor-Induced RNEU-specific CD8 T Cell Tolerance. A, Treatment scheme for tumor implantation with $1x10^6$ Myc-CaP/Neu cells. Seven or twenty-four days after androgen-deprivation (ADT) was administrated, $1x10^6$ high-avidity CFSE-labeled Thy1.2$^+$ RNEU$_{420–429}$-specific CD8 T cells were adoptively transferred (AT) into the mice. On day 5, tumor-draining lymph nodes (TDLNs)

were harvested and analyzed by flow cytometry. **B,** Tumor infiltrating lymphocytes (TIL; CD3), regulatory T cells (FoxP3), myeloid-derived suppressor cells (Ly6G), and Mϕ (F4/80) of indicated murine allografts (representative immunohistochemistry; repeated x 2). Scale bar = 50 μm. **C,** Counts of immune cells in tumor microenvironment (TME). **D,** Percentages of proliferating TCRVβ4$^+$ CD8 T cells in TDLNs (representative flow plots and quantification; n ≥ 4 per group, repeated x 2). **E,** Percentages of cytokine production by RNEU-specific TCRVβ4$^+$ CD8 T cells (representative flow plots; repeated x 2). **F,** Percentages of polyfunctional TCRVβ4$^+$ CD8$^+$ IFNγ$^+$GzB$^+$TNFα$^+$ in TDLNs (n ≥ 4 per group, repeated x 2). Proliferating TCRVβ4$^+$ CD8 T cells, and their cytokine production, were calculated as fraction of TCRVβ4$^+$ CD8 T cells. IL-2 production was evaluated as a fraction of polyfunctional IFNγ$^+$GzB$^+$TNFα$^+$ TCRVβ4$^+$ CD8 T cells.

2.3 Discussion

We previously showed that androgen-derivation therapy (ADT) has an additive effect when combined with immunotherapeutic interventions.[55] However, the lack of models to study antigen-specific CD8 T cell responses to neoantigens expressed in an androgen-independent manner has limited understanding of the cellular and molecular mechanisms involved in antigen-specific immune responses to PCa antigens that are not androgen-regulated. In this study, we developed a model to study antigen-specific CD8 T cell peripheral tolerance in an implantable, androgen-responsive murine cell line in which expression of a bona-fide cancer antigen is uncoupled from androgen receptor signaling. We found that tumor cells expressing Her-2/neu maintain their immunogenicity *in vivo*, and recruit RNEU-specific CD8 T cells. Furthermore, we found this recognition led to a reduction of effector cytokine production in the context of a suppressive TME. This tolerance was robust and was not significantly mitigated by either the TLR-agonist Poly I:C or by ADT. These data are consistent with clinical data showing that use of immunotherapy has generally met with limited clinical success in PCa.[347]

These data are potentially discordant with our prior work using a variant of the TRAMP model that expresses influenza hemagglutinin under the control of the androgen-responsive, prostate-specific minimal rat probasin promoter.[348] There, we found that ADT results in *de novo* presentation of a prostate-restricted antigen in TDLN when castration (ADT) is performed 1 day prior to adoptive transfer of antigen-specific CD4 T cells. In those studies we also showed that CD4 T cell proliferation was diminished when ADT was performed 10 days prior to adoptive transfer.[327] Thus, those results are likely consistent with the notion that persistent expression of tissue antigen is important in the establishment of peripheral tolerance. Consistent with this, studies from another group showed that ADT dramatically decreased probasin-driven expression of ovalbumin in POET-1 mice.[331] Here, in the presence of both antigen and antigen-specific CD8 T cells, we found more profound tolerance – that was not significantly mitigated by ADT. The differences between the prior models and the current one are possibly related to how the T-cell recognized antigen is expressed; in prior studies antigen expression was driven by the androgen-responsive probasin promoter and was thus transiently decreased after ADT. By contrast, here the bona-fide tumor antigen Her-2 was constitutively expressed in an androgen-insensitive manner – with persistent presentation likely driving the more robust tolerance seen in the new model.

Supporting persistent tolerance, we observed continued T_{reg} infiltration even late after ADT (24dP ADT; at onset of castration-resistance), supporting a long-lived tolerogenic mechanism. These data are consistent with our prior studies in

which we used the androgen-responsive murine PCa cell line Myc-CaP, and found that the initial pro-inflammatory infiltrate (apparent in the early post-ADT period) was subsequently followed by an infiltration of T_{regs} into the TME that diminished late after ADT.[55] Indeed, anti-CTLA-4 treatment prior to ADT resulted in T_{reg} depletion and delayed tumor growth in that model,[55] suggesting that tumor infiltrating T_{regs} may be an important mechanism of primary resistance to immunotherapy. These data align with the observation that CD8 T infiltration was accompanied by a proportional influx of T_{regs} in PCa patients upon neoadjuvant ADT treatment.[317] Interestingly, we found that PMN-MDSCs infiltrated tumors as castration-resistance emerges, suggesting their suppressive role may be important in the development of acquired resistance to immunotherapy. In line with this hypothesis, we and others have demonstrated that blocking PMN-MDSC trafficking into the tumor augments responses to immune checkpoint blockade.[349] In addition, the rationale for targeting these cells in combination with other immune therapeutic interventions has also been supported by studies using TRAMP mice,[350,351] and recently reviewed in the literature.[352] Further studies characterizing tumor infiltrating T_{regs} and PMN-MDSCs in the novel model presented here may aid in the development of new therapeutic approaches to overcome immunotherapy resistance in PCa, including metastatic PCa. Although, metastasis has not been observed in *MYC* driven Myc-CaP tumors,[338] a potential limitation of this model, the TME of prostate tumors in bone, the most clinical relevant metastatic niche, can be studied by direct intratibial injection of Myc-

CaP/Neu tumor cells[353] followed by adoptive transfer of CFSE-labeled RNEU-specific CD8 T cells.

In summary, we report a novel cell line / adoptive CD8 T cell transfer model to study antigen-specific T cell tolerance to PCa. Although the interventions explored here were insufficient to significantly break tolerance, this system may serve as a useful tool to further interrogate methods by which to augment antigen-specific CD8 T cell anti-tumor responses.

Chapter III – Tumor Cells Drive an Immunosuppressive Microenvironment

> "Where we're going is this much more individualized approach – just like infectious diseases. If you have a very bad infection – very bad – your doctor will take a sample of the bug, grow it, and pick an antibiotic or two or sometimes three – mix them together and hopefully cure you –and that's what we're trying to do in oncology now."
>
> Dr. George Demetri (2015) – a pioneer in the development of targeted therapy.
>
> Dana-Farber Cancer Institute.

3.1 Introduction

As discussed above,[354] myeloid-derived cells may be of critical importance in cancer progression and may also contribute to the failure of PCa patients to respond to treatment. Recent clinical studies showed that increased macrophage infiltration in the primary tumor at baseline correlates with failure of ADT.[141] In addition, a recent study reported that circulating MDSCs correlate with a failure to respond to cancer vaccines and immune checkpoint blockade.[275] Taken together, these data highlight the potential of targeting myeloid-derived cells or the mechanism(s) that regulate their recruitment to improve the response to immunotherapy in men with PCa. Understanding the alterations that lead to the

dysregulation of intrinsic signaling pathways in prostate tumor cells and the mechanisms by which they regulate the infiltration of myeloid-derived cells may have a significant impact on PCa treatment. Here, we identified the IL-8 / CXCR2 pathway as a major mechanism for PMN-MDSC recruitment to the TME of CRPC tumors following ADT.

3.2 Results

3.2.1 Androgen-Deprivation Therapy (ADT) Increases IL-8 Transcription in Prostate Cancer Cells

To identify immune-related tumor-cell intrinsic factors involved in PCa progression, we performed expression analyses on murine PCa cells pre- and post- castration. We used the MCRedAL PCa cell line; an RFP expressing version of the Myc-Cap cell line characterized by *MYC* overexpression.[337] Like human PCa, MCRedAL tumors are initially castration-sensitive (CS), but castration-resistance (CR) develops approximately 30 days after castration (Fig. 3.1A). Pre- and post- ADT tumor cells were sorted to > 96% purity (Fig. 3.1B) and analyzed (Fig. 3.1C-D). A number of cytokine and chemokine transcripts were significantly up-regulated post-ADT (Fig. 3.1D right), including *Cxcl15*, a CXC chemokine with a conserved ELR motif (Table 3.1), which is the likely murine homolog of human *IL-8* (*CXCL8*).[355-358] qRT-PCR and ELISA assays confirmed the upregulation of Cxcl15 post-ADT at the protein level (Fig. 3.1F). In addition to the chemokines above, GSEA revealed the upregulation of several pro-inflammatory pathways post-ADT (Fig. 3.1E). *In vitro* experiments using the human androgen-responsive LNCaP cell line corroborated a role for these pro-inflammatory signals, showing that in the

absence of androgen, TNFα upregulated IL-8 expression in a dose-dependent manner (Fig. 3.1G left); while AR signaling in the absence of inflammation did not affect IL-8 expression (Fig. 3.1G right). These data led to the hypothesis that AR signaling directly suppresses *IL-8* expression in PCa cells. We performed *in silico* ChIP-Seq analyses using human LNCaP cells (GSE83860) and found AR binding at the *IL-8* promoter in the presence of the potent androgen dihydrotestosterone (DHT; Fig. 3.1H top). This androgen dependent binding was verified by ChIP-qRT-PCR (Fig. 3.1I left).

Table 3.1 | Amino Acid Sequence Homology Between Human IL-8 (CXCL8) and the Murine Homologues.

RefSeq Accession #	Protein	Score	Expect	Identities	ELR/CXC motifs
NP_000575.1	CXCL8	202 bits (514)	1e-19	99/99 (100%)	**ELRCQCI**
EDL05301.1	Cxcl1	78.6 bits (192)	9e-26	35/66 (53%)	**ELRC**L**C**L
NP_033166.1	Cxcl2	68.9 bits (167)	6e-22	34/76 (45%)	**ELRC**L**C**L
NP_033167.2	Cxcl5	63.5 bits (153)	3e-19	27/66 (41%)	**ELR**VL**C**L
NP_035469.1	Cxcl15	47.4 bits (111)	8e-13	26/72 (36%)	**ELRC**L**CI**
AAH06640.1	Cxcl12	39.7 bits (91)	1e-10	26/82 (32%)	**SY**RC**P**C**-**
NP_705804.2	Cxcl17	No significant similarity found			

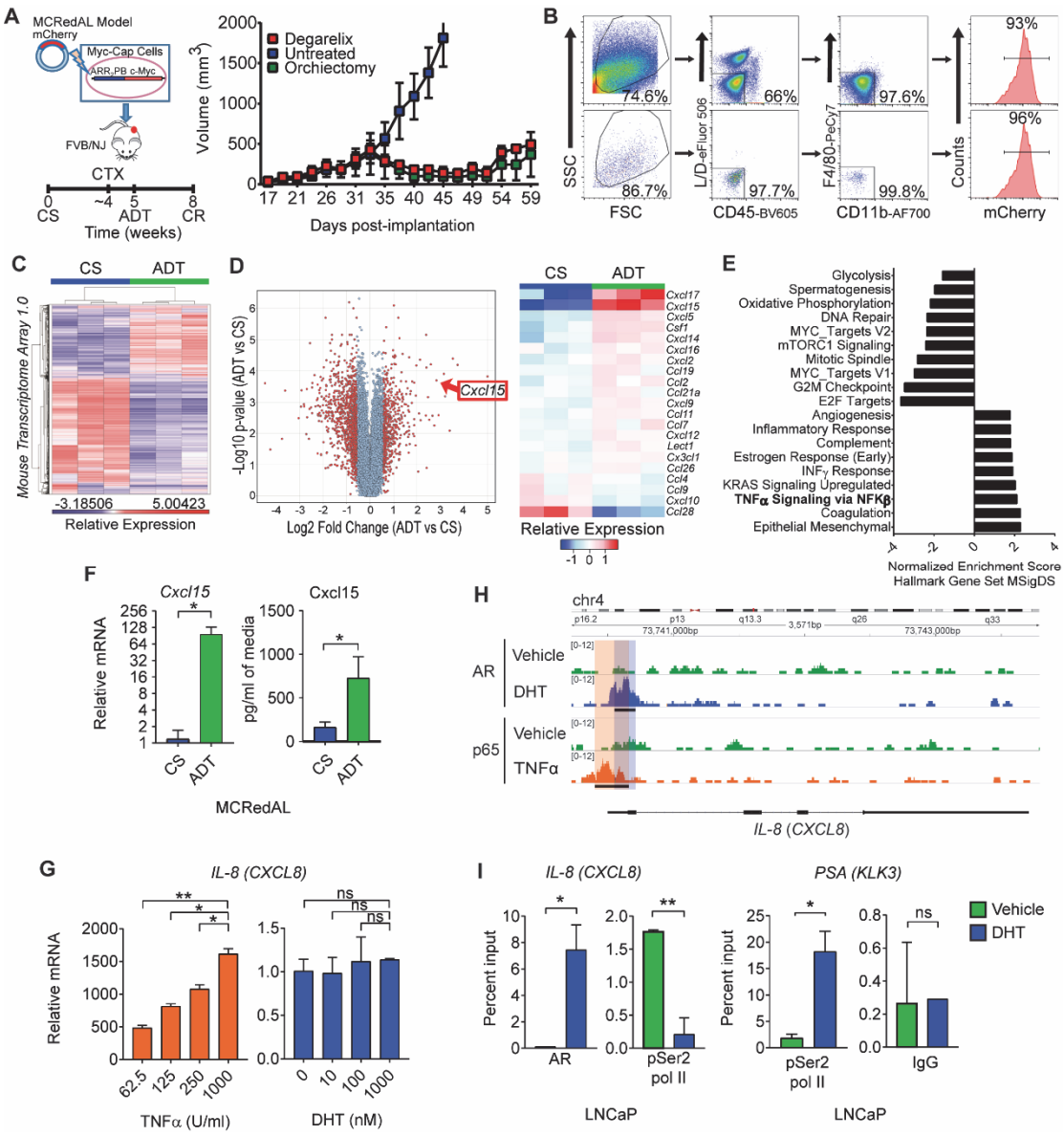

Figure 3.1 | Androgen-Deprivation Therapy (ADT) Increases IL-8 Expression in Prostate Cancer Cells. A, Androgen responsive tumor epithelial cells progress from castration-sensitive (CS) to androgen responsive (ADT), and eventually developed castration-resistance (CR). CR was tumor size defined as ≥ 30% of nadir tumor volume. Left, fluorescent tag-in strategy to generate mCherry^{+} Myc-Cap cells (MCRedAL cells). Right, tumor growth curve of MCRedAL tumors. CTX: Castration (n ≥ 3 per group, repeated x 2). **B,** Sorting strategy to isolate tumor epithelial cells from **A** based on their expression of mCherry and their CD45^{-} CD11b^{-}F4/80^{-} phenotype. **C,** Differential expression profile of tumor epithelial cells isolated from castration-sensitive (CS) and ADT-treated MCRedAL tumor bearing mice. Heatmap showing transcripts 3 standard deviations away from the mean (n = 3 per group). **D,** Differential chemokine expression of tumor epithelial cells

isolated from CS and ADT tumor bearing mice (replicate numbers as in **C**). Left, volcano plot showing gene expression among all MTA 1.0 microarray transcripts. Right, heatmap of normalized chemokine transcripts. **E,** Hallmarks gene sets pathway analysis post-ADT shows NF-κB up-regulation post-ADT. **F,** Gene and protein expression of Cxcl15 in indicated MCRedAL tumor cells *in vitro* by qRT-PCR and ELISA, respectively (n = 3 per group). **G,** qRT-PCR quantification of *IL-8* in LNCaP cells cultured at indicated concentrations of TNFα and DHT, cells cultured in androgen-free media as described in materials and methods (n = 3 per condition, repeated x 2). Expression levels normalized to mean ΔCT level in samples cultured in androgen free media without TNFα or DHT. **H,** ChIP-Seq analysis of AR and p65 (the the NF-κB subunit) at the *IL-8* (*CXCL8*) promoter in LNCaP cells cultured in the presence of either vehicle (DMSO), DHT (100 nM), or TNFα (1000 U/ml) (n = 2 per group; GSE83860). **I,** left: ChIP quantitative RT-PCR (qRT-PCR) analysis of AR and pSer2 Pol II at the *IL-8* (*CXCL8*) promoter (n = 3 per group). Right: percentage input bound in ChIP–qRT-PCR assays assessing binding of pSer2 Pol II and control IgG at *PSA* (*KLK3*) promoter loci. Experiments were performed in LNCaP cells treated for 24 h with or without DHT (100 nM; n = 3 per group). For **H**, loci with significant differential binding (black bar) were identified as described in materials and methods. Error bars represent standard error. Unpaired t-tests were performed, *p*-values ≤ 0.05 (*), 0.01 (**), 0.001 (***) and 0.0001 (****); *p*-values ≥ 0.05 (ns).

To further explore the role of AR in IL-8 regulation, we interrogated RNA polymerase binding and transcription marks found at sites of active promoters.[359] In the presence of DHT, binding of phosphorylated serine 2 RNA polymerase II (pSer2 pol II) to the IL-8 locus was substantially reduced, consistent with reduced transcriptional activity (Fig. 3.1I left). Conversely, pSer2 pol II binding to the promoter of the well-established AR-regulated gene *PSA* (*KLK3*), was significantly increased in the presence of DHT as expected (Fig. 3.1I right). Consistent with a role for inflammation, TNFα significantly increased p65 binding at the *IL-8* (*CXCL8*) promoter in LNCaP cells (Fig. 3.1H bottom). No significant binding of AR was detected at the promoters of the chemokines *CXCL1*, *CXCL2*, *CXCL5* or *CXCL12* (Fig. 3.2). These data suggest that AR directly suppresses *IL-8* expression

through repressive AR binding to the *IL-8* promoter. Taken together, we found that IL-8 transcription is up-regulated by pro-inflammatory signaling, and down-regulated by AR signaling.

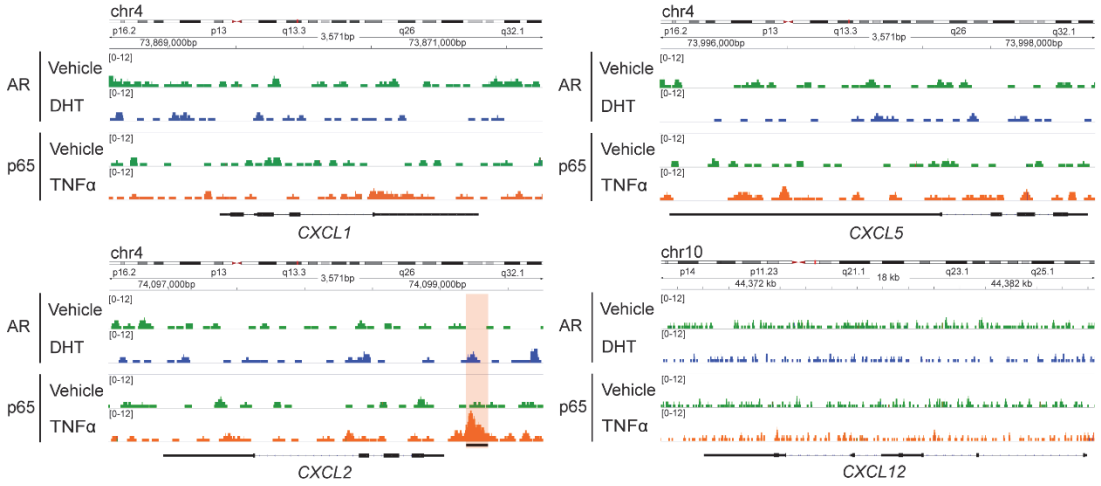

Figure 3.2 | Chemokine Regulation Upon AR signaling Stimulation and an Inflammatory Stimuli in Prostate Tumor Epithelial Cells. ChIP-Seq enrichment of AR at the *CXCR1, CXCR2, CXCR5,* and *CXCL12* promoters in LNCaP cells cultured in the presence of either vehicle (DMSO), AR signaling (DHT: 100 nM), or an inflammatory stimuli (TNFα: 1000 U/ml) (n = 2 per group; GSE83860).

3.2.2 IL-8 is Differentially Expressed in Castration-Resistant Versus Castration Sensitive Prostate Cancer Cells

We next investigated the effects of ADT on the expression of *Cxcl15 in vivo*, using RNA in situ hybridization (RISH) to study Myc-Cap tumors. We found that CR tumors expressed increased *Cxcl15* as compared to CS tumors, particularly in epithelial (PanCK^{+}) tumor cells (Fig. 3.3A). These findings were confirmed *in vitro*, both at the mRNA and protein level (Fig. 3.3B). To investigate these findings in the context of human PCa, we used three paired cell lines in which isogenic CR lines were derived from CS progenitors. For each pair, the CR line expressed

significantly increased IL-8 as compared to the CS counterpart, both at the mRNA and protein level (Fig. 3.3C-D). This observation held across a panel of AR expressing PCa cell lines; with higher levels of *IL-8* expression in cell lines from castration-resistant disease (Fig. 3.3E). To test whether AR modulates *Cxcl15* expression in benign prostate epithelium, we used RISH to study WT mice treated with ADT, and WT mice treated with ADT followed by testosterone (T) repletion (Fig. 1.1A-C). These data (Fig. 3.3F-G) showed increased epithelial *Cxcl15* expression in ADT samples with expression significantly decreased by testosterone repletion (Fig. 3.3G). This observation was further corroborated by interrogating a dataset (GSE8466) profiling human prostate epithelial cells isolated by laser-capture microdissection (LCM) from men undergoing ADT and ADT with testosterone supplementation. Testosterone repletion significantly reduced *IL-8* mRNA expression (Fig. 3.3H), supporting the hypothesis that AR signaling down-regulates IL-8 expression. In agreement with these data from benign prostate tissues, we LCM-enriched tumor prostate epithelium from high-risk PCa patients treated with ADT on a neo-adjuvant trial (NCT01696877) and found increased *IL-8* expression as compared to tumors from age and stage-matched untreated controls (Fig. 3.3I). Taken together, analyses using human tissues strongly support the notion that castration increases *IL-8* expression in prostate epithelial cells.

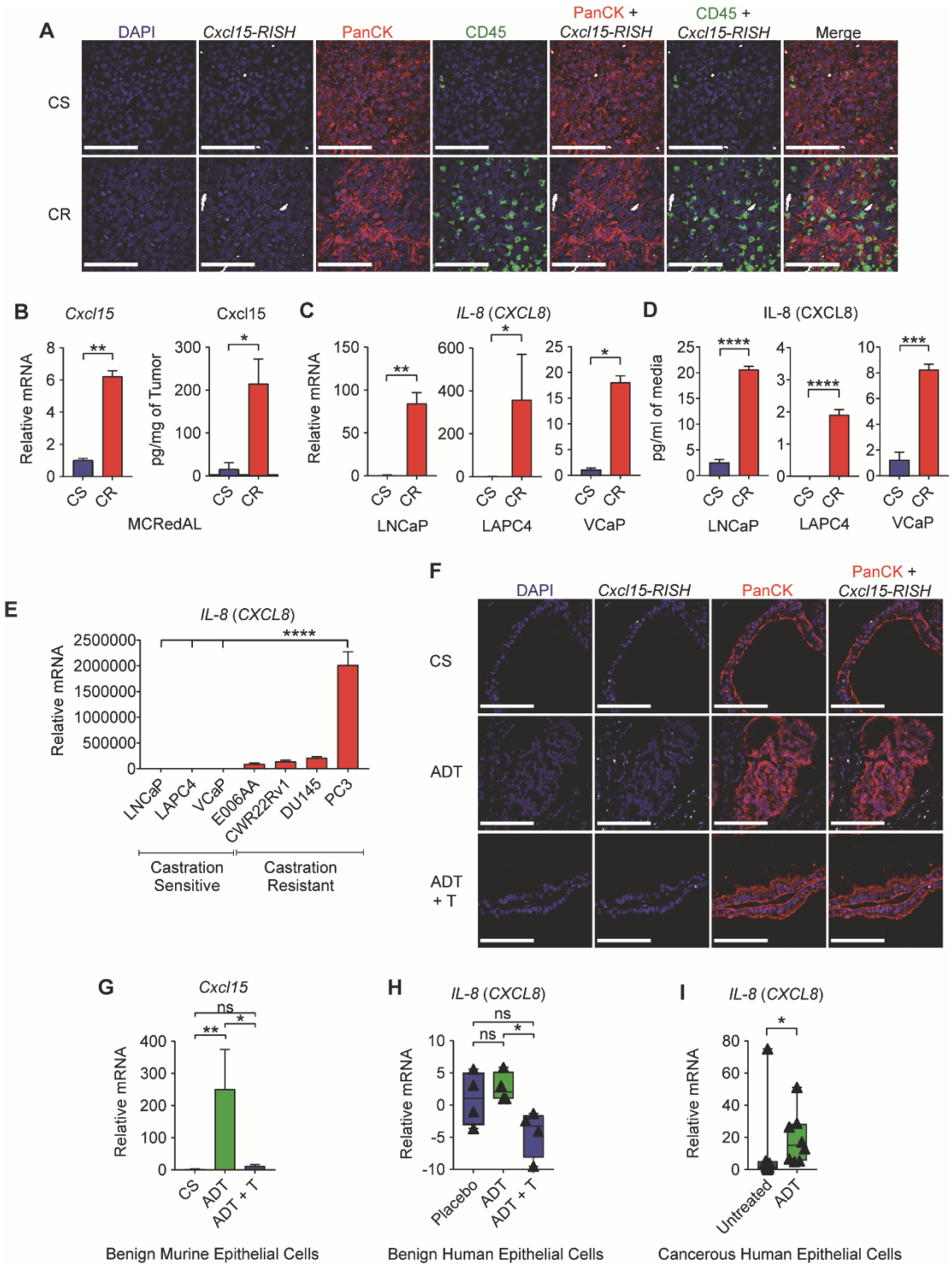

Figure 3.3 | IL-8 is Up-Regulated in Post-Castration and Castration-Resistant Prostate Cancer Cells. A, Representative images of *Cxcl15* fluorescent detection (murine homologue of IL-8) in Myc-Cap tumors. Tumors were harvested when volumes reached ~500mm^3 (CS group), 7 days after androgen-deprivation (ADT), or at the time of castration-resistance (CR) and hybridized with CF568-labeled

probe sets (white) to *Cxcl15*, CF640-labeled anti-PanCK antibody (red), and CF488-labeled anti-CD45 antibody (green). Nuclei counterstained with DAPI (blue). Repeated x 3. **B,** Gene and protein expression of Cxcl15 in MCRedAL cells of indicated tumor samples by qRT-PCR and ELISA, respectively (n = 3 per group, repeated x 2). **C,** qRT-PCR quantification of *IL-8* in human AR positive castration-sensitive cells (CS: LNCaP, LAPC4, and VCaP) and their castration-resistant counterparts (CR: LNCaP-abl, LAPC4-CR, and VCaP-CR), replicate numbers as in **B**. **D,** IL-8 protein expression in the isogenic cell pairs from **C** quantified by ELISA, replicate numbers as in **C**. **E,** qRT-PCR quantification of *IL-8* in AR positive castration-sensitive (LNCaP, LAPC4, and VCaP) and AR independent castration-resistant (E006AA, CWR22Rv1, DU145, and PC3) human PCa cell lines (n = 2 per group, repeated x 2). **F,** Representative images of *Cxcl15* fluorescent detection in benign murine prostate tissue samples from castration-sensitive (CS), androgen-deprivation treated (ADT), and ADT-treated mice that received testosterone repletion (ADT + T). Tissue sections hybridized with CF568-labeled probe sets (white) to *Cxcl15*, and CF640-labeled anti-PanCK antibody (red). Nuclei were counterstained with DAPI (blue). Repeated x 3. **G,** qRT-PCR analysis of *Cxcl15* expression in prostate luminal epithelial cells from indicated treatment groups (n = 3 per group). Prostate luminal epithelial cells were isolated based on their $GFP^{+}CD49f^{int}CD24^{+}CD45^{-}F4/80^{-}CD11b^{-}$ expression by flow sorting into Trizol LS. **H,** Expression of *IL-8* in human prostate epithelial cells micro-dissected from patients in a clinical trial (NCT00161486) receiving placebo, androgen-deprivation treatment (ADT), or ADT plus testosterone repletion (ADT + T). Z-score values of microarray transcripts from benign prostate biopsies were normalized to placebo samples (n = 4 per group; GSE8466). **I,** Expression of *IL-8* in human PCa epithelial cells micro-dissected from untreated or ADT-treated (NCT01696877; n = 8 per group) patients as determined by qRT-PCR. RISH images are at 60X magnification; scale bar = 100 μm. Gene expression levels were normalized to the mean ΔCT level in samples from CS, untreated or placebo groups. For **B-H**, unpaired t-tests were performed; for **I** a Mann-Whitney U test was used due to the non-normal data distribution observed. *p*-values ≤ 0.05 (*) and 0.01 (**); *p*-values ≥ 0.05 (ns) shown. The range in box and whiskers plots shows min and max values such that all data are included.

3.2.3 ADT-mediated IL-8 Up-Regulation Promotes PMN-MDSC Infiltration

We next quantified castration-mediated immune infiltration in Myc-Cap allografts (Fig. 3.4A). Consistent with prior data,[55] ADT promoted a transient T cell influx, without significant changes in tumor associated macrophage (TAM) populations (Fig. 3.4B). By contrast, PMN-MDSC infiltration was significantly increased in CR tumors (Fig. 3.4B), as verified by IHC (Fig. 3.4C). We found similar results in human PCa xenografts (Fig. 3.4D-E). PMN-MDSC infiltration also increased in WT mice treated with ADT, but not in WT mice treated with ADT then repleted with testosterone (Fig. 3.4F), supporting a causal relationship between ADT and PMN-MDSC infiltration.

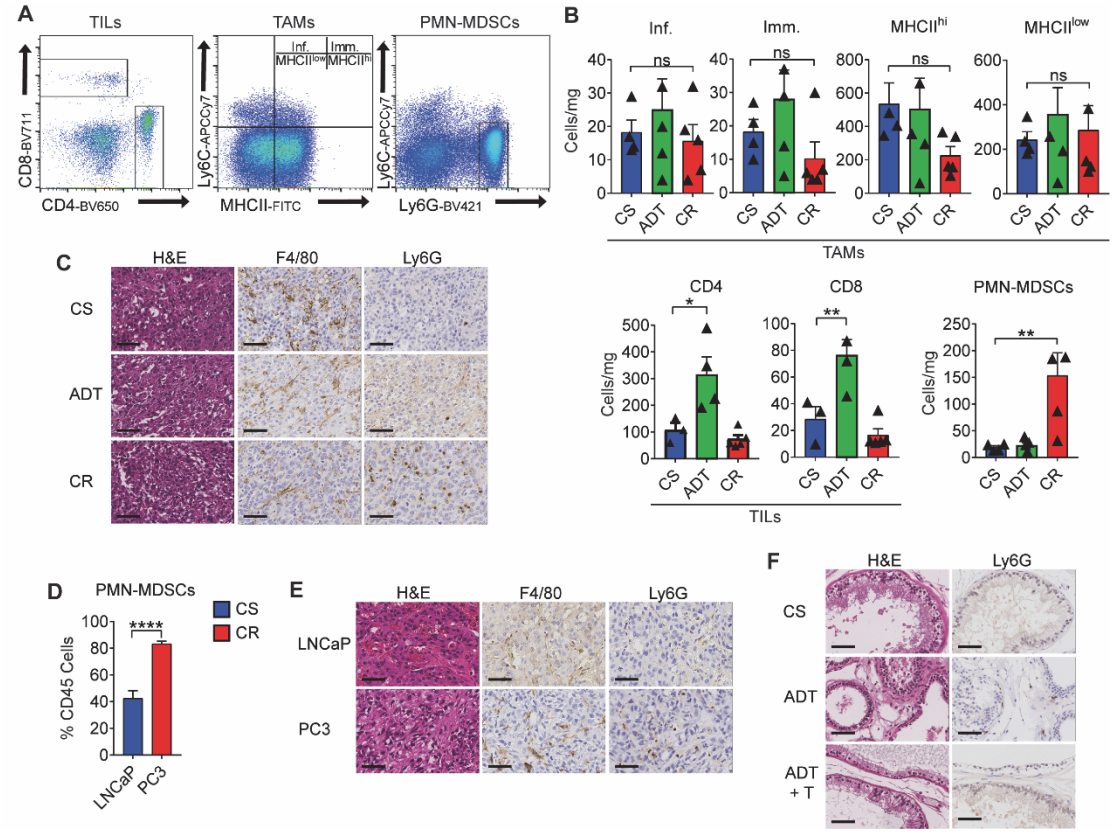

Figure 3.4 | Castration-mediated IL-8 Up-Regulation Promotes PMN-MDSC Infiltration. A, Gating strategy used to profile the immune compartment of the TME by flow cytometry. Tumor associated Mϕ (TAMs) gated based on $CD45^+Ly6G^-F4/80^+CD11b^+$, Inflammatory (Inf.) TAMs as $CD45^+CD11b^+F4/80^+Ly6C^+MHCII^-$, immature (Imm.) TAMs as $CD45^+CD11b^+F4/80^+Ly6C^+MHCII^+$, $MHCII^{hi}$ TAMs as $CD45^+CD11b^+F4/80^+Ly6C^-MHCII^+$, $MHCII^{low}$ TAMs as $CD45^+CD11b^+F4/80^+Ly6C^-MHCII^-$, tumor Infiltrating Lymphocytes (TILs) $CD45^+CD4^+$ or $CD45^+CD8^+$, tumor infiltrating polymorphonuclear myeloid-derived suppressor cells (PMN-MDSCs) as $CD45^+CD11b^+Ly6C^+Ly6G^+$. **B,** TAM, TIL, and PMN-MDSC density normalized to mg of tumor weight (cells/mg; n ≥ 3 per group, repeated x 2). **C,** Representative H&E and immunohistochemistry (F4/80 and Ly6G) of indicated murine allografts (repeated x 3). **D,** PMN-MDSCs as a percentage of $CD45^+$ cells in the TME of indicated human prostate tumors as determined by flow cytometry (n = 3 per group, repeated x 2). **E,** Representative H&E and immunohistochemistry (Ly6G and F4/80) sections of the indicated human prostate xenografts (repeated x 3). **F,** Representative H&E and immunohistochemistry of Ly6G in non-cancerous murine prostate from castration-sensitive (CS), androgen-deprivation treated (ADT) non-tumor bearing mice, and ADT treated mice that received testosterone repletion (ADT + T). Repeated x 2.

3.3 Discussion

We identified that ADT mediates increased IL-8 secretion by PCa epithelial cells by reliving AR mediated transitional repression. IL-8 up-regulation further drives prostate tumor infiltration with PMN-MDSCs. Recent studies have suggested potential mechanisms that explain the migration of PMN-MDSCs in response to a few of the ligands of Cxcr4 (Cxcl12) and Cxcr2 (IL-8 murine functional homologues: Cxcl1, Cxcl2, Cxcl5).[360,361] Here, we found Cxcl15 expression is upregulated after inhibition of AR-signaling in murine tumor epithelial cells in a manner similar to which IL-8 is up-regulated in human PCa epithelial cells (Fig. 3.3). Interestingly, we did not observe AR binding to the promoter of other chemokines reported to modulate neutrophil infiltration (Fig. 3.2). Complimentary to the mechanism described here, a recent study found that Cxcl12 expression

could be induced in prostate tumor cells by treatment with the tyrosine kinase inhibitor cabozatinib in Pten/tp53 deficient animals.[361]

Chapter IV – Targeting Tumor Intrinsic Mechanisms Alone or in Combination with Checkpoint Blockade

"Immunotherapy represents a new frontier in prostate cancer. We're also looking at how it can be used synergistically with traditional therapies, both in prostate cancer as well as in other tumor types."

Dr. Charles G. Drake (2016) – a pioneer in cancer immunotherapy.

Professor and hematology oncologist at Columbia University, and the co-director of the Cancer Immunotherapy Programs.

4.1 Introduction

We and others have shown that ADT initially increases CD8 T cell infiltration into prostate tumors,[141,238,327] and this response is augmented pre-clinically with anti-CTLA-4.[55] Emerging data suggest that immune-resistance in PCa involves dysfunctional myeloid cells known as MDSCs in the TME.[362] MDSCs secrete IL-23, which acts directly on PCa epithelial cells to drive castration-resistance.[289] Here we found that mitigating the suppressive effects of PMN-MDSCs influx driven by ADT increase anti-tumor immune responses when given in combination with ICB.

4.2 Results

4.2.1 Blockade of the IL-8 / CXCR2 Pathway Attenuates the Migration of PMN-MDSCs But Not Their Function

Molecular profiling of the infiltrating myeloid cells revealed a signature consistent with functional PMN-MDSCs, including up-regulation of *IL-1b*, *Arg2* and *IL-23a*[289] (Fig. 4.1A). In particular, increased expression of *IL-23a* and *Cxcr2* was verified by qRT-PCR (Fig. 4.1B) and flow cytometry (Fig. 4.1C). To test whether blocking the IL-8 / CXCR2 axis was sufficient to attenuate post-ADT PMN-MDSC infiltration, we treated prostate-tumor bearing mice with anti-CXCR2 and found that blocking CXCR2 significantly diminished tumor infiltration with PMN-MDSCs in both human (PC3) and murine (Myc-Cap) immunodeficient and immunocompetent models (Fig. 4.1D-F). To confirm this observation at the genetic level, we used CRISPR/Cas9 to generate human (PC3) and mouse (Myc-Cap) lines that were knocked out for human IL-8 or the murine IL-8 homolog Cxcl15, respectively. We observed a clear decrease in PMN-MDSC infiltration in both settings (Fig. 4.1E-G).

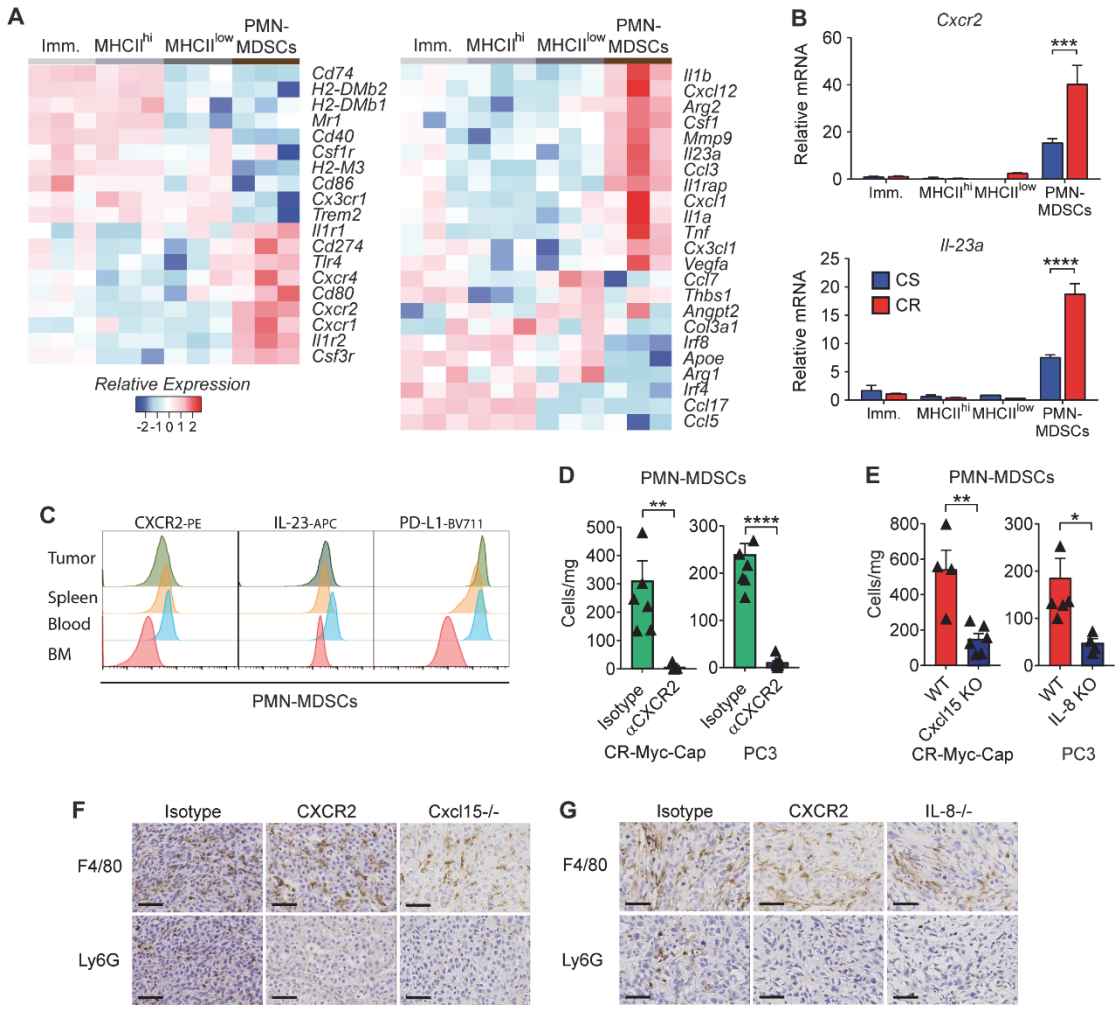

Figure 4.1 | PMN-MDSCs Infiltration Relays on IL-8 (Cxcl15) / CXCR2 Signaling Following ADT. **A,** Normalized expression of selected genes determined by NanoString nCounter gene analysis in sorted myeloid fractions defined as in **Fig. 3.4A** (n = 3 per group). **B,** qRT-PCR quantification of *Cxcr2* and *Il-23* in indicated populations of Myc-Cap tumors (n = 3 per group). **C,** Representative histograms of protein expression determined by flow cytometry in PMN-MDSCs from indicated organs (repeated x 2). **D** and **E,** Density of PMN-MDSCs normalized to mg of tumor weight (cells/mg) in Myc-Cap and PC3 tumors (n ≥ 4 per group, repeated x 2). Cells quantified by flow cytometry as in **Fig. 3.4A**, tumors implanted and harvested as in materials and methods. H&E and IHC images at 40X magnification; scale bar = 50 μm. Gene expression levels normalized to the mean ΔCT level in samples from the Immature TAMs (Imm.) group. Unpaired t-tests performed, *p*-values ≤ 0.05 (*), 0.01 (**), 0.001 (***) and 0.0001 (****); *p*-values ≥ 0.05 (ns). **F,** Representative H&E and immunohistochemistry (Ly6G and F4/80) on CR-Myc-Cap allografts treated as

indicated (repeated x 3). **G,** Representative H&E and immunohistochemistry (Ly6G and F4/80) in PC3 tumor xenografts treated as indicated (repeated x 3). H&E and IHC images are 40X magnification; scale bar = 50 μm. Unpaired t-tests were performed, *p*-values ≤ 0.0001 (****).

We next asked whether the supernatant from castration-resistant MCRedAL (CR-MCRedAL) cells was sufficient to drive PMN-MDSC migration *in vitro*. In line with *in vivo* results (Fig. 4.1D-G and Fig. 4.2A-C), we found that PMN-MDSC migrated towards the supernatant of CR tumors and migration was significantly attenuated by CXCR2 blockade (Fig. 4.2D). Human PCa (PC3) showed an identical pattern. To confirm a role for IL-8 in PMN-MDSC migration, we generated IL-8 KO CR-LNCaP (LNCaP-abl) using CRISPR/Cas9. Supernatants from IL-8 KO cells were significantly attenuated in their ability to promote PMN-MDSC migration (Fig. 4.2E). These PMN-MDSCs were functional and suppressed CD8 T cell proliferation in a dose-dependent manner (Fig. 4.2F-I). Although CXCR2 blockade decreased PMN-MDSC migration, it did not significantly alter suppressor function (Fig. 4.2J). Similarly, Cxcl15 loss did not diminish the suppressive function of PMN-MDSCs (Fig. 4.2K). Taken together these findings reinforce a functional role for castration-mediated IL-8 secretion in PMN-MDSC migration.

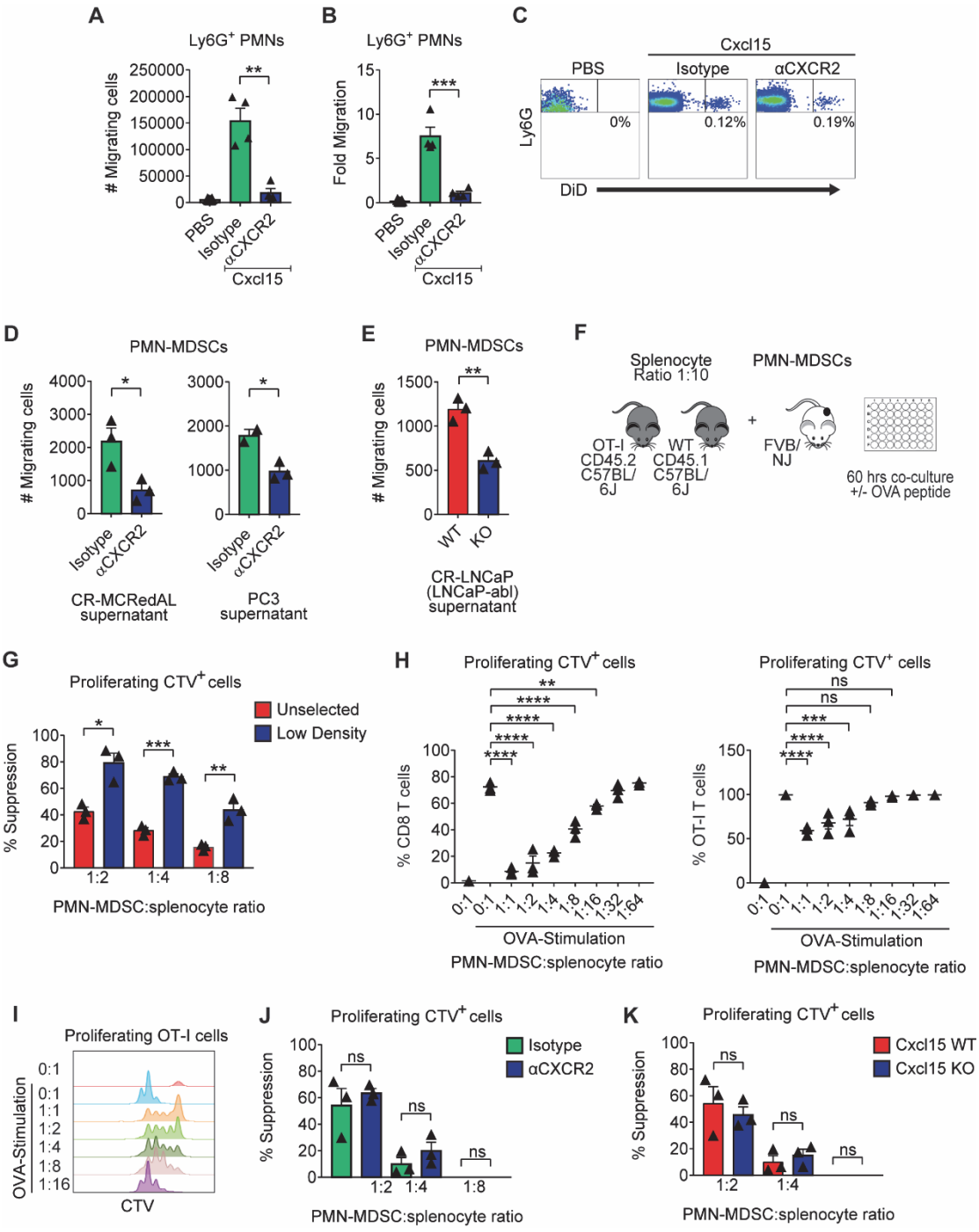

Figure 4.2 | PMN-MDSCs Migrate in Response to Cxcl15 and Suppress Antigen Specific T Cell Function. **A,** Analysis of Ly6G$^+$ PMNs in peritoneal washings receiving Cxcl15 (200ng/mouse, i.p.) in mice pre-treated with either isotype or αCXCR2 (n ≥ 4 per group, repeated x 2). **B,** Analysis of the fold change between the number of Ly6G$^+$ PMNs in peritoneal washings from **A** in relation to PMNs' numbers in peripheral blood of indicated treated mice. **C,** Representative

plots of Ly6G$^+$ PMNs in peritoneal washings from **A** of indicated treated mice (repeated x 2). **D,** PMN-MDSC *in vitro* migration towards tumor supernatants in the presence of either isotype or anti-CXCR2 (200 µg/ml). Antibodies were added at the beginning of the experiment (n ≥ 2 per group, repeated x 2). **E,** PMN-MDSC *in vitro* migration towards CR-LNCaP (LNCaP-abl) WT or IL-8 KO tumor supernatants (n = 3 per group, repeated x 2). **F,** Schematic representation of PMN-MDSC suppression assay. OT-I splenocytes (CD45.2) were mixed with naïve splenocytes (CD45.1) in a 1:10 ratio, labeled with CTV, and co-culture with PMN-MDSCs at the indicated ratios. T cell proliferation was stimulated (Stim) by OVA peptide (5pM) for 60 hours. **G,** Percent suppression when either unselected or low-density PMN-MDSCs were used for the experiment (n = 3 per group, repeated x 3). **H,** Percent of CD8 T cells (left) and antigen specific OT-I cells (CD45.2; right) proliferating at different proportions of PMN-MDSCs when stimulated with or without 5pM of OVA, replicate numbers as in **G**. **I,** Representative histograms of antigen specific OT-I cells proliferation based on the dilution of CTV dye when stimulated as in **H** (repeated x 2). **J,** Percent suppression in the presence of either isotype or anti-CXCR2 (200 µg/ml). Antibodies were added at the beginning of the experiment (n = 3 per group, repeated x 2). **K,** Percent suppression of PMN-MDSCs derived from spleens of WT or Cxcl15 KO Myc-Cap tumor bearing mice (n = 3 per group, repeated x 2). For **A-C**, PMNs were gated on CD45$^+$Ly6G$^+$ cells. Cell migration *in vivo* was evaluated 4 hours after PBS or cytokine treatment and normalized to 10,000 beads. PBS was injected as the control for these experiments. For **D-E**, PMN-MDSCs were isolated from spleens of mice bearing CR-Myc-Cap tumors and placed in the top chamber of a transwell. Culture supernatants were plated in the bottom chamber, and number of PMN-MDSCs migrating from the top to the bottom chamber after 2.5 hours was evaluated. For **G, J-K**, percent suppression (% Suppression) was calculated by the following formula: % Suppression = [1-(% divided cells of the condition / the average of % divided cells of T responder only conditions)] x 100. Unpaired t-tests were performed, *p*-values ≤ 0.05 (*), 0.01 (**), 0.001 (***) and 0.0001 (****); *p*-values ≥ 0.05 (ns).

4.2.2 CXCR2 Blockade Improves Response to Immune Checkpoint Blockade Following Androgen-Deprivation

Finally, we investigated the pre-clinical activity of blocking the IL-8 / CXCR2 axis at the time of androgen-deprivation in the Myc-Cap model. Notably, in the absence of immunotherapy the combination of ADT and CXCR2 blockade was not effective (Fig. 4.3A&C). In contrast, combining CXCR2 blockade with ICB (anti-CTLA-4; Fig. 4.3E) resulted in significantly increased survival (Fig. 4.3F). This triple combination (ADT + anti-CXCR2 + anti-CTLA-4) was effective even when tumors were relatively advanced (400 mm^3) at the time of treatment (Fig. 4.3G). Macrophage modulation with anti-CSF1R was not effective therapeutically in this setting (Fig. 4.3B&D).

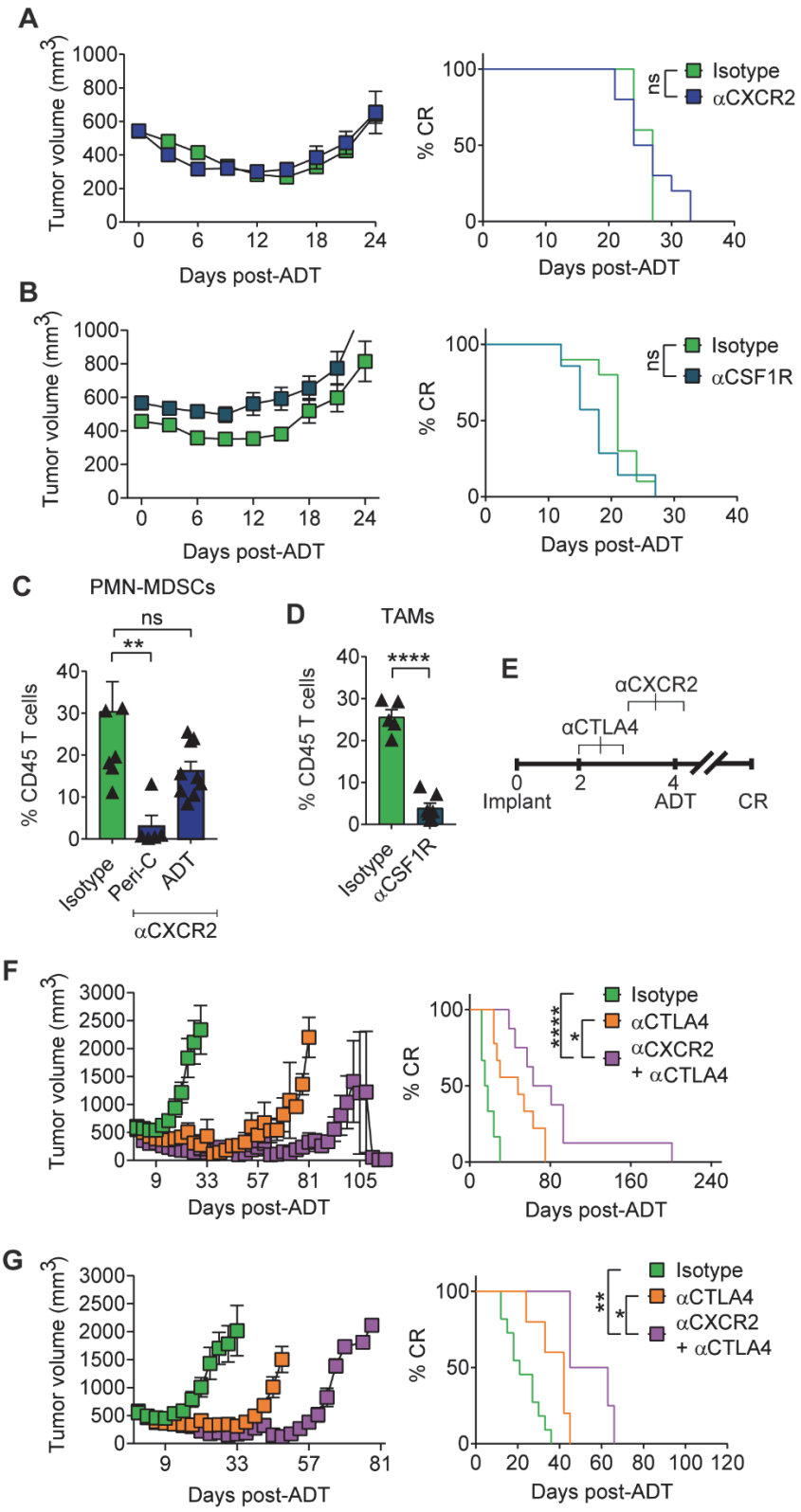
A
Tumor volume (mm3)
Days post-ADT
% CR
ns
Isotype
αCXCR2
B
αCSF1R
C
PMN-MDSCs
% CD45 T cells
Isotype
Peri-C
ADT
αCXCR2
D
TAMs
E
αCXCR2
αCTLA4
Implant
ADT
CR
F
αCXCR2
+ αCTLA4
G

Figure 4.3 | CXCR2 Blockade Improves Response to Immune Checkpoint Blockade Following Androgen-Deprivation Therapy. **A,** Tumor growth and survival curves of mice from isotype vs. αCXCR2 treatment groups (green vs. blue, respectively; n = 10 per group, repeated x 2). **B,** Tumor growth and survival curves of mice from isotype vs. αCSF1R treatment groups (green vs. purple, respectively; n ≥ 7 per group, repeated x 2). **C,** PMN-MDSCs as a percentage of $CD45^+$ cells in the TME of indicated treatment groups, repeated x 2. **D,** TAMs as a percentage of $CD45^+$ cells in the TME of indicated treatment groups, replicate numbers as in **B**. **E,** Treatment scheme, scale = weeks. Animals sacrificed for immune phenotyping 1 week post-ADT. **F,** Tumor growth and survival curves of mice from isotype vs. anti-CTLA-4 vs. anti-CTLA-4 + anti-CXCR2 groups treated as described in **E** (black line vs. orange line vs. purple line, respectively; n ≥ 8 per group, repeated x 2). Treatment was initiated when tumor volumes reached $200mm^3$. **G,** Tumor growth and survival curves of mice from isotype vs. αCTLA-4 vs. αCTLA-4 + αCXCR2 treatment groups (green vs. orange vs. purple, respectively; n ≥ 7 per group, repeated x 2). Treatment started when tumor volumes reached $400mm^3$. Average tumor volume (±s.e.m.) for each experimental group. Wilcoxon test used for survival analysis. Flow cytometry as in materials and methods. Unpaired t-tests performed, *p*-values ≤ 0.05 (*), 0.01 (**), 0.001 (***) and 0.0001 (****); *p*-values ≥ 0.05 (ns).

Mechanistically, the increased anti-tumor effects mediated by the addition of anti-CXCR2 to ADT + anti-CTLA-4 did not appear to be due to increased T cell infiltration (Fig. 4.4A&C-D), nor due to decreased T_{reg} infiltration (Fig. 4.4B), but rather correlated with an increase in polyfunctional effector CD8 T cells in tumor-draining lymph nodes (TDLN) and spleens (Fig. 4.4E-F).

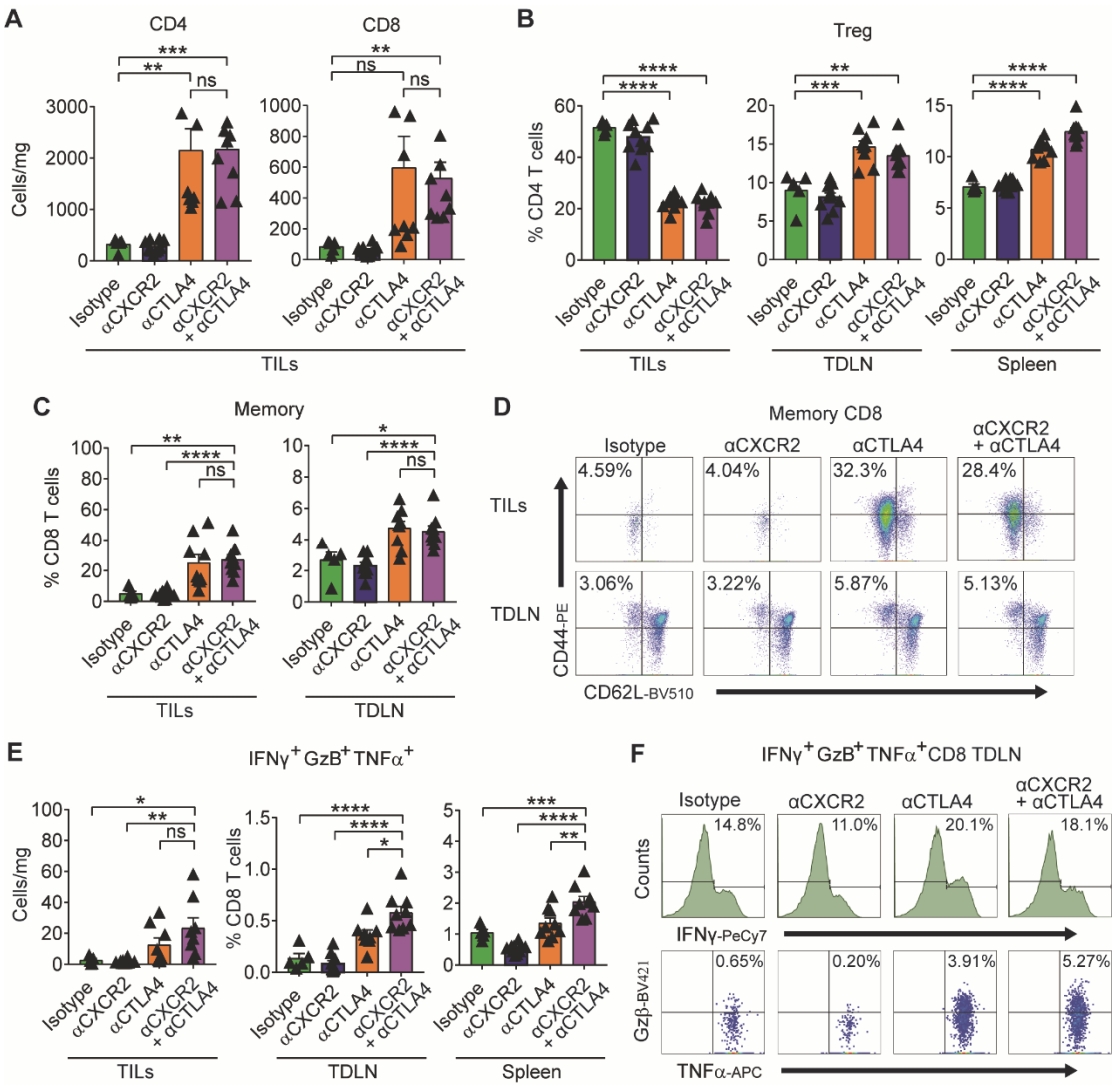

Figure 4.4 | The Therapeutic Effect of the Triple Combination is Associated with PMN-MDSC Reduction. **A,** Tumor infiltrating lymphocyte (TILs) density in indicated treatment groups (n ≥ 5 per group, repeated x 2). **B,** Treg percentages (as fraction of CD4) in indicated tissues (n ≥ 5 per group, repeated x 2). **C,** Memory CD8 T cells as a percentage of $CD45^+CD8^+$ TILs and TDLN of indicated treatment groups, replicate numbers as in **A**. **D,** Representative plot of memory $CD8^+$ TILs and TDLN of indicated treatment groups (repeated x 2). **E,** Polyfunctional CD8 T cells, left panel = density, center/right panels = percentage of total CD8, animals numbers as in **A**. **F,** Representative histograms and dot plots of polyfunctional $CD8^+$ $IFN\gamma^+GzB^+TNF\alpha^+$ from tumor draining lymph nodes (TDLN).For For **A-F**, treatment started when tumor volumes reached 200mm^3. Average tumor volume (±s.e.m.) for each experimental group. Wilcoxon test was used for survival analysis. Flow cytometry as in materials and methods. Unpaired t-tests were

performed, *p*-values ≤ 0.05 (*), 0.01 (**), 0.001 (***) and 0.0001 (****); *p*-values ≥ 0.05 (ns).

4.3 Discussion

We found that blocking CXCR2 at the time of ADT attenuates PMN-MDSC infiltration, rendering prostate tumors more sensitive to ICB. It is noteworthy that in other murine models the recruitment of PMN-MDSC and neutrophils may be driven by other chemokines, including Cxcl1[360] and Cxcl12.[361] Our findings are corroborated by clinical data showing that PMN-MDSCs accumulate in the blood of patients with advanced PCa,[135,136,363] and that an intra-tumoral PMN signature is associated with poor outcome.[364] Our data are also supported by pre-clinical studies showing that blocking MDSC function increases the efficacy of ICB in animal models of CRPC.[362] Consistent with recent data, we found that the PMN-MDSCs infiltrating prostate tumors express IL-23.[289] We further showed that inhibiting the recruitment of these cells peri-castration augmented the CD8 T cell effector function initiated by ICB. Based on these findings, our group has launched an investigator-initiated phase Ib/II trial (NCT03689699) to test whether adding ICB and anti-IL-8 to a short course of ADT can prevent PMN-MDSC infiltration and delay progression in men with castration-sensitive PCa. In summary, targeting the IL-8 / CXCR2 pathway following ADT in combination with ICB may represent a novel treatment paradigm to improve responses to immunotherapy and delay the onset of castration-resistance in PCa patients.

Concluding Remarks

The promise of cancer immunotherapy in PCa and other so called ‘cold’ tumors, is likely to lay in combination therapy. Even though prostate tumor-associated antigens lead to pro-inflammatory CD4 and CD8 T-cell responses, the immunosuppressive microenvironment of PCa tumors renders these antigen-specific T-cell responses tolerant. Although androgen-derivation therapy (ADT) drives the infiltration of T cells into the TME, it also up-regulates the expression of interleukin-8 (IL-8) and it’s likely murine homolog Cxcl15, which in turns drives the recruitment of polymorphonuclear myeloid-derived suppressor cells (PMN-MDSCs). Indeed, combining immune checkpoint blockade with a treatment intervention that mitigates the recruitment of PMN-MDSCs prior to ADT delays the onset of castration-resistance disease.

References

1 Siegel, R. L., Miller, K. D. & Jemal, A. Cancer statistics, 2020. *CA Cancer J Clin* **70**, 7-30, doi:10.3322/caac.21590 (2020).

2 Tosoian, J. J. *et al.* Active surveillance program for prostate cancer: an update of the Johns Hopkins experience. *J Clin Oncol* **29**, 2185-2190, doi:10.1200/JCO.2010.32.8112 (2011).

3 Freedland, S. J. & Moul, J. W. Prostate specific antigen recurrence after definitive therapy. *J Urol* **177**, 1985-1991, doi:S0022-5347(07)00275-3 [pii] 10.1016/j.juro.2007.01.137 (2007).

4 Harris, W. P., Mostaghel, E. A., Nelson, P. S. & Montgomery, B. Androgen deprivation therapy: progress in understanding mechanisms of resistance and optimizing androgen depletion. *Nat Clin Pract Urol* **6**, 76-85, doi:10.1038/ncpuro1296 (2009).

5 Drake, C. G., Sharma, P. & Gerritsen, W. Metastatic castration-resistant prostate cancer: new therapies, novel combination strategies and implications for immunotherapy. *Oncogene* **33**, 5053-5064, doi:10.1038/onc.2013.497 (2014).

6 Topalian, S. L., Drake, C. G. & Pardoll, D. M. Immune checkpoint blockade: a common denominator approach to cancer therapy. *Cancer Cell* **27**, 450-461, doi:S1535-6108(15)00089-6 [pii];10.1016/j.ccell.2015.03.001 [doi] (2015).

7 Drake, C. G., Lipson, E. J. & Brahmer, J. R. Breathing new life into immunotherapy: review of melanoma, lung and kidney cancer. *Nat. Rev. Clin. Oncol* **11**, 24-37, doi:nrclinonc.2013.208 [pii];10.1038/nrclinonc.2013.208 [doi] (2014).

8 Sauter, B. *et al.* Consequences of cell death: exposure to necrotic tumor cells, but not primary tissue cells or apoptotic cells, induces the maturation of immunostimulatory dendritic cells. *J. Exp. Med* **191**, 423-434 (2000).

9 Murphy, K., et al. The Adaptive Immune Response: T-cell-Mediated Immunity. In: Janeway's Immunobiology. 9th ed. *Garland Science/Taylor & Francis* (2017).

10 Medzhitov, R. & Janeway, C., Jr. Innate immune recognition: mechanisms and pathways. *Immunol. Rev* **173**, 89-97 (2000).

11 Dunn, G. P., Old, L. J. & Schreiber, R. D. The immunobiology of cancer immunosurveillance and immunoediting. *Immunity* **21**, 137-148 (2004).

12 Teng, M. W., Ngiow, S. F., Ribas, A. & Smyth, M. J. Classifying Cancers Based on T-cell Infiltration and PD-L1. *Cancer Res* **75**, 2139-2145, doi:10.1158/0008-5472.CAN-15-0255 (2015).

13 Mao W, D. C. Immunotherapy for Prostate Cancer: An Evolving Landscape. In: Laurence Zitvogel & Guido Kroemer, editors. Oncoimmunology: a practical guide for cancer immunotherapy. *Springer*, pp. 593–606 (2018).

14 Xing, Y. & Hogquist, K. A. T-cell tolerance: central and peripheral. *Cold Spring Harb Perspect Biol* **4**, doi:10.1101/cshperspect.a006957 (2012).

15 Bousso, P., Bhakta, N. R., Lewis, R. S. & Robey, E. Dynamics of thymocyte-stromal cell interactions visualized by two-photon microscopy. *Science* **296**, 1876-1880, doi:10.1126/science.1070945 (2002).

16 Ueno, T. *et al.* CCR7 signals are essential for cortex-medulla migration of developing thymocytes. *J Exp Med* **200**, 493-505, doi:10.1084/jem.20040643 (2004).

17 Laan, M. & Peterson, P. The many faces of aire in central tolerance. *Front Immunol* **4**, 326, doi:10.3389/fimmu.2013.00326 (2013).

18 Palmer, E. Negative selection--clearing out the bad apples from the T-cell repertoire. *Nat Rev Immunol* **3**, 383-391, doi:10.1038/nri1085 (2003).

19 Walker, L. S. & Abbas, A. K. The enemy within: keeping self-reactive T cells at bay in the periphery. *Nat Rev Immunol* **2**, 11-19, doi:10.1038/nri701 (2002).

20 Wells, A. D. New insights into the molecular basis of T cell anergy: anergy factors, avoidance sensors, and epigenetic imprinting. *J Immunol* **182**, 7331-7341, doi:10.4049/jimmunol.0803917 (2009).

21 Schwartz, R. H., Mueller, D. L., Jenkins, M. K. & Quill, H. T-cell clonal anergy. *Cold Spring Harb Symp Quant Biol* **54 Pt 2**, 605-610, doi:10.1101/sqb.1989.054.01.072 (1989).

22 Quill, H. & Schwartz, R. H. Stimulation of normal inducer T cell clones with antigen presented by purified Ia molecules in planar lipid membranes:

specific induction of a long-lived state of proliferative nonresponsiveness. *J Immunol* **138**, 3704-3712 (1987).

23 Crespo, J., Sun, H., Welling, T. H., Tian, Z. & Zou, W. T cell anergy, exhaustion, senescence, and stemness in the tumor microenvironment. *Curr Opin Immunol* **25**, 214-221, doi:10.1016/j.coi.2012.12.003 (2013).

24 Parish, I. A. & Heath, W. R. Too dangerous to ignore: self-tolerance and the control of ignorant autoreactive T cells. *Immunol Cell Biol* **86**, 146-152, doi:10.1038/sj.icb.7100161 (2008).

25 Hui, L. & Chen, Y. Tumor microenvironment: Sanctuary of the devil. *Cancer Lett* **368**, 7-13, doi:10.1016/j.canlet.2015.07.039 (2015).

26 Attanasio, J. & Wherry, E. J. Costimulatory and Coinhibitory Receptor Pathways in Infectious Disease. *Immunity* **44**, 1052-1068, doi:10.1016/j.immuni.2016.04.022 (2016).

27 Wherry, E. J. & Kurachi, M. Molecular and cellular insights into T cell exhaustion. *Nat Rev Immunol* **15**, 486-499, doi:10.1038/nri3862 (2015).

28 Blackburn, S. D. *et al.* Coregulation of CD8+ T cell exhaustion by multiple inhibitory receptors during chronic viral infection. *Nat Immunol* **10**, 29-37, doi:10.1038/ni.1679 (2009).

29 Liston, A. & Gray, D. H. Homeostatic control of regulatory T cell diversity. *Nat Rev Immunol* **14**, 154-165, doi:10.1038/nri3605 (2014).

30 Cabrera, T. *et al.* High frequency of altered HLA class I phenotypes in invasive breast carcinomas. *Hum Immunol* **50**, 127-134, doi:10.1016/0198-8859(96)00145-0 (1996).

31 Marincola, F. M., Jaffee, E. M., Hicklin, D. J. & Ferrone, S. Escape of human solid tumors from T-cell recognition: molecular mechanisms and functional significance. *Adv Immunol* **74**, 181-273, doi:10.1016/s0065-2776(08)60911-6 (2000).

32 Natali, P. G. *et al.* Selective changes in expression of HLA class I polymorphic determinants in human solid tumors. *Proc Natl Acad Sci U S A* **86**, 6719-6723, doi:10.1073/pnas.86.17.6719 (1989).

33 Blades, R. A., Keating, P. J., McWilliam, L. J., George, N. J. & Stern, P. L. Loss of HLA class I expression in prostate cancer: implications for immunotherapy. *Urology* **46**, 681-686; discussion 686-687, doi:10.1016/S0090-4295(99)80301-X (1995).

34 McGranahan, N. *et al.* Allele-Specific HLA Loss and Immune Escape in Lung Cancer Evolution. *Cell* **171**, 1259-1271 e1211, doi:10.1016/j.cell.2017.10.001 (2017).

35 Almand, B. *et al.* Clinical significance of defective dendritic cell differentiation in cancer. *Clin Cancer Res* **6**, 1755-1766 (2000).

36 Vicari, A. P., Caux, C. & Trinchieri, G. Tumour escape from immune surveillance through dendritic cell inactivation. *Semin Cancer Biol* **12**, 33-42, doi:10.1006/scbi.2001.0400 (2002).

37 Pinzon-Charry, A., Maxwell, T. & Lopez, J. A. Dendritic cell dysfunction in cancer: a mechanism for immunosuppression. *Immunol Cell Biol* **83**, 451-461, doi:10.1111/j.1440-1711.2005.01371.x (2005).

38 Brunet, J. F. *et al.* A new member of the immunoglobulin superfamily--CTLA-4. *Nature* **328**, 267-270, doi:10.1038/328267a0 (1987).

39 Ishida, Y., Agata, Y., Shibahara, K. & Honjo, T. Induced expression of PD-1, a novel member of the immunoglobulin gene superfamily, upon programmed cell death. *EMBO J* **11**, 3887-3895 (1992).

40 Freeman, G. J. *et al.* Engagement of the PD-1 immunoinhibitory receptor by a novel B7 family member leads to negative regulation of lymphocyte activation. *J Exp Med* **192**, 1027-1034, doi:10.1084/jem.192.7.1027 (2000).

41 Topalian, S. L. *et al.* Safety, activity, and immune correlates of anti-PD-1 antibody in cancer. *N. Engl. J. Med* **366**, 2443-2454, doi:10.1056/NEJMoa1200690 [doi] (2012).

42 Leach, D. R., Krummel, M. F. & Allison, J. P. Enhancement of antitumor immunity by CTLA-4 blockade. *Science* **271**, 1734-1736, doi:10.1126/science.271.5256.1734 (1996).

43 O'Day, S. J. *et al.* Efficacy and safety of ipilimumab monotherapy in patients with pretreated advanced melanoma: a multicenter single-arm phase II study. *Ann Oncol* **21**, 1712-1717, doi:10.1093/annonc/mdq013 (2010).

44 Chen, L. Co-inhibitory molecules of the B7-CD28 family in the control of T-cell immunity. *Nat Rev Immunol* **4**, 336-347, doi:10.1038/nri1349 (2004).

45 Spranger, S. & Gajewski, T. F. Mechanisms of Tumor Cell–Intrinsic Immune Evasion. *Annual Review of Cancer Biology* **2**, 213-228, doi:10.1146/annurev-cancerbio-030617-050606 (2018).

46 Harding, F. A., McArthur, J. G., Gross, J. A., Raulet, D. H. & Allison, J. P. CD28-mediated signalling co-stimulates murine T cells and prevents induction of anergy in T-cell clones. *Nature* **356**, 607-609, doi:10.1038/356607a0 (1992).

47 Wolchok, J. D. *et al.* Development of ipilimumab: a novel immunotherapeutic approach for the treatment of advanced melanoma. *Ann. N. Y. Acad. Sci* **1291**, 1-13, doi:10.1111/nyas.12180 [doi] (2013).

48 Chen, L. & Flies, D. B. Molecular mechanisms of T cell co-stimulation and co-inhibition. *Nat Rev Immunol* **13**, 227-242, doi:10.1038/nri3405 (2013).

49 Pardoll, D. M. The blockade of immune checkpoints in cancer immunotherapy. *Nat Rev Cancer* **12**, 252-264, doi:10.1038/nrc3239 (2012).

50 Wing, K. *et al.* CTLA-4 control over Foxp3+ regulatory T cell function. *Science* **322**, 271-275, doi:10.1126/science.1160062 (2008).

51 Tivol, E. A. *et al.* Loss of CTLA-4 leads to massive lymphoproliferation and fatal multiorgan tissue destruction, revealing a critical negative regulatory role of CTLA-4. *Immunity* **3**, 541-547, doi:10.1016/1074-7613(95)90125-6 (1995).

52 Waterhouse, P. *et al.* Lymphoproliferative disorders with early lethality in mice deficient in Ctla-4. *Science* **270**, 985-988, doi:10.1126/science.270.5238.985 (1995).

53 Drake, C. G., Jaffee, E. & Pardoll, D. M. Mechanisms of immune evasion by tumors. *Adv Immunol* **90**, 51-81, doi:10.1016/S0065-2776(06)90002-9 (2006).

54 Beer, T. M. *et al.* Randomized, Double-Blind, Phase III Trial of Ipilimumab Versus Placebo in Asymptomatic or Minimally Symptomatic Patients With Metastatic Chemotherapy-Naive Castration-Resistant Prostate Cancer. *J Clin Oncol* **35**, 40-47, doi:10.1200/JCO.2016.69.1584 [pii], 10.1200/JCO.2016.69.1584 (2017).

55 Shen, Y. C. *et al.* Combining intratumoral Treg depletion with androgen deprivation therapy (ADT): preclinical activity in the Myc-CaP model. *Prostate Cancer Prostatic Dis* **21**, 113-125, doi:10.1038/s41391-017-0013-x (2018).

56 Gao, J. *et al.* VISTA is an inhibitory immune checkpoint that is increased after ipilimumab therapy in patients with prostate cancer. *Nat Med* **23**, 551-555, doi:10.1038/nm.4308 (2017).

57 Leach, D. R., Krummel, M. F. & Allison, J. P. Enhancement of antitumor immunity by CTLA-4 blockade. *Science* **271**, 1734-1736 (1996).

58 Arce Vargas, F. *et al.* Fc Effector Function Contributes to the Activity of Human Anti-CTLA-4 Antibodies. *Cancer Cell* **33**, 649-663 e644, doi:10.1016/j.ccell.2018.02.010 (2018).

59 Kwon, E. D. *et al.* Ipilimumab versus placebo after radiotherapy in patients with metastatic castration-resistant prostate cancer that had progressed after docetaxel chemotherapy (CA184-043): a multicentre, randomised, double-blind, phase 3 trial. *Lancet Oncol* **15**, 700-712, doi:S1470-2045(14)70189-5 [pii];10.1016/S1470-2045(14)70189-5 [doi] (2014).

60 Fizazi, K. *et al.* Final Analysis of the Ipilimumab Versus Placebo Following Radiotherapy Phase III Trial in Postdocetaxel Metastatic Castration-resistant Prostate Cancer Identifies an Excess of Long-term Survivors. *Eur Urol*, doi:10.1016/j.eururo.2020.07.032 (2020).

61 Keir, M. E. *et al.* Tissue expression of PD-L1 mediates peripheral T cell tolerance. *J. Exp. Med* **203**, 883-895 (2006).

62 Dong, H., Zhu, G., Tamada, K. & Chen, L. B7-H1, a third member of the B7 family, co-stimulates T-cell proliferation and interleukin-10 secretion. *Nat. Med* **5**, 1365-1369, doi:10.1038/70932 [doi] (1999).

63 Goldberg, M. V. *et al.* Role of PD-1 and its ligand, B7-H1, in early fate decisions of CD8 T cells. *Blood* **110**, 186-192, doi:10.1182/blood-2006-12-062422 (2007).

64 Salmon, H. *et al.* Expansion and Activation of CD103(+) Dendritic Cell Progenitors at the Tumor Site Enhances Tumor Responses to Therapeutic PD-L1 and BRAF Inhibition. *Immunity* **44**, 924-938, doi:10.1016/j.immuni.2016.03.012 (2016).

65 Chemnitz, J. M., Parry, R. V., Nichols, K. E., June, C. H. & Riley, J. L. SHP-1 and SHP-2 associate with immunoreceptor tyrosine-based switch motif of programmed death 1 upon primary human T cell stimulation, but only receptor ligation prevents T cell activation. *J Immunol* **173**, 945-954, doi:10.4049/jimmunol.173.2.945 (2004).

66 Peled, M. *et al.* Affinity purification mass spectrometry analysis of PD-1 uncovers SAP as a new checkpoint inhibitor. *Proc Natl Acad Sci U S A* **115**, E468-E477, doi:10.1073/pnas.1710437115 (2018).

67 Nishimura, H., Minato, N., Nakano, T. & Honjo, T. Immunological studies on PD-1 deficient mice: implication of PD-1 as a negative regulator for B cell responses. *Int Immunol* **10**, 1563-1572, doi:10.1093/intimm/10.10.1563 (1998).

68 Nishimura, H., Nose, M., Hiai, H., Minato, N. & Honjo, T. Development of lupus-like autoimmune diseases by disruption of the PD-1 gene encoding an ITIM motif-carrying immunoreceptor. *Immunity* **11**, 141-151, doi:10.1016/s1074-7613(00)80089-8 (1999).

69 Nishimura, H. *et al.* Autoimmune dilated cardiomyopathy in PD-1 receptor-deficient mice. *Science* **291**, 319-322, doi:10.1126/science.291.5502.319 (2001).

70 Zou, W., Wolchok, J. D. & Chen, L. PD-L1 (B7-H1) and PD-1 pathway blockade for cancer therapy: Mechanisms, response biomarkers, and combinations. *Sci Transl Med* **8**, 328rv324, doi:10.1126/scitranslmed.aad7118 (2016).

71 Haffner, M. C. *et al.* Comprehensive Evaluation of Programmed Death-Ligand 1 Expression in Primary and Metastatic Prostate Cancer. *Am J Pathol* **188**, 1478-1485, doi:10.1016/j.ajpath.2018.02.014 (2018).

72 Taube, J. M. *et al.* Colocalization of inflammatory response with b7-h1 expression in human melanocytic lesions supports an adaptive resistance mechanism of immune escape. *Sci. Transl. Med* **4**, 127ra137, doi:4/127/127ra37 [pii];10.1126/scitranslmed.3003689 [doi] (2012).

73 Ribas, A. Adaptive Immune Resistance: How Cancer Protects from Immune Attack. *Cancer Discov* **5**, 915-919, doi:10.1158/2159-8290.CD-15-0563 (2015).

74 Martin, A. M. *et al.* Paucity of PD-L1 expression in prostate cancer: innate and adaptive immune resistance. *Prostate Cancer Prostatic Dis* **18**, 325-332, doi:10.1038/pcan.2015.39 (2015).

75 Spranger, S. *et al.* Up-regulation of PD-L1, IDO, and T(regs) in the melanoma tumor microenvironment is driven by CD8(+) T cells. *Sci Transl Med* **5**, 200ra116, doi:10.1126/scitranslmed.3006504 (2013).

76 Venturini, N. J. & Drake, C. G. Immunotherapy for Prostate Cancer. *Cold Spring Harb Perspect Med* **9**, doi:10.1101/cshperspect.a030627 (2019).

77 Li, Y. *et al.* The Clinicopathologic and Prognostic Significance of Programmed Cell Death Ligand 1 (PD-L1) Expression in Patients With Prostate Cancer: A Systematic Review and Meta-Analysis. *Front Pharmacol* **9**, 1494, doi:10.3389/fphar.2018.01494 (2018).

78 Bono, J. S. D. *et al.* KEYNOTE-199: Pembrolizumab (pembro) for docetaxel-refractory metastatic castration-resistant prostate cancer (mCRPC). *Journal of Clinical Oncology* **36**, 5007-5007, doi:10.1200/JCO.2018.36.15_suppl.5007 (2018).

79 McDermott, D. F. *et al.* Pembrolizumab monotherapy as first-line therapy in advanced clear cell renal cell carcinoma (accRCC): Results from cohort A of KEYNOTE-427. *Journal of Clinical Oncology* **36**, 4500-4500, doi:10.1200/JCO.2018.36.15_suppl.4500 (2018).

80 Bellmunt, J. *et al.* Pembrolizumab as Second-Line Therapy for Advanced Urothelial Carcinoma. *N Engl J Med* **376**, 1015-1026, doi:10.1056/NEJMoa1613683 (2017).

81 Galon, J. *et al.* Cancer classification using the Immunoscore: a worldwide task force. *J Transl Med* **10**, 205, doi:10.1186/1479-5876-10-205 (2012).

82 Bonaventura, P. *et al.* Cold Tumors: A Therapeutic Challenge for Immunotherapy. *Front Immunol* **10**, 168, doi:10.3389/fimmu.2019.00168 (2019).

83 Chen, D. S. & Mellman, I. Oncology meets immunology: the cancer-immunity cycle. *Immunity* **39**, 1-10, doi:10.1016/j.immuni.2013.07.012 (2013).

84 Mildner, A. & Jung, S. Development and function of dendritic cell subsets. *Immunity* **40**, 642-656, doi:10.1016/j.immuni.2014.04.016 (2014).

85 Merad, M., Sathe, P., Helft, J., Miller, J. & Mortha, A. The dendritic cell lineage: ontogeny and function of dendritic cells and their subsets in the steady state and the inflamed setting. *Annu Rev Immunol* **31**, 563-604, doi:10.1146/annurev-immunol-020711-074950 (2013).

86 Haniffa, M. *et al.* Human tissues contain CD141hi cross-presenting dendritic cells with functional homology to mouse CD103+ nonlymphoid dendritic cells. *Immunity* **37**, 60-73, doi:10.1016/j.immuni.2012.04.012 (2012).

87 van der Aa, E., van Montfoort, N. & Woltman, A. M. BDCA3(+)CLEC9A(+) human dendritic cell function and development. *Semin Cell Dev Biol* **41**, 39-48, doi:10.1016/j.semcdb.2014.05.016 (2015).

88 Durham, N. M. & Drake, C. G. *Cancer Immunotherapy: Chapter 18. Dendritic Cell Vaccines: Sipuleucel-T and Other Approaches*. (Elsevier Inc. Chapters, 2013).

89 Ghiringhelli, F. *et al.* Tumor cells convert immature myeloid dendritic cells into TGF-beta-secreting cells inducing CD4+CD25+ regulatory T cell proliferation. *J Exp Med* **202**, 919-929, doi:10.1084/jem.20050463 (2005).

90 Allavena, P. *et al.* IL-10 prevents the differentiation of monocytes to dendritic cells but promotes their maturation to macrophages. *Eur J Immunol* **28**, 359-369, doi:Doi 10.1002/(Sici)1521-4141(199801)28:01<359::Aid-Immu359>3.0.Co;2-4 (1998).

91 Buelens, C. *et al.* Interleukin-10 prevents the generation of dendritic cells from human peripheral blood mononuclear cells cultured with interleukin-4 and granulocyte/macrophage-colony-stimulating factor. *Eur J Immunol* **27**, 756-762, doi:10.1002/eji.1830270326 (1997).

92 Munn, D. H., Sharma, M. D. & Mellor, A. L. Ligation of B7-1/B7-2 by human CD4+ T cells triggers indoleamine 2,3-dioxygenase activity in dendritic cells. *J Immunol* **172**, 4100-4110 (2004).

93 Platten, M., von Knebel Doeberitz, N., Oezen, I., Wick, W. & Ochs, K. Cancer Immunotherapy by Targeting IDO1/TDO and Their Downstream Effectors. *Front Immunol* **5**, 673, doi:10.3389/fimmu.2014.00673 (2014).

94 Murray, P. J. & Wynn, T. A. Protective and pathogenic functions of macrophage subsets. *Nat Rev Immunol* **11**, 723-737, doi:10.1038/nri3073 (2011).

95 Condamine, T., Mastio, J. & Gabrilovich, D. I. Transcriptional regulation of myeloid-derived suppressor cells. *J Leukoc Biol* **98**, 913-922, doi:10.1189/jlb.4RI0515-204R (2015).

96 Solito, S. *et al.* Myeloid-derived suppressor cell heterogeneity in human cancers. *Ann N Y Acad Sci* **1319**, 47-65, doi:10.1111/nyas.12469 (2014).

97 Bronte, V. *et al.* Recommendations for myeloid-derived suppressor cell nomenclature and characterization standards. *Nat Commun* **7**, 12150, doi:10.1038/ncomms12150 (2016).

98 Marvel, D. & Gabrilovich, D. I. Myeloid-derived suppressor cells in the tumor microenvironment: expect the unexpected. *J Clin Invest* **125**, 3356-3364, doi:10.1172/JCI80005 (2015).

99 Kumar, V., Patel, S., Tcyganov, E. & Gabrilovich, D. I. The Nature of Myeloid-Derived Suppressor Cells in the Tumor Microenvironment. *Trends Immunol* **37**, 208-220, doi:10.1016/j.it.2016.01.004 (2016).

100 Chetram, M. A., Don-Salu-Hewage, A. S. & Hinton, C. V. ROS enhances CXCR4-mediated functions through inactivation of PTEN in prostate cancer cells. *Biochem Biophys Res Commun* **410**, 195-200, doi:10.1016/j.bbrc.2011.05.074 (2011).

101 Cubillos-Ruiz, J. R. *et al.* ER Stress Sensor XBP1 Controls Anti-tumor Immunity by Disrupting Dendritic Cell Homeostasis. *Cell* **161**, 1527-1538, doi:10.1016/j.cell.2015.05.025 (2015).

102 Molon, B. *et al.* Chemokine nitration prevents intratumoral infiltration of antigen-specific T cells. *J Exp Med* **208**, 1949-1962, doi:10.1084/jem.20101956 (2011).

103 Nagaraj, S. *et al.* Altered recognition of antigen is a mechanism of CD8+ T cell tolerance in cancer. *Nat Med* **13**, 828-835, doi:nm1609 [pii], 10.1038/nm1609 (2007).

104 Hanson, E. M., Clements, V. K., Sinha, P., Ilkovitch, D. & Ostrand-Rosenberg, S. Myeloid-derived suppressor cells down-regulate L-selectin expression on CD4+ and CD8+ T cells. *J Immunol* **183**, 937-944, doi:10.4049/jimmunol.0804253 (2009).

105 Floriano-Sanchez, E., Castro-Marin, M. & Cardenas-Rodriguez, N. [Molecular markers associated with prostate cancer: 3-nitrotyrosine and genetic and proteic expression of Mn-superoxide dismutasa (Mn-SOD)]. *Arch Esp Urol* **62**, 702-711 (2009).

106 Franklin, R. A. & Li, M. O. Ontogeny of Tumor-associated Macrophages and Its Implication in Cancer Regulation. *Trends Cancer* **2**, 20-34, doi:10.1016/j.trecan.2015.11.004 (2016).

107 Auffray, C., Sieweke, M. H. & Geissmann, F. Blood monocytes: development, heterogeneity, and relationship with dendritic cells. *Annu Rev Immunol* **27**, 669-692, doi:10.1146/annurev.immunol.021908.132557 (2009).

108 Sica, A., Erreni, M., Allavena, P. & Porta, C. Macrophage polarization in pathology. *Cell Mol Life Sci* **72**, 4111-4126, doi:10.1007/s00018-015-1995-y (2015).

109 Mantovani, A., Sozzani, S., Locati, M., Allavena, P. & Sica, A. Macrophage polarization: tumor-associated macrophages as a paradigm for polarized M2 mononuclear phagocytes. *Trends Immunol* **23**, 549-555 (2002).

110 Murray, P. J. *et al.* Macrophage activation and polarization: nomenclature and experimental guidelines. *Immunity* **41**, 14-20, doi:10.1016/j.immuni.2014.06.008 (2014).

111 Movahedi, K. *et al.* Different tumor microenvironments contain functionally distinct subsets of macrophages derived from Ly6C(high) monocytes. *Cancer Res* **70**, 5728-5739, doi:10.1158/0008-5472.CAN-09-4672 (2010).

112 De Marzo, A. M. *et al.* Inflammation in prostate carcinogenesis. *Nat Rev Cancer* **7**, 256-269, doi:10.1038/nrc2090 (2007).

113 Sfanos, K. S. & De Marzo, A. M. Prostate cancer and inflammation: the evidence. *Histopathology* **60**, 199-215, doi:10.1111/j.1365-2559.2011.04033.x (2012).

114 Gurel, B. *et al.* Chronic inflammation in benign prostate tissue is associated with high-grade prostate cancer in the placebo arm of the prostate cancer prevention trial. *Cancer Epidemiol Biomarkers Prev* **23**, 847-856, doi:10.1158/1055-9965.EPI-13-1126 (2014).

115 Le Magnen, C. *et al.* Cooperation of loss of NKX3.1 and inflammation in prostate cancer initiation. *Dis Model Mech* **11**, doi:10.1242/dmm.035139 (2018).

116 Simons, B. W. *et al.* A human prostatic bacterial isolate alters the prostatic microenvironment and accelerates prostate cancer progression. *J Pathol* **235**, 478-489, doi:10.1002/path.4472 (2015).

117 Yu, S. H. *et al.* A Paracrine Role for IL6 in Prostate Cancer Patients: Lack of Production by Primary or Metastatic Tumor Cells. *Cancer Immunol Res* **3**, 1175-1184, doi:10.1158/2326-6066.CIR-15-0013 (2015).

118 Smith, P. C., Hobisch, A., Lin, D. L., Culig, Z. & Keller, E. T. Interleukin-6 and prostate cancer progression. *Cytokine Growth Factor Rev* **12**, 33-40 (2001).

119 Ara, T. & DeClerck, Y. A. Interleukin-6 in bone metastasis and cancer progression. *Eur J Cancer* **46**, 1223-1231, doi:10.1016/j.ejca.2010.02.026 (2010).

120 Roca, H. *et al.* CCL2 and interleukin-6 promote survival of human CD11b+ peripheral blood mononuclear cells and induce M2-type macrophage polarization. *J Biol Chem* **284**, 34342-34354, doi:10.1074/jbc.M109.042671 (2009).

121 Bettelli, E., Oukka, M. & Kuchroo, V. K. T(H)-17 cells in the circle of immunity and autoimmunity. *Nat Immunol* **8**, 345-350, doi:10.1038/ni0407-345 (2007).

122 Zou, W. & Restifo, N. P. T(H)17 cells in tumour immunity and immunotherapy. *Nat Rev Immunol* **10**, 248-256, doi:10.1038/nri2742 (2010).

123 Wang, L. *et al.* IL-17 can promote tumor growth through an IL-6-Stat3 signaling pathway. *J Exp Med* **206**, 1457-1464, doi:10.1084/jem.20090207 (2009).

124 Li, Q. *et al.* Interleukin-17 Indirectly Promotes M2 Macrophage Differentiation through Stimulation of COX-2/PGE2 Pathway in the Cancer Cells. *Cancer Res Treat* **46**, 297-306, doi:10.4143/crt.2014.46.3.297 (2014).

125 Park, J. Y., Pillinger, M. H. & Abramson, S. B. Prostaglandin E2 synthesis and secretion: the role of PGE2 synthases. *Clin Immunol* **119**, 229-240, doi:10.1016/j.clim.2006.01.016 (2006).

126 Heusinkveld, M. *et al.* M2 macrophages induced by prostaglandin E2 and IL-6 from cervical carcinoma are switched to activated M1 macrophages by CD4+ Th1 cells. *J Immunol* **187**, 1157-1165, doi:10.4049/jimmunol.1100889 (2011).

127 Engblom, C., Pfirschke, C. & Pittet, M. J. The role of myeloid cells in cancer therapies. *Nature Reviews Cancer* **16**, 447-462 (2016).

128 Nuhn, P. *et al.* Association of pretreatment neutrophil-to-lymphocyte ratio (NLR) and overall survival (OS) in patients with metastatic castration-resistant prostate cancer (mCRPC) treated with first-line docetaxel. *BJU Int* **114**, E11-17, doi:10.1111/bju.12531 (2014).

129 Brusa, D. *et al.* Circulating immunosuppressive cells of prostate cancer patients before and after radical prostatectomy: profile comparison. *Int J Urol* **20**, 971-978, doi:10.1111/iju.12086 (2013).

130 Vuk-Pavlovic, S. *et al.* Immunosuppressive CD14+HLA-DRlow/- monocytes in prostate cancer. *Prostate* **70**, 443-455, doi:10.1002/pros.21078 (2010).

131 Idorn, M., Kollgaard, T., Kongsted, P., Sengelov, L. & Thor Straten, P. Correlation between frequencies of blood monocytic myeloid-derived suppressor cells, regulatory T cells and negative prognostic markers in patients with castration-resistant metastatic prostate cancer. *Cancer Immunol Immunother* **63**, 1177-1187, doi:10.1007/s00262-014-1591-2 (2014).

132 Chi, N., Tan, Z., Ma, K., Bao, L. & Yun, Z. Increased circulating myeloid-derived suppressor cells correlate with cancer stages, interleukin-8 and -6 in prostate cancer. *Int J Clin Exp Med* **7**, 3181-3192 (2014).

133 Hossain, D. M. *et al.* TLR9-Targeted STAT3 Silencing Abrogates Immunosuppressive Activity of Myeloid-Derived Suppressor Cells from Prostate Cancer Patients. *Clin Cancer Res* **21**, 3771-3782, doi:10.1158/1078-0432.CCR-14-3145 (2015).

134 Komatsu, N. *et al.* Gene expression profiles in peripheral blood as a biomarker in cancer patients receiving peptide vaccination. *Cancer* **118**, 3208-3221, doi:10.1002/cncr.26636 (2012).

135 Kawahara, T. *et al.* Neutrophil-to-lymphocyte ratio predicts prostatic carcinoma in men undergoing needle biopsy. *Oncotarget* **6**, 32169-32176, doi:10.18632/oncotarget.5081 (2015).

136 Yin, X. *et al.* Prognostic Role of Neutrophil-to-Lymphocyte Ratio in Prostate Cancer: A Systematic Review and Meta-analysis. *Medicine (Baltimore)* **95**, e2544, doi:10.1097/MD.0000000000002544 (2016).

137 Meisel, A. *et al.* Severe neutropenia during cabazitaxel treatment is associated with survival benefit in men with metastatic castration-resistant prostate cancer (mCRPC): A post-hoc analysis of the TROPIC phase III trial. *Eur J Cancer* **56**, 93-100, doi:10.1016/j.ejca.2015.12.009 (2016).

138 Condamine, T. *et al.* Lectin-type oxidized LDL receptor-1 distinguishes population of human polymorphonuclear myeloid-derived suppressor cells in cancer patients. *Science Immunology* **1**, aaf8943 (2016).

139 Lanciotti, M. *et al.* The role of M1 and M2 macrophages in prostate cancer in relation to extracapsular tumor extension and biochemical recurrence after radical prostatectomy. *Biomed Res Int* **2014**, 486798, doi:10.1155/2014/486798 (2014).

140 Nonomura, N. *et al.* Infiltration of tumour-associated macrophages in prostate biopsy specimens is predictive of disease progression after hormonal therapy for prostate cancer. *BJU Int* **107**, 1918-1922, doi:10.1111/j.1464-410X.2010.09804.x (2011).

141 Gannon, P. O. *et al.* Characterization of the intra-prostatic immune cell infiltration in androgen-deprived prostate cancer patients. *J Immunol Methods* **348**, 9-17, doi:10.1016/j.jim.2009.06.004 (2009).

142 Zhu, P. *et al.* Macrophage/cancer cell interactions mediate hormone resistance by a nuclear receptor derepression pathway. *Cell* **124**, 615-629, doi:10.1016/j.cell.2005.12.032 (2006).

143 Escamilla, J. *et al.* CSF1 receptor targeting in prostate cancer reverses macrophage-mediated resistance to androgen blockade therapy. *Cancer Res* **75**, 950-962, doi:10.1158/0008-5472.CAN-14-0992 (2015).

144 Halin, S., Rudolfsson, S. H., Van Rooijen, N. & Bergh, A. Extratumoral macrophages promote tumor and vascular growth in an orthotopic rat prostate tumor model. *Neoplasia* **11**, 177-186 (2009).

145 Xu, J. *et al.* CSF1R signaling blockade stanches tumor-infiltrating myeloid cells and improves the efficacy of radiotherapy in prostate cancer. *Cancer Res* **73**, 2782-2794, doi:10.1158/0008-5472.CAN-12-3981 (2013).

146 Fridman, W. H. *et al.* The immune microenvironment: a major player in human cancers. *Int Arch Allergy Immunol* **164**, 13-26, doi:10.1159/000362332 (2014).

147 Sciarra, A. *et al.* Characterization of circulating blood dendritic cell subsets DC123+ (lymphoid) and DC11C+ (myeloid) in prostate adenocarcinoma patients. *Prostate* **67**, 1-7, doi:10.1002/pros.20431 (2007).

148 Sheikh, N. A. *et al.* Sipuleucel-T immune parameters correlate with survival: an analysis of the randomized phase 3 clinical trials in men with castration-resistant prostate cancer. *Cancer Immunol Immunother* **62**, 137-147, doi:10.1007/s00262-012-1317-2 (2013).

149 Gundem, G. *et al.* The evolutionary history of lethal metastatic prostate cancer. *Nature* **520**, 353-357, doi:10.1038/nature14347 (2015).

150 Mantovani, A., Allavena, P., Sica, A. & Balkwill, F. Cancer-related inflammation. *Nature* **454**, 436-444, doi:10.1038/nature07205 (2008).

151 Joyce, J. A. & Pollard, J. W. Microenvironmental regulation of metastasis. *Nat Rev Cancer* **9**, 239-252, doi:10.1038/nrc2618 (2009).

152 Lin, E. Y., Nguyen, A. V., Russell, R. G. & Pollard, J. W. Colony-stimulating factor 1 promotes progression of mammary tumors to malignancy. *J Exp Med* **193**, 727-740 (2001).

153 Smith, M. R. *et al.* Denosumab and bone-metastasis-free survival in men with castration-resistant prostate cancer: results of a phase 3, randomised, placebo-controlled trial. *Lancet* **379**, 39-46, doi:10.1016/S0140-6736(11)61226-9 (2012).

154 Sugiyama, T., Kohara, H., Noda, M. & Nagasawa, T. Maintenance of the hematopoietic stem cell pool by CXCL12-CXCR4 chemokine signaling in bone marrow stromal cell niches. *Immunity* **25**, 977-988, doi:S1074-7613(06)00515-2 [pii], 10.1016/j.immuni.2006.10.016 (2006).

155 Chen, Q. & Zhong, T. The association of CXCR4 expression with clinicopathological significance and potential drug target in prostate cancer: a meta-analysis and literature review. *Drug Des Devel Ther* **9**, 5115-5122, doi:10.2147/DDDT.S82475 (2015).

156 Sun, Y. X. *et al.* Skeletal localization and neutralization of the SDF-1(CXCL12)/CXCR4 axis blocks prostate cancer metastasis and growth in osseous sites in vivo. *J Bone Miner Res* **20**, 318-329, doi:10.1359/JBMR.041109 (2005).

157 Lacey, D. L. *et al.* Bench to bedside: elucidation of the OPG-RANK-RANKL pathway and the development of denosumab. *Nat Rev Drug Discov* **11**, 401-419, doi:10.1038/nrd3705 (2012).

158 Luo, J. L. *et al.* Nuclear cytokine-activated IKKalpha controls prostate cancer metastasis by repressing Maspin. *Nature* **446**, 690-694, doi:10.1038/nature05656 (2007).

159 Toso, A. *et al.* Enhancing chemotherapy efficacy in Pten-deficient prostate tumors by activating the senescence-associated antitumor immunity. *Cell Rep* **9**, 75-89, doi:10.1016/j.celrep.2014.08.044 (2014).

160 Borrello, M. G. *et al.* Induction of a proinflammatory program in normal human thyrocytes by the RET/PTC1 oncogene. *Proc Natl Acad Sci U S A* **102**, 14825-14830, doi:10.1073/pnas.0503039102 (2005).

161 Spranger, S., Bao, R. & Gajewski, T. F. Melanoma-intrinsic beta-catenin signalling prevents anti-tumour immunity. *Nature* **523**, 231-235, doi:10.1038/nature14404 (2015).

162 Peng, W. *et al.* Loss of PTEN Promotes Resistance to T Cell-Mediated Immunotherapy. *Cancer Discov* **6**, 202-216, doi:10.1158/2159-8290.CD-15-0283 (2016).

163 Topalian, S. L. *et al.* Safety, activity, and immune correlates of anti-PD-1 antibody in cancer. *N Engl J Med* **366**, 2443-2454, doi:10.1056/NEJMoa1200690 (2012).

164 Kwon, E. D. *et al.* Ipilimumab versus placebo after radiotherapy in patients with metastatic castration-resistant prostate cancer that had progressed after docetaxel chemotherapy (CA184-043): a multicentre, randomised, double-blind, phase 3 trial. *The lancet oncology* **15**, 700-712 (2014).

165 Slovin, S. F. *et al.* Ipilimumab alone or in combination with radiotherapy in metastatic castration-resistant prostate cancer: results from an open-label, multicenter phase I/II study. *Ann Oncol* **24**, 1813-1821, doi:10.1093/annonc/mdt107 (2013).

166 Graff, J. N. *et al.* Early evidence of anti-PD-1 activity in enzalutamide-resistant prostate cancer. *Oncotarget*, doi:10.18632/oncotarget.10547 (2016).

167 Robinson, D. *et al.* Integrative clinical genomics of advanced prostate cancer. *Cell* **161**, 1215-1228, doi:10.1016/j.cell.2015.05.001 (2015).

168 Vignarajan, S. *et al.* Loss of PTEN stabilizes the lipid modifying enzyme cytosolic phospholipase A(2)alpha via AKT in prostate cancer cells. *Oncotarget* **5**, 6289-6299, doi:10.18632/oncotarget.2198 (2014).

169 Conley-LaComb, M. K. *et al.* PTEN loss mediated Akt activation promotes prostate tumor growth and metastasis via CXCL12/CXCR4 signaling. *Mol Cancer* **12**, 85, doi:10.1186/1476-4598-12-85 (2013).

170 Lotan, T. L. *et al.* PTEN loss is associated with upgrading of prostate cancer from biopsy to radical prostatectomy. *Modern Pathol* **28**, 128-137, doi:10.1038/modpathol.2014.85 (2015).

171 Lotan, T. L. *et al.* PTEN Loss as Determined by Clinical-grade Immunohistochemistry Assay Is Associated with Worse Recurrence-free Survival in Prostate Cancer. *Eur Urol Focus* **2**, 180-188, doi:10.1016/j.euf.2015.07.005 (2016).

172 Garcia, A. J. *et al.* Pten null prostate epithelium promotes localized myeloid-derived suppressor cell expansion and immune suppression during tumor initiation and progression. *Mol Cell Biol* **34**, 2017-2028, doi:10.1128/MCB.00090-14 (2014).

173 Maxwell, P. J., Neisen, J., Messenger, J. & Waugh, D. J. Tumor-derived CXCL8 signaling augments stroma-derived CCL2-promoted proliferation and CXCL12-mediated invasion of PTEN-deficient prostate cancer cells. *Oncotarget* **5**, 4895-4908, doi:10.18632/oncotarget.2052 (2014).

174 Armstrong, C. W. *et al.* PTEN deficiency promotes macrophage infiltration and hypersensitivity of prostate cancer to IAP antagonist/radiation combination therapy. *Oncotarget* **7**, 7885-7898, doi:10.18632/oncotarget.6955 (2016).

175 Neisen, J. L., McCabe, N., Kennedy, R. D. & Waugh, D. J. J. Cabozantinib attenuates CXCL8-driven macrophage-dependent migration and invasion of PTEN-deficient prostate cancer. *Cancer Research* **75**, doi:10.1158/1538-7445.Chtme14-A49 (2015).

176 Hurst, S. M. *et al.* Il-6 and its soluble receptor orchestrate a temporal switch in the pattern of leukocyte recruitment seen during acute inflammation. *Immunity* **14**, 705-714 (2001).

177 Pootrakul, L. *et al.* Expression of stress response protein Grp78 is associated with the development of castration-resistant prostate cancer. *Clin Cancer Res* **12**, 5987-5993, doi:10.1158/1078-0432.CCR-06-0133 (2006).

178 Tan, S. S. *et al.* GRP78 up-regulation is associated with androgen receptor status, Hsp70-Hsp90 client proteins and castrate-resistant prostate cancer. *J Pathol* **223**, 81-87, doi:10.1002/path.2795 (2011).

179 Yadav, R. K., Chae, S. W., Kim, H. R. & Chae, H. J. Endoplasmic reticulum stress and cancer. *J Cancer Prev* **19**, 75-88, doi:10.15430/JCP.2014.19.2.75 (2014).

180 Storm, M., Sheng, X., Arnoldussen, Y. J. & Saatcioglu, F. Prostate cancer and the unfolded protein response. *Oncotarget*, doi:10.18632/oncotarget.9912 (2016).

181 Hetz, C., Chevet, E. & Harding, H. P. Targeting the unfolded protein response in disease. *Nat Rev Drug Discov* **12**, 703-719, doi:10.1038/nrd3976 (2013).

182 Roller, C. & Maddalo, D. The Molecular Chaperone GRP78/BiP in the Development of Chemoresistance: Mechanism and Possible Treatment. *Front Pharmacol* **4**, 10, doi:10.3389/fphar.2013.00010 (2013).

183 Lee, B. R. *et al.* Elevated endoplasmic reticulum stress reinforced immunosuppression in the tumor microenvironment via myeloid-derived suppressor cells. *Oncotarget* **5**, 12331-12345, doi:10.18632/oncotarget.2589 (2014).

184 Fu, Y. *et al.* Pten null prostate tumorigenesis and AKT activation are blocked by targeted knockout of ER chaperone GRP78/BiP in prostate epithelium. *Proc Natl Acad Sci U S A* **105**, 19444-19449, doi:10.1073/pnas.0807691105 (2008).

185 Volmer, R., van der Ploeg, K. & Ron, D. Membrane lipid saturation activates endoplasmic reticulum unfolded protein response transducers through their transmembrane domains. *P Natl Acad Sci USA* **110**, 4628-4633, doi:10.1073/pnas.1217611110 (2013).

186 Van de Sande, T., De Schrijver, E., Heyns, W., Verhoeven, G. & Swinnen, J. V. Role of the phosphatidylinositol 3'-kinase/PTEN/Akt kinase pathway in the overexpression of fatty acid synthase in LNCaP prostate cancer cells. *Cancer Res* **62**, 642-646 (2002).

187 Rysman, E. *et al.* De novo lipogenesis protects cancer cells from free radicals and chemotherapeutics by promoting membrane lipid saturation. *Cancer Res* **70**, 8117-8126, doi:10.1158/0008-5472.CAN-09-3871 (2010).

188 Yang, M. *et al.* Blood fatty acid patterns are associated with prostate cancer risk in a prospective nested case-control study. *Cancer Causes Control* **27**, 1153-1161, doi:10.1007/s10552-016-0794-6 (2016).

189 Mahadevan, N. R. *et al.* Transmission of endoplasmic reticulum stress and pro-inflammation from tumor cells to myeloid cells. *Proc Natl Acad Sci U S A* **108**, 6561-6566, doi:10.1073/pnas.1008942108 (2011).

190 Sodhi, C. P. *et al.* Intestinal Epithelial TLR-4 Activation Is Required for the Development of Acute Lung Injury after Trauma/Hemorrhagic Shock via the Release of HMGB1 from the Gut. *J Immunol* **194**, 4931-4939, doi:10.4049/jimmunol.1402490 (2015).

191 Pierre, N. *et al.* Toll-like receptor 4 knockout mice are protected against endoplasmic reticulum stress induced by a high-fat diet. *PLoS One* **8**, e65061, doi:10.1371/journal.pone.0065061 (2013).

192 Condamine, T. *et al.* ER stress response regulates the fate of myeloid-derived suppressor cells through TRAIL receptors mediated apoptosis. *Journal of Immunology* **192** (2014).

193 Thorpe, J. A. & Schwarze, S. R. IRE1α controls cyclin A1 expression and promotes cell proliferation through XBP-1. *Cell Stress and Chaperones* **15**, 497-508 (2010).

194 Herber, D. L. *et al.* Lipid accumulation and dendritic cell dysfunction in cancer. *Nat Med* **16**, 880-886, doi:10.1038/nm.2172 (2010).

195 Ramakrishnan, R. *et al.* Oxidized lipids block antigen cross-presentation by dendritic cells in cancer. *J Immunol* **192**, 2920-2931, doi:10.4049/jimmunol.1302801 (2014).

196 Salimu, J. *et al.* Cross-Presentation of the Oncofetal Tumor Antigen 5T4 from Irradiated Prostate Cancer Cells--A Key Role for Heat-Shock Protein 70 and Receptor CD91. *Cancer Immunol Res* **3**, 678-688, doi:10.1158/2326-6066.CIR-14-0079 (2015).

197 Liu, Y. Fatty acid oxidation is a dominant bioenergetic pathway in prostate cancer. *Prostate Cancer Prostatic Dis* **9**, 230-234, doi:10.1038/sj.pcan.4500879 (2006).

198 Comiskey, M. C., Dallos, M. C. & Drake, C. G. Immunotherapy in Prostate Cancer: Teaching an Old Dog New Tricks. *Curr Oncol Rep* **20**, 75, doi:10.1007/s11912-018-0712-z (2018).

199 Mehra, N. In-depth assessment of metastatic prostate cancer with high tumor mutational burden. *Annals of Oncology* **9**, viii271-viii302. 210.1093/annonc/mdy1284 (2018).

200 Abida, W. *et al.* Analysis of the Prevalence of Microsatellite Instability in Prostate Cancer and Response to Immune Checkpoint Blockade. *JAMA Oncol* **5**, 471-478, doi:10.1001/jamaoncol.2018.5801 (2019).

201 Rodrigues, D. N. *et al.* Immunogenomic analyses associate immunological alterations with mismatch repair defects in prostate cancer. *J Clin Invest* **128**, 5185, doi:10.1172/JCI125184 (2018).

202 Antonarakis, E. S. *et al.* Clinical Features and Therapeutic Outcomes in Men with Advanced Prostate Cancer and DNA Mismatch Repair Gene Mutations. *Eur Urol* **75**, 378-382, doi:10.1016/j.eururo.2018.10.009 (2019).

203 Wang, F. *et al.* Evaluation of POLE and POLD1 Mutations as Biomarkers for Immunotherapy Outcomes Across Multiple Cancer Types. *JAMA Oncology* **5**, 1504-1506, doi:10.1001/jamaoncol.2019.2963 (2019).

204 Allison, J. Jim Allison: Breakthrough. *DADA FILMS* (2019).

205 Simpson, T. R. *et al.* Fc-dependent depletion of tumor-infiltrating regulatory T cells co-defines the efficacy of anti-CTLA-4 therapy against melanoma. *J. Exp. Med* **210**, 1695-1710, doi:jem.20130579 [pii];10.1084/jem.20130579 [doi] (2013).

206 Le, D. T. *et al.* Mismatch repair deficiency predicts response of solid tumors to PD-1 blockade. *Science* **357**, 409-413, doi:10.1126/science.aan6733 (2017).

207 Pritchard, C. C. *et al.* Complex MSH2 and MSH6 mutations in hypermutated microsatellite unstable advanced prostate cancer. *Nat Commun* **5**, 4988, doi:10.1038/ncomms5988 (2014).

208 Mercader, M. *et al.* T cell infiltration of the prostate induced by androgen withdrawal in patients with prostate cancer. *Proc. Natl. Acad. Sci. U. S. A* **98**, 14565-14570 (2001).

209 Drake, C. G. *et al.* Androgen ablation mitigates tolerance to a prostate/prostate cancer-restricted antigen. *Cancer Cell* **7**, 239-249 (2005).

210 Graff, J. N. *et al.* Pembrolizumab (Pembro) plus enzalutamide (Enz) in metastatic castration resistant prostate cancer (mCRPC): Extended follow up. *Journal of Clinical Oncology* **36**, 5047-5047, doi:10.1200/JCO.2018.36.15_suppl.5047 (2018).

211 Boudadi, K. *et al.* Ipilimumab plus nivolumab and DNA-repair defects in AR-V7-expressing metastatic prostate cancer. *Oncotarget* **9**, 28561-28571, doi:10.18632/oncotarget.25564 (2018).

212 Sharma, P. *et al.* Nivolumab Plus Ipilimumab for Metastatic Castration-Resistant Prostate Cancer: Preliminary Analysis of Patients in the CheckMate 650 Trial. *Cancer Cell*, doi:10.1016/j.ccell.2020.08.007 (2020).

213 Alexandrov, L. B. *et al.* Signatures of mutational processes in human cancer. *Nature* **500**, 415-421, doi:10.1038/nature12477 (2013).

214 Lawrence, M. S. *et al.* Mutational heterogeneity in cancer and the search for new cancer-associated genes. *Nature* **499**, 214-218, doi:10.1038/nature12213 (2013).

215 Ophir, E., Bobisse, S., Coukos, G., Harari, A. & Kandalaft, L. E. Personalized approaches to active immunotherapy in cancer. *Biochim Biophys Acta* **1865**, 72-82, doi:10.1016/j.bbcan.2015.07.004 (2016).

216 Rausch, M. P. & Hastings, K. T. GILT modulates CD4+ T-cell tolerance to the melanocyte differentiation antigen tyrosinase-related protein 1. *J Invest Dermatol* **132**, 154-162, doi:10.1038/jid.2011.236 (2012).

217 Kantoff, P. W. *et al.* Sipuleucel-T immunotherapy for castration-resistant prostate cancer. *N Engl J Med* **363**, 411-422, doi:10.1056/NEJMoa1001294 (2010).

218 Murphy, G. P. *et al.* Higher-dose and less frequent dendritic cell infusions with PSMA peptides in hormone-refractory metastatic prostate cancer patients. *Prostate* **43**, 59-62 (2000).

219 Gulley, J. L. *et al.* Results of PROSPECT: A randomized phase 3 trial of PROSTVAC-V/F (PRO) in men with asymptomatic or minimally symptomatic metastatic, castration-resistant prostate cancer. *Journal of Clinical Oncology* **36**, 5006-5006, doi:10.1200/JCO.2018.36.15_suppl.5006 (2018).

220 van den Eertwegh, A. J. *et al.* Combined immunotherapy with granulocyte-macrophage colony-stimulating factor-transduced allogeneic prostate cancer cells and ipilimumab in patients with metastatic castration-resistant prostate cancer: a phase 1 dose-escalation trial. *Lancet Oncol* **13**, 509-517, doi:10.1016/S1470-2045(12)70007-4 (2012).

221 MN., S. *et al.* KEYNOTE-046: ADXS-PSA plus pembrolizumab (pembro) in metastatic castration-resistant prostate cancer (mCRPC). *Journal of Clinical Oncology* **36** (2018).

222 Stieglmaier, J., Benjamin, J. & Nagorsen, D. Utilizing the BiTE (bispecific T-cell engager) platform for immunotherapy of cancer. *Expert Opin Biol Ther* **15**, 1093-1099, doi:10.1517/14712598.2015.1041373 (2015).

223 Yu H, Pan J, Guo Z, Yang C & L, M. CART cell therapy for prostate cancer: status and promise. *OncoTargets and therapy* **12**, 391-395, doi:doi:10.2147/OTT.S185556 (2019).

224 Porter, D. L., Levine, B. L., Kalos, M., Bagg, A. & June, C. H. Chimeric antigen receptor-modified T cells in chronic lymphoid leukemia. *N Engl J Med* **365**, 725-733, doi:10.1056/NEJMoa1103849 (2011).

225 Porter, D. L. *et al.* Chimeric antigen receptor T cells persist and induce sustained remissions in relapsed refractory chronic lymphocytic leukemia. *Sci Transl Med* **7**, 303ra139, doi:10.1126/scitranslmed.aac5415 (2015).

226 Maude, S. L. *et al.* Chimeric antigen receptor T cells for sustained remissions in leukemia. *N Engl J Med* **371**, 1507-1517, doi:10.1056/NEJMoa1407222 (2014).

227 Park, J. H. *et al.* Long-Term Follow-up of CD19 CAR Therapy in Acute Lymphoblastic Leukemia. *N Engl J Med* **378**, 449-459, doi:10.1056/NEJMoa1709919 (2018).

228 Schuster, S. J. *et al.* Chimeric Antigen Receptor T Cells in Refractory B-Cell Lymphomas. *N Engl J Med* **377**, 2545-2554, doi:10.1056/NEJMoa1708566 (2017).

229 Mirzaei, H. R., Rodriguez, A., Shepphird, J., Brown, C. E. & Badie, B. Chimeric Antigen Receptors T Cell Therapy in Solid Tumor: Challenges and Clinical Applications. *Front Immunol* **8**, 1850, doi:10.3389/fimmu.2017.01850 (2017).

230 J., B. *et al.* Preclinical evaluation of AMG 160, a next-generation bispecific T cell engager (BiTE) targeting the prostate-specific membrane antigen PSMA for metastatic castration-resistant prostate cancer (mCRPC). *Journal of Clinical Oncology* **37** (2019).

231 HD., H. *et al.* Phase 1 study of pasotuxizumab (BAY 2010112), a PSMA-targeting bispecific T cell engager (BiTE) immunotherapy for metastatic castration-resistant prostate cancer (mCRPC). *Journal of Clinical Oncology* **37** (2019).

232 Tran, B. *et al.* Phase I study of AMG 160, a half-life extended bispecific T-cell engager (HLE BiTE) immune therapy targeting prostate-specific membrane antigen (PSMA), in patients with metastatic castration-resistant prostate cancer (mCRPC). *Journal of Clinical Oncology* **38**, TPS261-TPS261, doi:10.1200/JCO.2020.38.6_suppl.TPS261 (2020).

233 Feldmann, A. *et al.* Retargeting of T cells to prostate stem cell antigen expressing tumor cells: comparison of different antibody formats. *Prostate* **71**, 998-1011, doi:10.1002/pros.21315 (2011).

234 Morgenroth, A. *et al.* Targeting of tumor cells expressing the prostate stem cell antigen (PSCA) using genetically engineered T-cells. *Prostate* **67**, 1121-1131, doi:10.1002/pros.20608 (2007).

235 Feldmann, A. *et al.* Retargeting of T lymphocytes to PSCA- or PSMA positive prostate cancer cells using the novel modular chimeric antigen receptor platform technology "UniCAR". *Oncotarget* **8**, 31368-31385, doi:10.18632/oncotarget.15572 (2017).

236 Sharabi, A. B., Lim, M., DeWeese, T. L. & Drake, C. G. Radiation and checkpoint blockade immunotherapy: radiosensitisation and potential mechanisms of synergy. *Lancet Oncol* **16**, e498-e509, doi:S1470-2045(15)00007-8 [pii];10.1016/S1470-2045(15)00007-8 [doi] (2015).

237 Pfannenstiel, L. W., Lam, S. S., Emens, L. A., Jaffee, E. M. & Armstrong, T. D. Paclitaxel enhances early dendritic cell maturation and function through TLR4 signaling in mice. *Cell Immunol* **263**, 79-87, doi:10.1016/j.cellimm.2010.03.001 (2010).

238 Mercader, M. *et al.* T cell infiltration of the prostate induced by androgen withdrawal in patients with prostate cancer. *Proc Natl Acad Sci U S A* **98**, 14565-14570, doi:10.1073/pnas.251140998 (2001).

239 Sorrentino, C., Musiani, P., Pompa, P., Cipollone, G. & Di Carlo, E. Androgen deprivation boosts prostatic infiltration of cytotoxic and regulatory T lymphocytes and has no effect on disease-free survival in prostate cancer patients. *Clin Cancer Res* **17**, 1571-1581, doi:10.1158/1078-0432.CCR-10-2804 (2011).

240 Arredouani, M. S. *et al.* Androgen ablation augments human HLA2.1-restricted T cell responses to PSA self-antigen in transgenic mice. *Prostate* **70**, 1002-1011, doi:10.1002/pros.21134 (2010).

241 Antonarakis, E. S. *et al.* Sequencing of Sipuleucel-T and Androgen Deprivation Therapy in Men with Hormone-Sensitive Biochemically Recurrent Prostate Cancer: A Phase II Randomized Trial. *Clin Cancer Res* **23**, 2451-2459, doi:10.1158/1078-0432.CCR-16-1780 (2017).

242 Drake, C. G., Lipson, E. J. & Brahmer, J. R. Breathing new life into immunotherapy: review of melanoma, lung and kidney cancer. *Nature reviews Clinical oncology* **11**, 24-37 (2014).

243 Belgiovine, C., D'Incalci, M., Allavena, P. & Frapolli, R. Tumor-associated macrophages and anti-tumor therapies: complex links. *Cell Mol Life Sci* **73**, 2411-2424, doi:10.1007/s00018-016-2166-5 (2016).

244 Pegram, H. J., Chekmasova, A. A., Imperato, G. H. & Brentjens, R. J. *Interleukin 12: Stumbling Blocks and Stepping Stones to Effective Anti-Tumor Therapy*. (INTECH Open Access Publisher, 2012).

245 Temizoz, B., Kuroda, E. & Ishii, K. J. Vaccine adjuvants as potential cancer immunotherapeutics. *Int Immunol* **28**, 329-338, doi:10.1093/intimm/dxw015 (2016).

246 Gupta, N., Al Ustwani, O., Shen, L. & Pili, R. Mechanism of action and clinical activity of tasquinimod in castrate-resistant prostate cancer. *Onco Targets Ther* **7**, 223-234, doi:10.2147/OTT.S53524 (2014).

247 Deronic, A., Leanderson, T. & Ivars, F. The anti-tumor effect of the quinoline-3-carboxamide tasquinimod: blockade of recruitment of CD11b(+) Ly6C(hi) cells to tumor tissue reduces tumor growth. *BMC Cancer* **16**, 440, doi:10.1186/s12885-016-2481-0 (2016).

248 Shen, L. *et al.* Tasquinimod modulates suppressive myeloid cells and enhances cancer immunotherapies in murine models. *Cancer Immunol Res* **3**, 136-148, doi:10.1158/2326-6066.CIR-14-0036 (2015).

249 Sternberg, C. *et al.* Randomized, Double-Blind, Placebo-Controlled Phase III Study of Tasquinimod in Men With Metastatic Castration-Resistant Prostate Cancer. *J Clin Oncol* **34**, 2636-2643, doi:10.1200/JCO.2016.66.9697 (2016).

250 Sternberg, C. N., Armstrong, A. J., Pili, R., Nederman, T. & Carducci, M. A. A Phase 3, randomized, double-blind, placebo-controlled study of tasquinimod (TASQ) in men with metastatic castration-resistant prostate cancer (mCRPC), secondary endpoints. *Journal of Clinical Oncology* **34** (2016).

251 Zeng, Q. & Hong, W. The emerging role of the hippo pathway in cell contact inhibition, organ size control, and cancer development in mammals. *Cancer Cell* **13**, 188-192, doi:10.1016/j.ccr.2008.02.011 (2008).

252 Liu-Chittenden, Y. *et al.* Genetic and pharmacological disruption of the TEAD-YAP complex suppresses the oncogenic activity of YAP. *Genes Dev* **26**, 1300-1305, doi:10.1101/gad.192856.112 (2012).

253 Nguyen, L. T. *et al.* ERG Activates the YAP1 Transcriptional Program and Induces the Development of Age-Related Prostate Tumors. *Cancer Cell* **27**, 797-808, doi:10.1016/j.ccell.2015.05.005 (2015).

254 Wang, G. *et al.* Targeting YAP-Dependent MDSC Infiltration Impairs Tumor Progression. *Cancer Discov* **6**, 80-95, doi:10.1158/2159-8290.CD-15-0224 (2016).

255 Ciprotti, M. *et al.* Phase I Imaging and Pharmacodynamic Trial of CS-1008 in Patients With Metastatic Colorectal Cancer. *J Clin Oncol* **33**, 2609-2616, doi:10.1200/JCO.2014.60.4256 (2015).

256 Ries, C. H. *et al.* Targeting tumor-associated macrophages with anti-CSF-1R antibody reveals a strategy for cancer therapy. *Cancer Cell* **25**, 846-859, doi:10.1016/j.ccr.2014.05.016 (2014).

257 Wallner, L. *et al.* Inhibition of interleukin-6 with CNTO328, an anti-interleukin-6 monoclonal antibody, inhibits conversion of androgen-dependent prostate cancer to an androgen-independent phenotype in orchiectomized mice. *Cancer Res* **66**, 3087-3095, doi:10.1158/0008-5472.CAN-05-3447 (2006).

258 Dorff, T. B. *et al.* Clinical and correlative results of SWOG S0354: a phase II trial of CNTO328 (siltuximab), a monoclonal antibody against interleukin-6, in chemotherapy-pretreated patients with castration-resistant prostate cancer. *Clin Cancer Res* **16**, 3028-3034, doi:10.1158/1078-0432.CCR-09-3122 (2010).

259 Fizazi, K. *et al.* Randomised phase II study of siltuximab (CNTO 328), an anti-IL-6 monoclonal antibody, in combination with mitoxantrone/prednisone versus mitoxantrone/prednisone alone in metastatic castration-resistant prostate cancer. *Eur J Cancer* **48**, 85-93, doi:10.1016/j.ejca.2011.10.014 (2012).

260 Villiger, P. M. *et al.* Tocilizumab for induction and maintenance of remission in giant cell arteritis: a phase 2, randomised, double-blind, placebo-

controlled trial. *Lancet* **387**, 1921-1927, doi:10.1016/S0140-6736(16)00560-2 (2016).

261 Watanabe, R., Goronzy, J. J., Berry, G., Liao, Y. J. & Weyand, C. M. Giant Cell Arteritis: From Pathogenesis to Therapeutic Management. *Curr Treatm Opt Rheumatol* **2**, 126-137, doi:10.1007/s40674-016-0043-x (2016).

262 Hou, D. Y. *et al.* Inhibition of indoleamine 2,3-dioxygenase in dendritic cells by stereoisomers of 1-methyl-tryptophan correlates with antitumor responses. *Cancer Res* **67**, 792-801, doi:10.1158/0008-5472.CAN-06-2925 (2007).

263 Holmgaard, R. B., Zamarin, D., Munn, D. H., Wolchok, J. D. & Allison, J. P. Indoleamine 2,3-dioxygenase is a critical resistance mechanism in antitumor T cell immunotherapy targeting CTLA-4. *Journal of Experimental Medicine* **210**, 1389-1402, doi:10.1084/jem.20130066 (2013).

264 Egerdie, R. B. *et al.* Responder analysis of the effects of denosumab on bone mineral density in men receiving androgen deprivation therapy for prostate cancer. *Prostate Cancer Prostatic Dis* **15**, 308-312, doi:10.1038/pcan.2012.18 (2012).

265 Smith, M. R. *et al.* Denosumab for the prevention of skeletal complications in metastatic castration-resistant prostate cancer: comparison of skeletal-related events and symptomatic skeletal events. *Ann Oncol* **26**, 368-374, doi:10.1093/annonc/mdu519 (2015).

266 Park, H. M., Cho, H. I., Shin, C. A., Shon, H. J. & Kim, T. G. Zoledronic acid induces dose-dependent increase of antigen-specific CD8 T-cell responses in combination with peptide/poly-IC vaccine. *Vaccine* **34**, 1275-1281, doi:10.1016/j.vaccine.2016.01.026 (2016).

267 Porvasnik, S. *et al.* Effects of CXCR4 antagonist CTCE-9908 on prostate tumor growth. *Prostate* **69**, 1460-1469, doi:10.1002/pros.21008 (2009).

268 Wong, D., Kandagatla, P., Korz, W. & Chinni, S. R. Targeting CXCR4 with CTCE-9908 inhibits prostate tumor metastasis. *BMC Urol* **14**, 12, doi:10.1186/1471-2490-14-12 (2014).

269 Russell, N. *et al.* Plerixafor and granulocyte colony-stimulating factor for first-line steady-state autologous peripheral blood stem cell mobilization in lymphoma and multiple myeloma: results of the prospective PREDICT trial. *Haematologica* **98**, 172-178, doi:10.3324/haematol.2012.071456 (2013).

270 Yang, L. *et al.* Abrogation of TGF beta signaling in mammary carcinomas recruits Gr-1+CD11b+ myeloid cells that promote metastasis. *Cancer Cell* **13**, 23-35, doi:10.1016/j.ccr.2007.12.004 (2008).

271 Hotte, S. J. *et al.* 405 POSTER Final results of a Phase I/II study of CTCE-9908, a novel anticancer agent that inhibits CXCR4, in patients with advanced solid cancers. *EJC Supplements* **6**, 127, doi:10.1016/S1359-6349(08)72339-5 (2008).

272 Skerlj, R. *et al.* Design of novel CXCR4 antagonists that are potent inhibitors of T-tropic (X4) HIV-1 replication. *Bioorg Med Chem Lett* **21**, 1414-1418, doi:10.1016/j.bmcl.2011.01.021 (2011).

273 Amaya-Chanaga, C. I. *et al.* BMS-936564 (Anti-CXCR4 Antibody) Induces Specific Leukemia Cell Mobilization and Objective Clinical Responses In CLL Patients Treated Under a Phase I Clinical Trial. *Blood* **122**, 4190-4190 (2013).

274 Dunn, G. P., Bruce, A. T., Ikeda, H., Old, L. J. & Schreiber, R. D. Cancer immunoediting: from immunosurveillance to tumor escape. *Nat Immunol* **3**, 991-998, doi:10.1038/ni1102-991, ni1102-991 [pii] (2002).

275 Santegoets, S. J. *et al.* Myeloid derived suppressor and dendritic cell subsets are related to clinical outcome in prostate cancer patients treated with prostate GVAX and ipilimumab. *J Immunother Cancer* **2**, 31, doi:10.1186/s40425-014-0031-3 (2014).

276 Small, E. J. *et al.* Placebo-controlled phase III trial of immunologic therapy with sipuleucel-T (APC8015) in patients with metastatic, asymptomatic hormone refractory prostate cancer. *J Clin Oncol* **24**, 3089-3094, doi:10.1200/JCO.2005.04.5252 (2006).

277 Higano, C. S. *et al.* Integrated data from 2 randomized, double-blind, placebo-controlled, phase 3 trials of active cellular immunotherapy with sipuleucel-T in advanced prostate cancer. *Cancer* **115**, 3670-3679, doi:10.1002/cncr.24429 (2009).

278 Kantoff, P. W. *et al.* Sipuleucel-T immunotherapy for castration-resistant prostate cancer. *N Engl J Med* **363**, 411-422, doi:10.1056/NEJMoa1001294 (2010).

279 Lee, P. & Gujar, S. Potentiating prostate cancer immunotherapy with oncolytic viruses. *Nat Rev Urol* **15**, 235-250, doi:10.1038/nrurol.2018.10 (2018).

280 de Almeida, D. V. P., Fong, L., Rettig, M. B. & Autio, K. A. Immune Checkpoint Blockade for Prostate Cancer: Niche Role or Next Breakthrough? *Am Soc Clin Oncol Educ Book* **40**, 1-18, doi:10.1200/EDBK_278853 (2020).

281 Kiessling, A. *et al.* Tumor-associated antigens for specific immunotherapy of prostate cancer. *Cancers (Basel)* **4**, 193-217, doi:10.3390/cancers4010193 (2012).

282 Obradovic, A. Z. *et al.* T-Cell Infiltration and Adaptive Treg Resistance in Response to Androgen Deprivation With or Without Vaccination in Localized Prostate Cancer. *Clin Cancer Res* **26**, 3182-3192, doi:10.1158/1078-0432.CCR-19-3372 (2020).

283 Wang, X. *et al.* A luminal epithelial stem cell that is a cell of origin for prostate cancer. *Nature* **461**, 495-500, doi:10.1038/nature08361 (2009).

284 Meeker, A. K. *et al.* Telomere shortening is an early somatic DNA alteration in human prostate tumorigenesis. *Cancer Res* **62**, 6405-6409 (2002).

285 Koh, C. M. *et al.* MYC and Prostate Cancer. *Genes Cancer* **1**, 617-628, doi:10.1177/1947601910379132 (2010).

286 Brooks, J. D. *et al.* CG island methylation changes near the GSTP1 gene in prostatic intraepithelial neoplasia. *Cancer Epidemiol Biomarkers Prev* **7**, 531-536 (1998).

287 Dubbink, H. J. *et al.* Tissue specific and androgen-regulated expression of human prostate-specific transglutaminase. *The Biochemical journal* **315 (Pt 3)**, 901-908, doi:10.1042/bj3150901 (1996).

288 Evans, M. J. *et al.* Noninvasive measurement of androgen receptor signaling with a positron-emitting radiopharmaceutical that targets prostate-specific membrane antigen. *Proc Natl Acad Sci U S A* **108**, 9578-9582, doi:10.1073/pnas.1106383108 (2011).

289 Calcinotto, A. *et al.* IL-23 secreted by myeloid cells drives castration-resistant prostate cancer. *Nature* **559**, 363-369, doi:10.1038/s41586-018-0266-0 (2018).

290 van der Toom, E. E. *et al.* Prostate-specific markers to identify rare prostate cancer cells in liquid biopsies. *Nat Rev Urol* **16**, 7-22, doi:10.1038/s41585-018-0119-5 (2019).

291 Dahlman, A. *et al.* Effect of androgen deprivation therapy on the expression of prostate cancer biomarkers MSMB and MSMB-binding protein CRISP3. *Prostate Cancer Prostatic Dis* **13**, 369-375, doi:10.1038/pcan.2010.25 (2010).

292 Tiwari, R. *et al.* Androgen deprivation upregulates SPINK1 expression and potentiates cellular plasticity in prostate cancer. *Nat Commun* **11**, 384, doi:10.1038/s41467-019-14184-0 (2020).

293 Wang, Z. A. *et al.* Lineage analysis of basal epithelial cells reveals their unexpected plasticity and supports a cell-of-origin model for prostate cancer heterogeneity. *Nat Cell Biol* **15**, 274-283, doi:10.1038/ncb2697 (2013).

294 Lizio, M. *et al.* Update of the FANTOM web resource: expansion to provide additional transcriptome atlases. *Nucleic Acids Res* **47**, D752-D758, doi:10.1093/nar/gky1099 (2019).

295 Consortium, G. T. The Genotype-Tissue Expression (GTEx) project. *Nat Genet* **45**, 580-585, doi:10.1038/ng.2653 (2013).

296 Cao, Z. *et al.* Overexpression of transglutaminase 4 and prostate cancer progression: a potential predictor of less favourable outcomes. *Asian J Androl* **15**, 742-746, doi:10.1038/aja.2013.79 (2013).

297 Cancer Genome Atlas Research, N. The Molecular Taxonomy of Primary Prostate Cancer. *Cell* **163**, 1011-1025, doi:10.1016/j.cell.2015.10.025 (2015).

298 Taylor, B. S. *et al.* Integrative genomic profiling of human prostate cancer. *Cancer Cell* **18**, 11-22, doi:10.1016/j.ccr.2010.05.026 (2010).

299 Larman, H. B. *et al.* Autoantigen discovery with a synthetic human peptidome. *Nat Biotechnol* **29**, 535-541, doi:10.1038/nbt.1856 (2011).

300 Larman, H. B. *et al.* PhIP-Seq characterization of autoantibodies from patients with multiple sclerosis, type 1 diabetes and rheumatoid arthritis. *J Autoimmun* **43**, 1-9, doi:10.1016/j.jaut.2013.01.013 (2013).

301 GuhaThakurta, D. *et al.* Humoral Immune Response against Nontargeted Tumor Antigens after Treatment with Sipuleucel-T and Its Association with Improved Clinical Outcome. *Clin Cancer Res* **21**, 3619-3630, doi:10.1158/1078-0432.CCR-14-2334 (2015).

302 Antonarakis, E. S. *et al.* Antigen-Specific CD8 Lytic Phenotype Induced by Sipuleucel-T in Hormone-Sensitive or Castration-Resistant Prostate Cancer

and Association with Overall Survival. *Clin Cancer Res* **24**, 4662-4671, doi:10.1158/1078-0432.CCR-18-0638 (2018).

303 Wargowski, E. *et al.* Prime-boost vaccination targeting prostatic acid phosphatase (PAP) in patients with metastatic castration-resistant prostate cancer (mCRPC) using Sipuleucel-T and a DNA vaccine. *J Immunother Cancer* **6**, 21, doi:10.1186/s40425-018-0333-y (2018).

304 Hagihara, K. *et al.* Neoadjuvant sipuleucel-T induces both Th1 activation and immune regulation in localized prostate cancer. *Oncoimmunology* **8**, e1486953, doi:10.1080/2162402X.2018.1486953 (2019).

305 Kloss, C. C. *et al.* Dominant-Negative TGF-beta Receptor Enhances PSMA-Targeted Human CAR T Cell Proliferation And Augments Prostate Cancer Eradication. *Mol Ther* **26**, 1855-1866, doi:10.1016/j.ymthe.2018.05.003 (2018).

306 Junghans, R. P. *et al.* Phase I Trial of Anti-PSMA Designer CAR-T Cells in Prostate Cancer: Possible Role for Interacting Interleukin 2-T Cell Pharmacodynamics as a Determinant of Clinical Response. *Prostate* **76**, 1257-1270, doi:10.1002/pros.23214 (2016).

307 Mahadevan, M. *et al.* Generation of robust cytotoxic T lymphocytes against prostate specific antigen by transduction of dendritic cells using protein and recombinant adeno-associated virus. *Cancer Immunol Immunother* **56**, 1615-1624, doi:10.1007/s00262-007-0307-2 (2007).

308 Zhang, D., Zhao, S., Li, X., Kirk, J. S. & Tang, D. G. Prostate Luminal Progenitor Cells in Development and Cancer. *Trends Cancer* **4**, 769-783, doi:10.1016/j.trecan.2018.09.003 (2018).

309 Crowley, L. *et al.* A single-cell atlas of the mouse and human prostate reveals heterogeneity and conservation of epithelial progenitors. *bioRxiv* (2020).

310 Rivera-Gonzalez, G. C. *et al.* Retinoic acid and androgen receptors combine to achieve tissue specific control of human prostatic transglutaminase expression: a novel regulatory network with broader significance. *Nucleic Acids Res* **40**, 4825-4840, doi:10.1093/nar/gks143 (2012).

311 Shaikhibrahim, Z., Lindstrot, A., Buettner, R. & Wernert, N. Analysis of laser-microdissected prostate cancer tissues reveals potential tumor markers. *Int J Mol Med* **28**, 605-611, doi:10.3892/ijmm.2011.746 (2011).

312 An, G., Meka, C. S., Bright, S. P. & Veltri, R. W. Human prostate-specific transglutaminase gene: promoter cloning, tissue-specific expression, and down-regulation in metastatic prostate cancer. *Urology* **54**, 1105-1111, doi:10.1016/s0090-4295(99)00298-8 (1999).

313 Sequeiros, T. *et al.* Targeted proteomics in urinary extracellular vesicles identifies biomarkers for diagnosis and prognosis of prostate cancer. *Oncotarget* **8**, 4960-4976, doi:10.18632/oncotarget.13634 (2017).

314 Cho, S. Y. *et al.* Differential alternative splicing of human transglutaminase 4 in benign prostate hyperplasia and prostate cancer. *Exp Mol Med* **42**, 310-318, doi:10.3858/emm.2010.42.4.031 (2010).

315 Jiang, W. G. *et al.* Prostate transglutaminase (TGase-4, TGaseP) enhances the adhesion of prostate cancer cells to extracellular matrix, the potential role of TGase-core domain. *J Transl Med* **11**, 269, doi:10.1186/1479-5876-11-269 (2013).

316 Ablin, R. J., Owen, S. & Jiang, W. G. Prostate Transglutaminase (TGase-4) Induces Epithelial-to-Mesenchymal Transition in Prostate Cancer Cells. *Anticancer Res* **37**, 481-487, doi:10.21873/anticanres.11340 (2017).

317 Obradovic, A. Z. *et al.* T-Cell Infiltration and Adaptive Treg Resistance in Response to Androgen Deprivation With or Without Vaccination in Localized Prostate Cancer. *Clin Cancer Res*, doi:10.1158/1078-0432.CCR-19-3372 (2020).

318 Landegren, N. *et al.* Transglutaminase 4 as a prostate autoantigen in male subfertility. *Sci Transl Med* **7**, 292ra101, doi:10.1126/scitranslmed.aaa9186 (2015).

319 Dieterich, W. *et al.* Identification of tissue transglutaminase as the autoantigen of celiac disease. *Nat Med* **3**, 797-801, doi:10.1038/nm0797-797 (1997).

320 Sardy, M., Karpati, S., Merkl, B., Paulsson, M. & Smyth, N. Epidermal transglutaminase (TGase 3) is the autoantigen of dermatitis herpetiformis. *J Exp Med* **195**, 747-757, doi:10.1084/jem.20011299 (2002).

321 Hadjivassiliou, M. *et al.* Autoantibodies in gluten ataxia recognize a novel neuronal transglutaminase. *Ann Neurol* **64**, 332-343, doi:10.1002/ana.21450 (2008).

322 Bilusic, M., Madan, R. A. & Gulley, J. L. Immunotherapy of Prostate Cancer: Facts and Hopes. *Clin Cancer Res* **23**, 6764-6770, doi:10.1158/1078-0432.CCR-17-0019 (2017).

323 Zahm, C. D., Colluru, V. T. & McNeel, D. G. DNA vaccines for prostate cancer. *Pharmacol Ther* **174**, 27-42, doi:10.1016/j.pharmthera.2017.02.016 (2017).

324 Patel, A. & Fong, L. Immunotherapy for Prostate Cancer: Where Do We Go From Here?-PART 1: Prostate Cancer Vaccines. *Oncology (Williston Park)* **32**, 112-120 (2018).

325 Collins, J. M., Redman, J. M. & Gulley, J. L. Combining vaccines and immune checkpoint inhibitors to prime, expand, and facilitate effective tumor immunotherapy. *Expert Rev Vaccines* **17**, 697-705, doi:10.1080/14760584.2018.1506332 (2018).

326 Morgan, D. J., Kreuwel, H. T. & Sherman, L. A. Antigen concentration and precursor frequency determine the rate of CD8+ T cell tolerance to peripherally expressed antigens. *J Immunol* **163**, 723-727 (1999).

327 Drake, C. G. *et al.* Androgen ablation mitigates tolerance to a prostate/prostate cancer-restricted antigen. *Cancer Cell* **7**, 239-249, doi:10.1016/j.ccr.2005.01.027 (2005).

328 Emens, L. A. Cancer vaccines: on the threshold of success. *Expert Opin Emerg Drugs* **13**, 295-308, doi:10.1517/14728214.13.2.295 (2008).

329 Jackson, S. R., Yuan, J. & Teague, R. M. Targeting CD8+ T-cell tolerance for cancer immunotherapy. *Immunotherapy* **6**, 833-852, doi:10.2217/imt.14.51 (2014).

330 Bruno, T. C. *et al.* Anti-tumor effects of endogenous prostate cancer-specific CD8 T cells in a murine TCR transgenic model. *Prostate* **72**, 514-522, doi:10.1002/pros.21453 (2012).

331 Lees, J. R. *et al.* Deletion is neither sufficient nor necessary for the induction of peripheral tolerance in mature CD8+ T cells. *Immunology* **117**, 248-261, doi:10.1111/j.1365-2567.2005.02293.x (2006).

332 Bai, A., Higham, E., Eisen, H. N., Wittrup, K. D. & Chen, J. Rapid tolerization of virus-activated tumor-specific CD8+ T cells in prostate tumors of TRAMP mice. *Proc Natl Acad Sci U S A* **105**, 13003-13008, doi:10.1073/pnas.0805599105 (2008).

333 Shafer-Weaver, K. A. *et al.* Immunity to murine prostatic tumors: continuous provision of T-cell help prevents CD8 T-cell tolerance and activates tumor-infiltrating dendritic cells. *Cancer Res* **69**, 6256-6264, doi:10.1158/0008-5472.CAN-08-4516 (2009).

334 Reilly, R. T. *et al.* HER-2/neu is a tumor rejection target in tolerized HER-2/neu transgenic mice. *Cancer Res* **60**, 3569-3576 (2000).

335 Sunay, M. M. *et al.* Sorafenib combined with HER-2 targeted vaccination can promote effective T cell immunity in vivo. *Int Immunopharmacol* **46**, 112-123, doi:10.1016/j.intimp.2017.02.028 (2017).

336 Black, C. M., Armstrong, T. D. & Jaffee, E. M. Apoptosis-regulated low-avidity cancer-specific CD8(+) T cells can be rescued to eliminate HER2/neu-expressing tumors by costimulatory agonists in tolerized mice. *Cancer Immunol Res* **2**, 307-319, doi:10.1158/2326-6066.CIR-13-0145 (2014).

337 Watson, P. A. *et al.* Context-dependent hormone-refractory progression revealed through characterization of a novel murine prostate cancer cell line. *Cancer Res* **65**, 11565-11571, doi:10.1158/0008-5472.CAN-05-3441 (2005).

338 Ellwood-Yen, K. *et al.* Myc-driven murine prostate cancer shares molecular features with human prostate tumors. *Cancer cell* **4**, 223-238 (2003).

339 Koh, C. M. *et al.* MYC and Prostate Cancer. *Genes Cancer* **1**, 617-628, doi:10.1177/1947601910379132 (2010).

340 Ercolini, A. M. *et al.* Identification and characterization of the immunodominant rat HER-2/neu MHC class I epitope presented by spontaneous mammary tumors from HER-2/neu-transgenic mice. *J Immunol* **170**, 4273-4280, doi:10.4049/jimmunol.170.8.4273 (2003).

341 Sakamoto, C. *et al.* Therapeutic vaccination based on side population cells transduced by the granulocyte-macrophage colony-stimulating factor gene elicits potent antitumor immunity. *Cancer Gene Ther* **24**, 165-174, doi:10.1038/cgt.2016.80 (2017).

342 Dranoff, G. *et al.* Vaccination with irradiated tumor cells engineered to secrete murine granulocyte-macrophage colony-stimulating factor stimulates potent, specific, and long-lasting anti-tumor immunity. *Proc Natl Acad Sci U S A* **90**, 3539-3543, doi:10.1073/pnas.90.8.3539 (1993).

343 Arlen, P. M., Mohebtash, M., Madan, R. A. & Gulley, J. L. Promising novel immunotherapies and combinations for prostate cancer. *Future Oncol* **5**, 187-196, doi:10.2217/14796694.5.2.187 (2009).

344 Melero, I. *et al.* Therapeutic vaccines for cancer: an overview of clinical trials. *Nat Rev Clin Oncol* **11**, 509-524, doi:10.1038/nrclinonc.2014.111 (2014).

345 Martins, K. A., Bavari, S. & Salazar, A. M. Vaccine adjuvant uses of poly-IC and derivatives. *Expert Rev Vaccines* **14**, 447-459, doi:10.1586/14760584.2015.966085 (2015).

346 Garzon-Muvdi, T. *et al.* Dendritic cell activation enhances anti-PD-1 mediated immunotherapy against glioblastoma. *Oncotarget* **9**, 20681-20697, doi:10.18632/oncotarget.25061 (2018).

347 Mao, W. & Drake, C. G. in *Oncoimmunology: A Practical Guide for Cancer Immunotherapy* (eds Laurence Zitvogel & Guido Kroemer) 593-606 (Springer International Publishing, 2018).

348 Greenberg, N. M. *et al.* Prostate cancer in a transgenic mouse. *Proc Natl Acad Sci U S A* **92**, 3439-3443, doi:10.1073/pnas.92.8.3439 (1995).

349 Highfill, S. L. *et al.* Disruption of CXCR2-mediated MDSC tumor trafficking enhances anti-PD1 efficacy. *Sci Transl Med* **6**, 237ra267, doi:10.1126/scitranslmed.3007974 (2014).

350 Hurwitz, A. A. *et al.* Combination immunotherapy of primary prostate cancer in a transgenic mouse model using CTLA-4 blockade. *Cancer Res* **60**, 2444-2448 (2000).

351 Jayaprakash, P. *et al.* Targeted hypoxia reduction restores T cell infiltration and sensitizes prostate cancer to immunotherapy. *J Clin Invest* **128**, 5137-5149, doi:10.1172/JCI96268 (2018).

352 de Bono, J. S. *et al.* Prostate carcinogenesis: inflammatory storms. *Nat Rev Cancer*, doi:10.1038/s41568-020-0267-9 (2020).

353 Corey, E. *et al.* Establishment and characterization of osseous prostate cancer models: intra-tibial injection of human prostate cancer cells. *Prostate* **52**, 20-33, doi:10.1002/pros.10091 (2002).

354 Lopez-Bujanda, Z. & Drake, C. G. Myeloid-derived cells in prostate cancer progression: phenotype and prospective therapies. *J Leukoc Biol* **102**, 393-406, doi:10.1189/jlb.5VMR1116-491RR (2017).

355 Hol, J., Wilhelmsen, L. & Haraldsen, G. The murine IL-8 homologues KC, MIP-2, and LIX are found in endothelial cytoplasmic granules but not in Weibel-Palade bodies. *J Leukoc Biol* **87**, 501-508, doi:10.1189/jlb.0809532 (2010).

356 Rossi, D. L. *et al.* Lungkine, a novel CXC chemokine, specifically expressed by lung bronchoepithelial cells. *J Immunol* **162**, 5490-5497 (1999).

357 Schmitz, J. M., McCracken, V. J., Dimmitt, R. A. & Lorenz, R. G. Expression of CXCL15 (Lungkine) in murine gastrointestinal, urogenital, and endocrine organs. *J Histochem Cytochem* **55**, 515-524, doi:10.1369/jhc.6A7121.2007 (2007).

358 Chen, R. *et al.* Telomerase Deficiency Causes Alveolar Stem Cell Senescence-associated Low-grade Inflammation in Lungs. *J Biol Chem* **290**, 30813-30829, doi:10.1074/jbc.M115.681619 (2015).

359 Karlic, R., Chung, H. R., Lasserre, J., Vlahovicek, K. & Vingron, M. Histone modification levels are predictive for gene expression. *Proc Natl Acad Sci U S A* **107**, 2926-2931, doi:10.1073/pnas.0909344107 (2010).

360 Kumar, V. *et al.* Cancer-Associated Fibroblasts Neutralize the Anti-tumor Effect of CSF1 Receptor Blockade by Inducing PMN-MDSC Infiltration of Tumors. *Cancer Cell* **32**, 654-668 e655, doi:10.1016/j.ccell.2017.10.005 (2017).

361 Patnaik, A. *et al.* Cabozantinib Eradicates Advanced Murine Prostate Cancer by Activating Antitumor Innate Immunity. *Cancer Discov* **7**, 750-765, doi:10.1158/2159-8290.CD-16-0778 (2017).

362 Lu, X. *et al.* Effective combinatorial immunotherapy for castration-resistant prostate cancer. *Nature* **543**, 728-732, doi:10.1038/nature21676 (2017).

363 Alfaro, C. *et al.* Tumor-Produced Interleukin-8 Attracts Human Myeloid-Derived Suppressor Cells and Elicits Extrusion of Neutrophil Extracellular Traps (NETs). *Clin Cancer Res* **22**, 3924-3936, doi:10.1158/1078-0432.CCR-15-2463 (2016).

364 Gentles, A. J. *et al.* The prognostic landscape of genes and infiltrating immune cells across human cancers. *Nat Med* **21**, 938-945, doi:10.1038/nm.3909 (2015).

365 Antonarakis, E. S. *et al.* Neoadjuvant randomized trial of degarelix (Deg) ± cyclophosphamide/GVAX (Cy/GVAX) in men with high-risk prostate cancer

(PCa) undergoing radical prostatectomy (RP). *Journal of Clinical Oncology* **35**, 5077-5077, doi:10.1200/JCO.2017.35.15_suppl.5077 (2017).

366 Culig, Z. *et al.* Switch from antagonist to agonist of the androgen receptor bicalutamide is associated with prostate tumour progression in a new model system. *Br J Cancer* **81**, 242-251, doi:10.1038/sj.bjc.6690684 (1999).

367 Weiss, V. L. *et al.* Trafficking of high avidity HER-2/neu-specific T cells into HER-2/neu-expressing tumors after depletion of effector/memory-like regulatory T cells. *PLoS One* **7**, e31962, doi:10.1371/journal.pone.0031962 (2012).

368 Rao, V. *et al.* A Hoxb13-driven reverse tetracycline transactivator system for conditional gene expression in the prostate. *Prostate* **72**, 1045-1051, doi:10.1002/pros.22490 (2012).

369 Bargmann, C. I., Hung, M. C. & Weinberg, R. A. Multiple independent activations of the neu oncogene by a point mutation altering the transmembrane domain of p185. *Cell* **45**, 649-657 (1986).

370 Altschul, S. F. *et al.* Protein database searches using compositionally adjusted substitution matrices. *Febs J* **272**, 5101-5109, doi:10.1111/j.1742-4658.2005.04945.x (2005).

371 Pevsner, J. *Bioinformatics and functional genomics*. (John Wiley & Sons, 2015).

372 Malinen, M., Niskanen, E. A., Kaikkonen, M. U. & Palvimo, J. J. Crosstalk between androgen and pro-inflammatory signaling remodels androgen receptor and NF-kappaB cistrome to reprogram the prostate cancer cell transcriptome. *Nucleic Acids Res* **45**, 619-630, doi:10.1093/nar/gkw855 (2017).

373 Haffner, M. C. *et al.* Androgen-induced TOP2B-mediated double-strand breaks and prostate cancer gene rearrangements. *Nat Genet* **42**, 668-675, doi:10.1038/ng.613 (2010).

374 Carlson, A. L. *et al.* Tracking Single Cells in Live Animals Using a Photoconvertible Near-Infrared Cell Membrane Label. *Plos One* **8**, doi:ARTN e69257

10.1371/journal.pone.0069257 (2013).

375 Xu, G. J. *et al.* Systematic autoantigen analysis identifies a distinct subtype of scleroderma with coincident cancer. *Proc Natl Acad Sci U S A* **113**, E7526-E7534, doi:10.1073/pnas.1615990113 (2016).

376 Mohan, D. *et al.* PhIP-Seq characterization of serum antibodies using oligonucleotide-encoded peptidomes. *Nat Protoc* **13**, 1958-1978, doi:10.1038/s41596-018-0025-6 (2018).

377 Ritchie, M. E. *et al.* limma powers differential expression analyses for RNA-sequencing and microarray studies. *Nucleic Acids Res* **43**, e47, doi:10.1093/nar/gkv007 (2015).

378 Team, R. C. R: A language and environment for statistical computing. R Foundation for Statistical Computing. *Vienna, Austria* (2014).

379 Wickham, H. ggplot2: Elegant Graphics for Data Analysis. *eBook* (2016).

380 Kassambara A, K. M., Biecek P, Fabian S. Package 'survminer'. *Version 0.4.3 ed2018* (2018).

381 Melville, L. M. a. J. H. a. J. UMAP: Uniform Manifold Approximation and Projection for Dimension Reduction. *arXiv* **1802.03426** (2018).

382 Van Gassen, S. *et al.* FlowSOM: Using self-organizing maps for visualization and interpretation of cytometry data. *Cytometry A* **87**, 636-645, doi:10.1002/cyto.a.22625 (2015).

383 Langmead, B. & Salzberg, S. L. Fast gapped-read alignment with Bowtie 2. *Nat Methods* **9**, 357-359, doi:10.1038/nmeth.1923 (2012).

384 Mostaghel, E. A. *et al.* Intraprostatic androgens and androgen-regulated gene expression persist after testosterone suppression: therapeutic implications for castration-resistant prostate cancer. *Cancer Res* **67**, 5033-5041, doi:10.1158/0008-5472.CAN-06-3332 (2007).

Materials and Methods

Patient Samples

Serum samples from human prostate cancer patients were obtained from consented patients treated with ADT alone (degarelix; 240 mg SQ) or cyclophosphamide (200 mg/m^2 IV) followed by GVAX and ADT in a neo-adjuvant trial (NCT01696877) at the Johns Hopkins Sidney Kimmel Comprehensive Cancer Center (Baltimore, MD) under an IRB-approved clinical protocol (IRB # NA_00073453).[317,365] Men with high-risk localized prostate adenocarcinoma, defined as clinical stage T1c-T3b, N0, M0 and a Gleason sum ≥ 4+3 (grade group ≥3) in at least two cores were considered eligible if they were planning to undergo prostatectomy. All patients were required to have an Eastern Cooperative Oncology Group performance status of 0 or 1; and normal kidney, liver, and marrow function. Patients with nodal (N1) or distant (M1) metastases were excluded. Additional key exclusion criteria included prior immunotherapy or vaccine therapy for prostate cancer, prior radiation, hormonal, or chemotherapy, autoimmune disease requiring corticosteroids, and known allergy to cyclophosphamide or G-CSF/GM-CSF. All patients provided written, informed consent authorizing the collection of clinical data, serum and other biospecimens. Primary human peripheral blood mononuclear cells (PBMCs) from anonymous 35-year-old or older healthy male donors were acquired from the New York Blood Center.

Formalin fixed, paraffin embedded (FFPE) human prostate cancer samples were obtained from consented patients treated with ADT (degarelix; 240 mg SQ) in a

neo-adjuvant trial (NCT01696877)[365] and matched control radical prostatectomies were obtained from patients treated at the Johns Hopkins Sidney Kimmel Comprehensive Cancer Center (Baltimore, MD) under IRB-approved clinical protocol J1265. All patients provided written, informed consent.

Cell Lines

Myc-CaP, derived from spontaneous prostate cancer in c-Myc transgenic mice,[337,338] was a generous gift from Dr. C. Sawyers. To generate MCRedAL, Myc-Cap cells were transfected with pRetroQ-mCherry-C1 (Clontech) using lipofectamine 2000 (Invitrogen) and isolated by FACS sorting based on mCherry expression. Myc-CaP cells were transduced with viral particles containing the rat Her-2/neu transcript and isolated by FACS sorting based on Her-2/neu expression to establish Myc-CaP/Neu cells. Myc-Cap, MCRedAL, and Myc-CaP/Neu cells were cultured in DMEM as previously described.[337] LNCaP, VCaP, E006AA, CWR22Rv1, DU145, and PC3 cell lines were obtained and cultured as recommended by the ATCC. LAPC4 (a gift from Dr. S. Yegnasubramanian) were maintained in RPMI-1640 (Corning) supplemented with 10% fetal bovine serum (FBS; Gemini Bio-Products). Androgen independent LNCaP-abl cells were a gift from Dr. Z. Culig and cultured as described previously.[366] LAPC4-CR and VCaP-CR (a gift from S. Yegnasubramanian) were derived by passaging LAPC4 and VCaP cells through castrated animals and further subculturing in RPMI-1640 supplemented with 10% charcoal stripped serum (CSS; Gemini Bio-Products) supplemented with 1X B-27 Neuronal Supplement (Gibco). For experiments when cells were grown in androgen-free conditions, 10% FBS was substituted for 10%

CSS in complete media. For migration/chemotaxis assays, prostate cancer cell lines were cultured in complete media containing either 0.5% or 2.5% FBS for human and murine cells, respectively. All cell lines were cultured in 1% penicillin/streptomycin media at 37°C, 5% CO_2.

Mouse Strains

Seven-week-old FVB/NJ Thy1.1 male mice were purchased from The Jackson Laboratory (JAX stock #001800). FVB/N Thy1.2$^+$ mice were created by backcrossing the Thy1.2 allele onto the FVB/N background for 10 generations. These mice were then crossed to FVB/N clone 100 transgenic mice carrying T cells specific for MHC I (H-2D^q) rat neu immunodominant peptide ($RNEU_{420-429}$).[340] Breeding pairs of clone 100 transgenic mice and FVB/N Thy1.2 labeled mice were kindly transferred from the Laboratory of Dr. Elizabeth M. Jaffee at Johns Hopkins to Columbia University. Experimental animals were bred in-house and phenotyped with TCRVβ4 and Thy1.2 staining as previously described.[367] Mice were acclimated for at least 1 week before any experimental procedures were performed. Animals were kept in specific pathogen-free facilities in either Johns Hopkins University School of Medicine or Columbia University Medical Center. All animal experiments were performed in accordance with protocols approved by the Institutional Animal Care and Use Committee (IACUC) at the Johns Hopkins University School of Medicine and Columbia University Medical Center.

Seven-week-old FVB/NJ, J:NU, C57BL/6-Tg(TcraTcrb)1100Mjb/J (OT-I), and B6.SJL-PtprcaPepcb/BoyJ (CD45.1) male mice were purchased from The Jackson Laboratory. A breeding pair of *Hoxb13-rtTA*|*TetO-H2BGFP* (HOXB13-

GFP) mice[368] was received from UMBC and experimental animals were bred in-house. Animals were kept in a specific pathogen-free facility at either Johns Hopkins University School of Medicine or Columbia University Medical Center. All animal experiments were performed in accordance with protocols approved by the Institutional Animal Care and Use Committee (IACUC) at the respective institutions.

Her-2/Neu Transfection

Rat neu cDNA was cloned from pSV2-neu-N (gift from Bob Weinberg; Addgene plasmid # 10917)[369] and ligated into the pWPXL vector to replace EGFP sequence (gift from Didier Trono; Addgene plasmid # 12257); pMD2.G and psPAX2 plasmids were used as envelop and packing systems. All plasmids were transfected into 293T using lipofectamine 2000 (Invitrogen) and 293T cell supernatants were collected 48 hours post-transfection and used to transduce Myc-CaP cells. Viral load was titrated to mimic different multiplicity of infections (MOI 5 - 50) using appropriate volumes of medium with lentivirus containing polybrene (Sigma-Aldrich). The same parental Myc-CaP cells were transduced with a murine GM-CSF lentivirus using the same method for inserting the rat Her-2/neu containing the $RNEU_{420-429}$ peptide (PDSLRDLSVF) to create Myc-CaP/Neu cells. Successfully transduced cells were isolated based on their Her-2/neu expression by FACS for Myc-CaP/Neu and based on their GM-CSF expression levels by ELISA for GM-CSF secreting bystanders. Efficiency was evaluated 24 hours after transduction in both cases.

Adoptive transfer (AT) experiments

High-avidity RNEU-derived CD8 T cell were isolated untouched from the spleens of 8-week old male clone 100 transgenic mice using CD8a immunomagnetic negative selection beads (Miltenyi Biotec). CD8 T cells were then labeled with CFSE (Invitrogen) and resuspended in PBS. One million CFSE-labeled Thy1.2^{+} RNEU$_{420–429}$-specific CD8 T cells were adoptively transferred intravenously into 8-week old male FVB/NJ mice (JAX stock #001800) – that, unlike most strains, express the congenic marker Thy1.1.[367] On days 5 and 7, LNs (draining or inguinal) and spleens were harvested. CFSE dilution of the adoptively transferred Thy1.2^{+} RNEU-derived CD8 CTLs was measured by flow cytometry. To maximize identification of adoptively transferred CFSE-labeled RNEU$_{420–429}$-specific CD8 T cells, we first gated on the congenic marker Thy1.2 and next gated on the clonotypic Vβ chain, Vβ4.

Toll-like receptor 3 (TLR3) stimulation experiments.

Naïve mice received a low molecular weight (LMW) synthetic polyinosinic-polycytidylic acid (Poly I:C) intraperitoneally (IP) at a dose of 100 μg/mouse (InvivoGen). Twenty-four hours later, mice received an intravenous injection of the high-avidity CFSE-labeled Thy1.2^{+} RNEU$_{420–429}$-specific CD8 T cells.

Tumor Allografts and Xenografts

Eight-week-old male FVB/NJ and J:NU mice were subcutaneously inoculated with either Myc-CaP or MCRedAL (1×10^{6} cells/mouse), and LNCaP or PC3 (3×10^{6} cells/mouse) in the right flank, respectively. Tumor diameters were measured with electronic calipers every 3 days as indicated and the tumor volume was calculated

using the formula: [longest diameter × (shortest diameter)^2]/2. Myc-Cap tumor bearing mice received androgen-deprivation therapy (ADT) 4 weeks after tumor implantation when tumor volume reached ~500mm^3, as indicated in figure legends. ADT was administered via subcutaneous (sc) injection of degarelix acetate (a GnRH receptor antagonist; Ferring Pharmaceuticals Inc.) at a dosage of 0.625 mg/100 µl H_2O/25 g body weight every 30 days, unless otherwise indicated. Onset of castration-resistance was defined as the time to tumor size increased by 30% (~650 mm^3) after ADT. Chemical castration by ADT was compared to bilateral orchiectomy as described in Extended Data Fig. 1a.

Tumor Allografts

Eight-week-old male FVB/NJ mice were subcutaneously inoculated with either Myc-CaP or Myc-CaP/Neu (1×10^6 cells/mouse) in the right flank. Tumor diameters were measured with an electronic caliper every 3 days as indicated and the tumor volume was calculated using the formula: [longest diameter × (shortest diameter)^2]/2.

Whole Genome Expression Profiling and Analysis of MCRedAL Tumors

MCRedAL tumor were harvested when their tumor volume reached ~500mm^3 (CS group), and 7 days after chemical castration (ADT). MCRedAL cells were isolated based on their mCherry$^+$ CD45$^-$ F4/80$^-$ CD11b$^-$ expression by flow sorting on a DakoCytomation MoFlo. RNA was extracted using Trizol LS (Invitrogen) and treated with DNAse-I using RNA clean & Concentrator (Zymo Research). The analysis was performed using Affymetrix Mouse Clariom D (MTA 1.0) array according to the manufacturer's instructions. Resulting CEL files were analyzed

in Affymetrix Expression Console (v. 1.4) using the SST-RMA method, and all samples passed the quality control. Log2 probe intensities were extracted from CEL (signal intensity) files and normalized using RMA quantile normalization, then further analyzed using Partek Genomics Suite v6.6. Illustrations (volcano plots, heatmaps, and histograms) were generated using TIBCO Spotfire DecisionSite with Functional Genomics. Gene set enrichment analysis (GSEA) of differently expressed genes was performed using the hallmark gene sets Molecular Signature Database (MSigDB).

Nanostring

RNA extraction was performed using the Trizol LS reagent (Thermo Fisher) as per manufacturer's instructions. For NanoString analysis, the nCounter mouse PanCancer Immune Profiling panel was employed using the nCounter Analysis System (NanoString, Seattle, WA). Analysis was conducted using nSolver software (NanoString). Heatmap analyses were performed using The R Project for Statistical Computing (https://www.r-project.org/).

Pairwise Alignment

The homology of the murine chemokines Cxcl1, Cxcl2, Cxcl5, Cxcl15, Cxcl12, and Cxcl17 to human IL-8 was evaluated using BLASTP 2.9.0+ (https://blast.ncbi.nlm.nih.gov/Blast.cgi?PAGE=Proteins).[370] Proteins were consider homologous if they shared > 30% amino acid identity.[371] Expected values of <0.05 were consider statistically significant. The expected value includes an inherent Bonferroni correction.

Chromatin immunoprecipitation assay (ChIP)-Seq

ChIP-Seq data was obtained from https://www.ncbi.nlm.nih.gov/geo/query/acc.cgi?acc=GSE83860 which contains ChIP-Seq data acquired with androgen receptor (AR) and nuclear factor NF-kappa-B p65 subunit (p65) specific antibodies on cell lysates from LNCaP cells cultured under the following treatments: DMSO, DHT, and TNFα. For each treatment the dataset contains two ChIP-Seq replicates pulled down using the AR and p65 antibodies.[372] ChIP-Seq data were aligned to the hg38 reference version using the subread package, and then the BAM files were sorted and indexed using SAMtools. Loci with significant differential binding (FDR = 0.05) of pulled-down proteins to DNA were identified using the csaw package for ChIP-Seq analysis, closely following Lun and Smyth's script. ChIP-Seq visualization was performed using the Integrative Genomics Viewer (IGV) from the Broad Institute (http://software.broadinstitute.org/software/igv/).

ChIP-qRT-PCR

Chromatin immunoprecipitation was performed as described.[373] In brief, LNCaP cells were washed with serum-free media and then grown in media containing 10% charcoal stripped FBS for 48 hours. Cells were treated with 100nM DHT or vehicle for 8 hours. DNA was cross-linked with 1% formaldehyde in PBS for 10 minutes and crosslinking was quenched by addition of 0.125 M glycine. Fixed cells were then lysed in lysis buffer (1% SDS, 5mM EDTA, 50mM Tris HCl, pH8.1) and sonicated to a fragment size of 200-600 bp using a Covaris water bath sonicator (Woburn, MA). Sheared chromatin was then incubated with primary antibodies

(AR [06-680, Millipore], H3K4me3 [ab8580, Abcam], phospho-Ser5 RNA polymerase 2 [ab5131, Abcam], RNA polymerase 2 [4H8, Cell Signaling Technologies] or control IgG [Cell Signaling Technologies]) overnight at 4ºC. Complexes were immobilized on Dynabeads (Thermo Fisher) by incubating for 4 hours at 4ºC. Beads were sequentially washed with TSEI (0.1% SDS, 1% Triton X-100, 2mM EDTA, 20mM Tris HCl, pH 8.1, 150mM NaCl), TSEII (0.1% SDS, 1% Triton X-100, 2mM EDTA, 20mM Tris HCl, pH 8.1, 500mM NaCl) and TSEIII (0.25 M LiCl, 1% NP-40, 1% deoxycholate, 1mM EDTA, 10mM Tris HCl, pH 8.1). DNA was eluted with IP Elution buffer (1% SDS, 0.1M $NaHCO_3$, proteinase K) and incubated at 56ºC for 15 minutes. Enriched DNA libraries were analyzed using primers specific to IL-8 locus: Forward: 5' AGCTGCAGAAATCAGGAAGG 3' and Reverse: 5' TATAAAAAGCCACCGGAGCA 3' using quantitative (q) RT-PCR. Data is shown as relative enrichment normalized to input DNA.

Quantitative (q) RT-PCR

Total RNA was extracted using Trizol (Ambion). cDNA was prepared from total RNA preps using the RNA to cDNA EcoDry Premix (Clontech). Real-time assays were conducted using TaqMan real-time probes (Applied Biosystems). ΔΔ CT method was used for relative gene expression. Expression of the target gene was normalized to the reference gene (18S) and the mean expression level of the control group. LCM samples were normalized to 18S, TBP, and GAPDH reference genes.

Laser Capture Microscopy (LCM)

Formalin fixed-paraffin embedded radical prostatectomy specimens, from patients enrolled in a neoadjuvant clinical trial (NCT01696877)[365] who received 240 mg (SQ) of degarelix and matched control cases (patients that did not receive any hormone therapy), were sectioned at a thickness of 8 μm and transferred onto PEN membrane glass slides (Leica). Sections were deparaffinized, hydrated and stained with hematoxylin prior to microdissection. Individual cancer cells and cancer cell clusters were microdissected by a trained pathologist using a LMD 7000 laser capture microscope (Leica). RNA was recovered from the microdisseceted material using the RNeasy FFPE kit (Qiagen). Quantitative RT-PCR was performed as described above. For the analysis, a Mann-Whitney U test was performed.

IL-8 and Cxcl15 CRISPR/Cas9 Knock Outs

The 20 bp long gRNA, designed using Deskgen online software, for targeting IL-8 and Cxcl15 in exon 3 (5'- TTCAGTGTAAAGCTTTCTGA -3' and 5'- ACAGAGCAGTCCCAAAAAAT -3', respectively) were incorporated into two complementary 100-mer oligonucleotides and cloned into a gRNA containing plasmid containing the (NeoR/KanR) cassette (Addgene # 41824). The human codon optimized pCAGGS-Cas9-mCherry was used for gene-editing experiments (a gift from Stem Cell Core Facility at Columbia University). gRNA and Cas9 containing plasmids were introduced to prostate epithelial cells using the basic nucleofector kit (Amaxa, Lonza) following the manufacturer's instructions for primary mammalian epithelial cells (program W001). Successfully transfected

cells were selected by culturing in the presence of 400µg/ml of neomycin sulfate analog (G418; Sigma), and isolated based on their mCherry expression 24 hours after transfection. Knock out clones were screened for IL-8 and Cxcl15 expression by ELISA and gene-editing confirmed by PCR amplification and Sanger sequencing (GENEWIZ) using primers ~200bp away from the cut site (IL-8 Forward: 5'- TTTGGACTTAGACTTTATGCCTGAC -3; IL-8 Reverse: 5'- TCCTGGGCAAACTATGTATGG -3; Cxcl15 Forward: 5'- GCTAGGCACACTGATATGTGTTAAA -3; Cxcl15 Reverse: 5'- ACATTTGGGGATGCTACTGG -3).

Migration/Chemotaxis Assay

Cells and supernatants used in this assay were resuspended in culture media containing 0.5% or 2.5% FBS. Transwell plates of 3-mm pore size were coated with Fibronectin (Corning Costar) and loaded with 500 ml of medium or with different cell supernatants in triplicates (lower chamber). Cells were resuspended at $2x10^7$ cells/ml, and 200 ml of this suspension was placed in each of the inserts (upper chamber). After 2.5 hours of incubation at 37°C and 5% CO_2, inserts were removed and 10,000 beads (Thermo Fisher) were added to each well. In some cases, either isotype or anti-CXCR2 (200 µg/ml) were added at the beginning of the experiment. The cells in the lower chamber were collected along with the starting cell population, stained with L/D, CD11b, Ly6C, and Ly6G and evaluated by flow cytometry in a BD FACSCelesta™ (BD Biosciences). The ratio of beads to cells was determined, allowing calculation of the number of cells that had migrated to the bottom well. In vivo, LD-PMN-MDSCs were collected as described below

from splenocytes of CR-Myc-Cap tumor bearing mice and labeled with DiD (DiIC18(5) or 1,1'-Dioctadecyl-3,3,3',3'-

Tetramethylindodicarbocyanine, 4-Chlorobenzenesulfonate Salt; Invitrogen), a lipophilic membrane dye, as described previously.[374] DiD^+ LD-PMN-MDSCs were adoptively transferred into FVB/NJ recipient 8-week male mice and their ability to migrate in response to 200ng of recombinant Cxcl15 was evaluated 4 hours after injection. Beads were also used to calculate absolute numbers of $Ly6G^+$ PMNs and DiD^+ LD-PMN-MDSCs in vivo.

PMN-MDSC Enrichment

Animals were sacrificed and spleens were collected. After dissociating cell clumps, the cell suspension was centrifuged (740 g, 10 minutes, RT) and resuspended in 1 ml HBSS–EDTA containing 0.5% BSA. Cells were then resuspended in 50% Percoll solution and treated on a three-layer Percoll gradient (55%, 72%, and 81%) at (1500 g, 30 minutes, 10°C without break). LD-PMN-MDSCs were collected from the 50-55% and 55-72% interfaces. Red blood cells (RBCs) were eliminated with RBC lysis solution (Miltenyi).

In vitro Suppression Assays

PMN-MDSCs were isolated from the spleen of CR-Myc-Cap-tumor bearing mice using the neutrophil isolation kit (Miltenyi) according to the manufacturer's instructions; greater than 95% enrichment was confirmed by flow cytometry. Unless otherwise indicated, a density gradient separation was performed prior to column purification. OT-I (CD45.2) transgenic splenocytes were mixed at a 1:10 ratio with sex-matched CD45.1 splenocytes. Splenocytes containing CD8 T

responder cells were stained with CellTrace Violet (5μM CTV; Thermo Fisher) and plated on a 96-well round-bottom plate at a density of $2x10^5$ cells per well. PMN-MDSCs cells were added at 2-fold dilutions starting from $2x10^5$ cells, in the presence of their cognate peptides (5pM OVA) and incubated for 60 hours. Proliferation of CD8 T responder cells (gated as $L/D^-CD8^+CTV^+$) was quantified by flow cytometry based on the dilution of Cell Trace Violet (CTV). Percent suppression (% Suppression) was calculated by the following formula: % Suppression = [1-(% divided cells of the condition/ the average of % divided cells of T responder only conditions)] x 100.

Luminal Epithelial Regression/Regeneration

Eight-week-old male HOXB13-GFP mice carrying the Hoxb13-rtTA transgene and a Tetracycline operator–Histone 2B-Green Fluorescent Protein (TetO-H2BGFP), which results on GFP expression being restricted to luminal epithelial $Hoxb13^+$ cells (described previously[368]), were castrated via bilateral orchiectomy. A cycle of prostate regression/regeneration was induced as described previously.[283] Briefly, mice were allowed to regress for six weeks to reach the fully involuted state. Mice were randomized to ADT or ADT + testosterone (T) treatment groups. Testosterone was administered for four weeks for prostate regeneration by subcutaneous pellets; this regimen yields physiological levels of serum testosterone. All mice received 2mg/ml of Doxycycline (Sigma) in the drinking water to induce GFP expression[368] under the control of the luminal epithelial promoter, HoxB13, one week prior euthanizing them for their analysis.

Vaccination (GVAX) experiments

Naïve and tumor bearing mice received a whole-cell GM-CSF vaccine composed of a mixture of irradiated Myc-CaP cells expressing GM-CSF adjuvant ($3x10^6$) and Myc-CaP/Neu cell expressing Rat Her-2/neu protein (GVAX). The two types of cells were harvested, washed in PBS, and irradiated at 30,000 rads using a γ irradiator (GammaCell 1000 irradiator), and administered subcutaneously (SC) in equal aliquots in the remaining three limbs (50 µL volume).

Androgen-deprivation treatment (ADT) experiments

Myc-CaP/Neu tumor bearing mice received androgen-deprivation therapy (ADT) 2 weeks after tumor implantation. ADT was administered via subcutaneous (SC) injection of degarelix acetate (a GnRH receptor antagonist; Ferring Pharmaceuticals Inc.) at a dosage of 0.625 mg/100 µl H_2O/25 g body weight.

Antibody Blockade

Anti-CXCR2 (murine IgG1-D265A, clone: 11C8; a non-FcγR-binding mutant with deficient FcγR-mediated depletion), anti-CSF1R (rat IgG2a, clone: AFS98; with competent FcγR-mediated depletion), and anti-CTLA-4 (murine IgG2a, clone: 12C11; with competent FcγR-mediated depletion)[55] were used. Antibody treatment was administered via intraperitoneal (ip) injection at a dose of 50 mg/kg body weight for 3 doses every 4 days for CXCR2, 50 mg/kg body weight every 3 days for the duration of the experiment for CSF1R, and/or10 mg/kg body weight for 3 doses every 3 days for CTLA-4. Mouse IgG1 (clone: 4F7), rat IgG2a (clone: 2A3), and mouse IgG2a (clone: 4C6) were used as isotype controls. Anti-CXCR2 and anti-CSF1R treatments started 7 days

before ADT; while anti-CTLA-4 treatment was started either 3 or 12 days before ADT (400mm^3 vs. 200mm^3, respectively).

Antibody Profiling

Phage-ImmunoPrecipitation Sequencing (PhIP-Seq) antibody profiling was performed on 32 PCa patient serum samples using a 90-aa peptide human proteome T7 phage display library as described previously.[299,300,375,376] Briefly, 2 µg of IgG, based on ELISA measurement of total IgG, was mixed with 2.5×10^{10} particle forming units of the 90-aa human peptidome library and incubated at 4C overnight. IgG-bound phages where then immunoprecipitated using 20µl of protein A magnetic Dynal beads and 20µl of protein G coated Dynal beads (Invitrogen). After three bead washes, the library DNA inserts were amplified for 20 cycles of PCR using Herculase II Polymerase (Agilent). A second 20 cycle PCR reaction was performed in order to add sample-specific DNA barcodes and P5/P7 Illumina sequencing adapters. Sequencing was performed on an Illumina HiSeq 2500 in rapid mode (50 cycles, single end reads).

Transcription Profile of Prostate Luminal Epithelial Cells Following Androgen-Induced Regression/Regeneration of the Prostate

We evaluated the transcription profile of Castration-Resistant Luminal Epithelial Cells (CRLECs) from the above 'luminal epithelial regression/regeneration' experiments. Briefly, eight-week-old male Hoxb13-GFP mice carrying the Hoxb13-rtTA transgene and a Tetracycline operator–Histone 2B-Green Fluorescent Protein (TetO-H2BGFP), which results in GFP expression restricted to luminal epithelial Hoxb13$^+$ cells,[368] were castrated via bilateral orchiectomy. A

cycle of prostate regression/regeneration was induced by allowing murine prostates to regress for six weeks to reach the fully involuted state. Mice were randomized to untreated, ADT or ADT + testosterone repletion (TR) treatment groups. Testosterone was administered for four weeks for prostate regeneration by subcutaneous silastic implants yielding physiological levels of serum testosterone. All mice received 2mg/ml of doxycycline (Sigma) in the drinking water to induce GFP expression[368] under the control of the luminal epithelial promoter, Hoxb13, one week prior to euthanization. CRLE cells were isolated based on their GFP^+ expression and $CD45^-CD11b^-F4/80^-CD24^+CD49f^{int}$ status by flow sorting on a DakoCytomation MoFlo. Differential gene expression was computed using the R limma package.[377] Transcriptional distribution of Log2-fold-changes for each gene in ADT vs untreated samples were normalized to z-scores. Z-score values were obtained by scaling the data for each gene in each sample to: (expression - mean expression across all genes) / (standard deviation of expression across all genes). The expression of androgen-responsive genes between ADT+TR/ADT samples was further evaluated by Log2 fold-change. Androgen-responsive gene signature was defined by the differential analysis of murine CRLECs from GFP^+ luminal prostate epithelial cells comparing ADT vs untreated and ADT vs ADT+TR groups and included all differentially expressed genes with an ADT Log2-fold-change below the 0.005 percentile and a Bonferroni-corrected $p < 0.01$, as well as a set of known androgen-responsive genes (Klk1b8, Fkbp5, Nkx3.1, and Tmprss2). Statistical analysis was performed in R[378] and plotting was done using the ggplot2 R package (version 3.1.0).[379]

Quantification of Serum Testosterone

Whole blood was collected from the tail vein and allowed to clot for 1 h at 4 °C. Serum was obtained by centrifuging (1000 × g for 30 min) and collecting the supernatant. Sera were stored at −80 °C prior to analysis. Testosterone concentration was determined by enzyme-linked immunosorbent assay according to the manufacturer's instructions (Enzo, Farmingdale, NY).

Transcriptional Analysis Across Normal and Cancer Tissues

The expression profile of a subset of androgen-responsive genes was evaluated in publicly available dataset from mice (RIKEN FANTOM5)[294] and human (GTEx)[295] normal tissues (prostate, brain, colon, liver, lung, skin, kidney, and salivary gland), as well as in lineage-marked benign or tumor prostate epithelial cells from transgenic mice (GSE39509).[293] For the later, we used RNA-seq data from luminal origin tumors of *Nkx3.1*$^{CreERT2/+}$*; Pten*$^{flox/flox}$*; R26R-YFP/+* mice that were uninduced (benign), or at 3 months after induction. For tamoxifen induction, mice were administered 9 mg/40 g tamoxifen (Sigma) suspended in corn oil, or vehicle alone for negative controls, by oral gavage once daily for 4 consecutive days. In all presented boxplots, the medians for relative gene expression are shown. The 'hinges' represent the first and third quartile. The whiskers are the smallest and largest values after exclusion of outliers (greater than the 75th percentile plus 1.5 times the interquartile range (IQR), or less than 25th percentile minus 1.5 times the IQR). The expression levels of the complete signature of androgen-responsive genes, including KLK3/PSA, FKBP5, NKX3.1, and TMPRSS2, as well as the prostate-restricted TAAs: STEAP1 and TARP were also

evaluated. The statistical analysis was performed in R[378] and plotting was done using the ggplot2 R package (version 3.1.0).[379]

In addition, transglutaminase 4 (TGM4) expression was plotted across human cancer types in The Cancer Genome Atlas (TCGA) database (n = 11,284 samples), including 558 primary prostate adenocarcinomas (PRAD), and across an independent dataset that includes primary prostate adenocarcinomas with clinical information on time to biochemical recurrence (n = 218; GSE21032).[298] Biochemical recurrence was defined as PSA ≥0.2 ng/ml. Following radical prostatectomy, patients were followed with history, physical exam, and serum PSA testing every 3 months for the first year, 6 months for the second year, and annually thereafter. The subset of primary prostate cancer samples from this dataset were tested for association of TGM4 expression with survival by cox regression. Optimal cutpoint for TGM4 selection was determined by maximizing the log-rank statistic using the R survminer package.[380]

Relative expression was quantified accordingly to the normalization methods used in the different publicly available databases analyzed here. RNASeq data from RIKEN FANTOM5 and GTEx were normalized to Log10(TPM), while RNASeq data from the GSE39509 dataset was normalized to FPKM rather than TPM. Raw un-normalized RNASeq data from TCGA were normalized to Log10(TPM+1). Microarray data from GSE21032 was normalized with circular binary segmentation and analyzed with RAE as previously described.[298]

Monocyte Isolation and DC Maturation

Peripheral blood mononuclear cells (PBMCs) from 10 anonymous healthy male donors ≥ 35 years-old obtained from the New York Blood Center were isolated using Lymphoprep^{TM} and SepMate^{TM} PBMC isolation tubes (STEMCELL Technologies). Untouched classical monocytes ($CD14^{+}CD16^{-}$) were then isolated from the PBMC fraction using magnetic beads following the manufacturer's instructions (Pan Monocyte Isolation Kit; Miltenyi Biotec). Following density gradient isolation, monocytes were resuspended in media containing IL-4 (1000 IU/ml) and GM-CSF (1000 IU/ml) at a concentration of $2x10^6$ cells per ml and cultured for 3 days. Cells were maturated for 2 days by adding lipopolysaccharides (LPS) to a final concentration of 500 IU/ml (Sigma). Monocyte-derived dendritic cells (moDCs) were stimulated with 1 µg/ml of whole protein (TGM4, PAP, or PSA; Fisher Scientific & BioLegend) or viral peptide-libraries (CEFT or pp65; JPT Peptide Technologies) overnight before co-culturing with autologous T cells.

Antigen-driven T-cell Purification and Expansion

Functional assays of protein-stimulated T-cell expansion were performed for 10 healthy male donors. On day 0, naïve T cells ($CCR7^{+}CD45RA^{+}$) were isolated from PBMCs by negative selection following the manufacturer's instructions (Naïve Pan T-Cell Isolation Kit; Miltenyi Biotec). Naïve T cells were co-cultured with antigen-pulsed moDCs at a 1:10 ratio in cultured media (1:1 mix of AIM-V media and RPMI1640 [Thermo Fisher] with 10% human serum [Gemini Bio], 1% penicillin streptomycin [Life Technologies] and 1% GlutaMAX [Life Technologies]) supplemented with IL-7 (25ng/ml; Peprotech). IL-2 (25ng/ml; Peprotech) was

added to the cultures 72hrs following priming of naïve T cells. Media was supplemented every 1-3 days with fresh culture media containing the same concentrations of IL-2 and IL-7. Every 10 days, cells were co-incubated with a fresh set of antigen-pulsed moDCs. Cells were harvest and washed twice with PBS on day 30. As positive controls, cells were stimulated with a mixture of pathogen-associated peptides, CEFT pool and pp65 (JPT Peptide Technologies). Cells were stained for FACS analysis 10 days after the last stimulation, and also stimulated with antigen-pulsed moDCs for 12 hours to evaluate the effect of activation markers on expanded T cells following stimulation.

Flow Cytometry in Human Samples

Prior staining, cells were Fc-blocked with purified rat anti-mouse CD16/CD32 (Clone: 2.4 G2, Becton Dickinson BD) for 15 minutes at RT. Dead cells were discriminated using the LIVE/DEAD (L/D) fixable viability dye eFluor 506 dead cell stain kit (Thermo Fisher) and samples were stained for extracellular and intracellular markers. The following antibodies were used: CD3 (UCHT1), CD4 (A161A1), CD8 (SK1), CCR7 (3D12), CD45RA (MEM-56), CD69 (FN50), CD28 (CD28.2), CD27 (M-T271), CD161 (DX12), PD-1 (EH12.1), TIM3 (F38-2E2), CTLA-4 (L3D10), TBET (eBio4B10), GATA3 (TWAJ), RORg(t) (REA278), FOXP3 (PCH101), TCF1 (C63D9), and EOMES (WD1928). Extracellular staining was performed at room temperature for 30min. For intracellular staining, cells were fixed and permeabilized using BD Perm/Wash (BD Biosciences) at room temperature for 45 minutes. Cells were stimulated with protein-pulsed moDCs for 12 hours to evaluate their activation status. Gates for transcription factors were

determined by fluorescence minus one (FMO) controls. Staining was visualized by fluorescence activated cell sorting (FACS) analysis using a Cytek® Aurora (Cytek Biosciences) and analyzed using FlowJo® (Flowjo LLC) in combination with R packages UMAP (version 0.2.0.0)[381] and FlowSOM (version 1.14.1).[382]

Multiparametric Flow Cytometry Analysis

Following compensation, FCS files underwent standard pre-processing to remove debris, doublets and to enrich for live cells. Live, single cells were analyzed by manual gating and unsupervised computational methods in parallel.

For manual gating, T cells were identified based on CD3 expression followed by CD4 and CD8 extracellular markers using FlowJo V10.6. Naïve, effector, central memory, effector memory subpopulations within CD4 and CD8 T cells were identified based on CD45RA and CCR7 expression. Antigen-driven T cells were quantified following three rounds of prime/boost autologous stimulation based on CD69, TBET, CD27, CD28, PD1 and TIM3, expression by manual gating.

Unsupervised computational analysis was performed separately for unstimulated and stimulated samples. In each case, 10,000 cells of post-gated live, single $CD4^+$ or $CD8^+$ T cells from each of the 10 healthy donors were randomly selected using the DownSampleV3 plugin in FlowJo. Subsequently, unsupervised clustering was performed on the expression values of the activation and functional markers separately using the FlowSOM algorithm,[382] which uses a self-organizing map followed by hierarchical consensus meta-clustering to detect cell populations. Default parameters and a predetermined number of 10 clusters were used. The

median levels of the activation and functional markers across all cells per cluster were visualized in separate heatmaps. The subpopulations between clusters were based on the expression levels of activation and functional markers after applying the non-linear dimensionality reduction technique UMAP of the randomly selected cells using the R package UMAP for visualization of the multiparametric data.[381] The cells were colored according to their FlowSOM cluster membership.

Flow cytometry in Murine Samples

Single-cell suspensions from prostate tumor and tissues were prepared using the mouse tumor dissociation kit according to the manufacturer's recommendations (Miltenyi). Single-cell suspensions of tumor-draining lymph nodes (TDLNs) and spleens were homogenized mechanically with the back of a syringe. Cells were Fc-blocked with purified rat anti-mouse CD16/CD32 (Clone: 2.4 G2, Becton Dickinson BD) for 15 minutes at RT. Dead cells were discriminated using the LIVE/DEAD (L/D) fixable viability dye eFluor 506 or near-IR dead cell stain kit (Thermo Fisher) and samples were stained for extracellular and intracellular markers. The following antibodies were used: Her-2/neu (7.16.4), anti-mouse IgG2a (RMG2a-62), Thy1.2 (53-2.1), TCRVβ4 (KT4), CD45 (30F-11), CD45.2 (104), CD24 (M1/69), CD49f (GOH3), Ly6C (HK1.4), Ly6G (1A8), Gr1 (RB6-8C5), CD11b (M1/70), F4/80 (BM8), MHCII (2G9), PD-L1 (10F.9G2), CD4 (RM4-5), CD8 (53-6.7), CD44 (IM7), CD62L (MEL-14), CD25 (PC61), Ki67 (16A8), IFNγ (XMG1.2), TNFα (MP6-XT22), IL-2 (JES6-5H4), GZβ (GB11), CXCR2 (242216), and IL-23 (FC23CPG). For intracellular staining, cells were fixed and permeabilized using BD Perm/Wash (BD Biosciences) at room temperature for 45

minutes. For intracellular cytokine staining, cells were stimulated with PMA (50 ng/ml) and ionomycin (500 ng/ml) for 4 hours in the presence of protein transport inhibitor cocktail (eBiosciences). Gates of cytokines were determined by fluorescence minus one (FMO) controls. Staining was visualized by fluorescence activated cell sorting (FACS) analysis using a BD FACSCelesta™ (BD Biosciences) and analyzed using FlowJo® (Flowjo LLC). Prostate luminal epithelial cells are defined as $CD45^{-}CD11b^{-}F4/80^{-}CD24^{+}CD49f^{int}GFP^{+}$, and prostate epithelial tumor cells are defined as $CD45^{-}CD11b^{-}F4/80^{-}mCherry^{+}$. Tumor associated macrophages (TAMs) are referred to as $CD45^{+}CD11b^{+}F4/80^{+}$, inflammatory TAMs as $CD45^{+}CD11b^{+}F4/80^{+}Ly6C^{+}MHCII^{-}$, immature TAMs as $CD45^{+}CD11b^{+}F4/80^{+}Ly6C^{+}MHCII^{+}$, $MHCII^{hi}$ TAMs as $CD45^{+}CD11b^{+}F4/80^{+}Ly6C^{-}MHCII^{+}$, $MHCII^{low}$ TAMs as $CD45^{+}CD11b^{+}F4/80^{+}Ly6C^{-}MHCII^{-}$. PMN-MDSCs are defined as $CD45^{+}CD11b^{+}Ly6C^{+}Ly6G^{+}$. CD4 T cells as $CD45^{+}CD4^{+}$, regulatory T cells as $CD45^{+}CD4^{+}CD25^{+}$, CD8 T cells as $CD45^{+}CD8^{+}$, polyfunctional CD8 T Cells as $CD45^{+}CD8^{+}IFN\gamma^{+}TNF\alpha^{+}Gz\beta^{+}$, and memory CD8 T cells as $CD45^{+}CD8^{+}CD44^{+}CD62L^{-}$. 123Count eBeads counting beads (Thermo Fisher) were used to normalize the numbers of PMN-MDSCs in migration/chemotaxis experiments.

Protein Quantification

Tumors collected at different treatment time points were minced, lysed in CelLytic MT (Sigma) containing halt protease and phosphatase inhibitor (Thermo Fisher) in a 1:100 ratio, and incubated on ice for 30 minutes with intermittent vortexing. Tumor lysates were assayed for raw protein concentration with Coomassie assay

(Bio-Rad). IL-8 and Cxcl15 were analyzed by ELISA kits following the manufacturer's instructions (BD Bioscience and R&D Systems, respectively).

Immunohistochemical staining (IHC)

Tumor and tissue samples were fixed with either 10% formalin (Fisher Scientific, Pittsburgh, PA) or zinc fixative (BD) for 24 hours before paraffin embedding and sectioning. Sections were stained with hematoxylin and eosin (H&E), and antibodies against mouse Ly6G (1A8; BD Pharmingen), FoxP3 (D6O8R; Cell Signaling), CD3 (SP7; Spring Bioscience), F4/80 (BM8; eBioscience), and Her-2/neu (7.16.4; Emdmillipore). Staining was performed by the Molecular Pathology core of the Herbert Irving Comprehensive Cancer Center at Columbia University. All images were acquired on a Leica SCN 400 system with high throughput 384 slide autoloader (SL801) and a 40X objective; files were processed with Aperio ImageScope v12.3.1.6002. Marker-positive cell counts were obtained from 5 random 40X fields per histological section and results were averaged over the number of counted fields.

RNA In Situ Hybridization (RISH) and Immunohistochemistry

Manual fluorescent RISH was performed on formalin-fixed and zinc-fixed paraffin embedded sections using company protocols. Briefly, 5μm sections were cut, baked at 60 ℃ for 1 hour, dewaxed, and air-dried before pre-treatments. RISH Cxcl15 probe, 3-plex positive control probes (Polr2a, Ppib, Ubc) and 3-plex negative control probes (DapB of Bacillus subtilis strain) from Advanced Cell Diagnostics (ACD) were used in this study. Detection of specific probe binding sites was performed with RISH Multiplex Fluorescent Reagent Kit v2 Reagent kit

from ACD following the manufacturer's instructions. Tyramide CF568 (Biotium) was used to visualize RISH signal.

For a more precise identification of cells expressing Cxcl15, RISH was coupled to immunohistochemistry of PanCK (Poly; Dako) and CD45 (30-F11; BD Biosciences). Immediately after RISH detection, samples were permeabilized with 0.2% TBS-Tween 20 for 10 minutes at RT, and then blocked with 2.5% of normal goat serum (Vector) for 30 minutes at RT. Primary antibody for PanCK was diluted 1/400 in renaissance background reducing diluent (Biocare Medical) and incubated overnight at 4 °C. After washing off the primary antibody, the slides were incubated 15 minutes at RT horseradish peroxidase (HRP) secondary antibody (Vector). Tyramide CF640R (Biotium) was used to visualize PanCK staining. In some cases, CD45 staining was also performed. For this, HRP signal was abolished by a 30 minute incubation at RT with PeroxAbolish (Biocare Medical) and then blocked with 2.5% of normal goat serum (Vector) for 30 minutes at RT. Primary antibody for CD45 was diluted 1/50 in renaissance background reducing diluent (Biocare Medical) and incubated 90 minutes at RT. After washing off the primary antibody, the slides were incubated 15 minutes at RT HRP-secondary antibody (Vector). Tyramide CF488A (Biotium) was used to visualize CD45 staining. All images were acquired on a Nikon A1RMP confocal microscope using a 60X objective. Comparisons of ISH-IHC results were performed using ImageJ.

Immunocytochemistry (ICC)

Manual fluorescent staining was performed using company protocols. Briefly, tumor cells were grown on poly-D-Lysine coated coverslips for 24hrs and fixed with 10% neutral buffered formalin for 30min at RT. Samples were permeabilized with 0.2% TBS-Tween 20 for 10min at RT, then blocked with mouse IgG blocking reagent for 60min at RT, followed by 2.5% of normal goat serum (Vector) for 5min at RT. Primary antibody for Her-2/neu was diluted 1:100 in renaissance background reducing diluent (Biocare Medical) and incubated overnight at 4 °C. After washing off the primary antibody, the slides were incubated 10 min at RT with peroxidase micropolymer for detecting mouse primary antibodies on mouse tissue (Vector M.O.M.). Tyramide CF640R (Biotium) was used to visualize Her-2/neu staining. After washing off the primary antibody, the slides were incubated 15 min at RT with HRP secondary antibody (Vector). All images were acquired on a Nikon A1RMP confocal microscope using a 60X objective. Image analysis was performed using ImageJ.

Antibody Analysis

PhIP-seq data analysis was performed as described in the phip-stat package (https://github.com/lasersonlab/phip-stat). Reads were aligned to the phage library insert sequences using bowtie2[383] to generate a matrix of reads per million (RPM) values for each peptide in each sample (paired pre- and post-treatment serum). Using the phip-stat call-hits command with the '--fdr 0.05' option, we defined a set of statistically significant 'hits' where the RPM value was significantly higher than a set of control wells loaded with beads only. We also calculated the Log2 fold-

change (FC) in post-treatment reactivity compared to pre-treatment repertoire, with Laplace smoothing applied to avoid NA fold-change values from zero-inflated matrix. We further analyzed only peptides with a post-treatment 'hit', such that RPM value is higher than the statistical baseline. For PhIP-Seq Log2 FC analysis, RPM values were aggregated across peptides corresponding to each gene before computing FC for this analysis.

We generated a heatmap of sample-by-sample on-treatment vs pre-treatment Log2 FC for the set of genes defined as androgen-responsive within patients with prostate adenocarcinomas treated with ADT only or with GVAX followed by ADT treatment. This heatmap includes all androgen-responsive proteins profiled with at least one 'hit' by PhIP-Seq. Relationship between immune response to androgen-responsive tumor associated antigens (TAAs) and biochemical recurrence-free survival among patients with prostate adenocarcinoma in either treatment group was assessed by Kaplan Meier curve with cox regression p-value as well as by Fisher's Exact test comparing frequency of immune response to any androgen-response gene in patients with recurrence vs patients without recurrence. All comparisons were performed in the R statistical computation environment.[378] Patients with positive Log2 FC for any androgen-responsive TAAs were considered to mount an immune response to any androgen-responsive TAAs. Androgen-responsive genes were defined in the differential analysis of murine CRLECs from GFP^+ luminal prostate epithelial cells, combined with a set of known androgen-responsive genes (Klk1b8, Fkbp5, Nkx3.1, and Tmprss2).

Z-score Analysis

IL-8 expression was evaluated in a publicly available data set (GSE8466)[384] using z-score values of quantile-normalized microarray transcripts from benign prostate biopsies. Z-score values were obtained by scaling the data for each gene in each patient to: (expression - mean expression across all genes) / (standard deviation of expression across all genes).

Statistical Analysis

Statistical analysis was performed using R (version 3.6.1)[378] or Prism 7 (GraphPad). All statistical tests performed were two-sided with Bonferroni multiple-testing correction where applicable. Tests were considered statistically significant at p-values ≤0.05 (*), 0.01 (**), 0.001 (***) and 0.0001 (****).

Appendix A

Reprint permissions Figure I.1:

SPRINGER NATURE LICENSE
TERMS AND CONDITIONS

Jul 06, 2020

This Agreement between JOHNS HOPKINS UNIVERSITY -- Zoila Lopez Bujanda ("You") and Springer Nature ("Springer Nature") consists of your license details and the terms and conditions provided by Springer Nature and Copyright Clearance Center.

License Number	4863190956572
License date	Jul 06, 2020
Licensed Content Publisher	Springer Nature
Licensed Content Publication	Springer eBook
Licensed Content Title	Immunotherapy for Prostate Cancer: An Evolving Landscape
Licensed Content Author	Wendy Mao, Charles G. Drake
Licensed Content Date	Jan 1, 2018
Type of Use	Thesis/Dissertation
Requestor type	academic/university or research institute
Format	print and electronic
Portion	figures/tables/illustrations

Appendix B

Reprint permissions Figure I.2:

From: Haffner MD PhD, Michael C
Sent: Monday, July 6, 2020 3:02 PM
To: Lopez Bujanda, Zoila A.
Subject: Re: CSHL Press Reprint Permission Request Form

Absolutely - go for it!

Kind regards,

Michael.

On Jul 6, 2020, at 11:59 AM, Lopez Bujanda, Zoila A. <zal2108@cumc.columbia.edu> wrote:

Hi Michael,

Would it be okay if I include Figure 2 in my doctoral thesis? The figure, included in the review article below, shows two representative sections of metastatic prostate lesions stained for PD-L1.

Venturini NJ, Drake CG. Immunotherapy for Prostate Cancer. *Cold Spring Harb Perspect Med*. 2019;9(5):a030627. Published 2019 May 1. doi:10.1101/cshperspect.a030627

Thanks you very much in advance!

Areli

From: Brown, Carol
Sent: Monday, July 6, 2020 2:28 PM
To: Lopez Bujanda, Zoila A.
Subject: FW: CSHL Press Reprint Permission Request Form

I am unable to grant permission for the use of Fig 2, as it was supplied to us by a third party. See figure legend: (Images courtesy of M. Haffner, Johns Hopkins University). You will need to contact this individual to secure the rights you need.

I am happy to grant permission for the use of Fig 3 in your PhD thesis only. Please include complete reference and copyright to Cold Spring Harbor Laboratory Press.

Best wishes for success with your thesis,

Carol C. Brown
Books Development, Marketing and Sales
Cold Spring Harbor Laboratory Press
brown@cshl.edu

Appendix C

Reprint permissions Figure I.3:

ELSEVIER LICENSE
TERMS AND CONDITIONS

Sep 16, 2020

This Agreement between JOHNS HOPKINS UNIVERSITY -- Zoila Lopez Bujanda ("You") and Elsevier ("Elsevier") consists of your license details and the terms and conditions provided by Elsevier and Copyright Clearance Center.

License Number	4911120587270
License date	Sep 16, 2020
Licensed Content Publisher	Elsevier
Licensed Content Publication	Immunity
Licensed Content Title	Oncology Meets Immunology: The Cancer-Immunity Cycle
Licensed Content Author	Daniel S. Chen,Ira Mellman
Licensed Content Date	Jul 25, 2013
Licensed Content Volume	39
Licensed Content Issue	1
Licensed Content Pages	10
Start Page	1
End Page	10
Type of Use	reuse in a thesis/dissertation

Appendix D

Reprint permissions for full text on myeloid cells and Figures I.4 and I.5:

JOHN WILEY AND SONS LICENSE
TERMS AND CONDITIONS

Jul 15, 2020

This Agreement between JOHNS HOPKINS UNIVERSITY -- Zoila Lopez Bujanda ("You") and John Wiley and Sons ("John Wiley and Sons") consists of your license details and the terms and conditions provided by John Wiley and Sons and Copyright Clearance Center.

License Number	4870370891419
License date	Jul 15, 2020
Licensed Content Publisher	John Wiley and Sons
Licensed Content Publication	JOURNAL OF LEUKOCYTE BIOLOGY
Licensed Content Title	Myeloid-derived cells in prostate cancer progression: phenotype and prospective therapies
Licensed Content Author	Zoila Lopez-Bujanda, Charles G. Drake
Licensed Content Date	May 26, 2017
Licensed Content Volume	102
Licensed Content Issue	2
Licensed Content Pages	14

Appendix E

Reprint permissions for Figure I.6:

SPRINGER NATURE LICENSE
TERMS AND CONDITIONS

Jul 06, 2020

This Agreement between JOHNS HOPKINS UNIVERSITY -- Zoila Lopez Bujanda ("You") and Springer Nature ("Springer Nature") consists of your license details and the terms and conditions provided by Springer Nature and Copyright Clearance Center.

License Number	4863191379934
License date	Jul 06, 2020
Licensed Content Publisher	Springer Nature
Licensed Content Publication	Current Oncology Reports
Licensed Content Title	Immunotherapy in Prostate Cancer: Teaching an Old Dog New Tricks
Licensed Content Author	Michael C. Comiskey et al
Licensed Content Date	Aug 18, 2018
Type of Use	Thesis/Dissertation
Requestor type	academic/university or research institute
Format	print and electronic
Portion	figures/tables/illustrations

Curriculum Vitae

The Johns Hopkins University School of Medicine

Zoila Areli Lopez Bujanda 10/22/2020

Educational History:

PhD, expected	2020	Program in Pathobiology Mentor: Charles G. Drake, MD, PhD	Johns Hopkins School of Medicine
M.S.	2009	Molecular Biology	University of Sonora, Mexico
B.S.	2007	Chemical and Biological Sciences	University of Sonora, Mexico

Other Professional Experience

Visiting Student	2017-2020	Lab of Charles G. Drake, MD, PhD	Columbia University
Research Technologist	2010-2013	Lab of Saraswati Sukumar, PhD	Johns Hopkins Medical Institutions
Research Assistant	2010	Lab of Federico Avila Moreno, PhD	National Institute of Breath Diseases (INER), Mexico
Instructor	2009-2010	Chemistry	University of Valle de Mexico (UVM), Mexico
Translational Internship	2009	Lab of Saraswati Sukumar, PhD	Johns Hopkins Medical Institutions
Genetics' Internship	2006-2007	Lab of Paulino Martinez Portela, PhD	University of Santiago de Compostela, Spain

Scholarships, fellowships, or other external funding

Graduate Student under DOD Grant	2014-2016	Title: Immunological Targeting of Tumor-Initiating Prostate Cancer Cells (W81XWH-13-1-0369, PI: Charles G. Drake, MD, PhD)

Academic and other honors at Hopkins and elsewhere

2020	The Moos-Miller Underrepresented Trainee Scholarship	Keystone Symposia
2019	Young Investigator Award	Society for Immunotherapy of Cancer

2019	The Mette Strand Research Award	Johns Hopkins School of Medicine
2019	Scholar-in-Training Award	American Association for Cancer Research-Prostate Cancer Foundation
2019	Science Alliance Leadership Trainee	The New York Academy of Science
2015	HHMI International Student Fellowship Institutional Nominee	Johns Hopkins University
2009	Top Twenty Sonoran Student Leaders	Zepeda Vidal Foundation
2007	Cum Laude	University of Sonora
2006	Merit-based Scholarship to study abroad from Mexican Higher Education Institutions (ANUIES).	University of Sonora

Publications, peer reviewed

1. **Lopez-Bujanda ZA**, Obradovic A, Nirschl TR, O'Donnell T, Laserson U, Macedo-Gonzales RJ, Reshef R, Yuan T, Soni K, Antonarakis ES, Larman HB, Muranski P, and Drake CG (2020*) TGM4: An Immunogenic Prostate-Restricted Antigen. J Immunother Cancer. *Under Revision.
2. **Lopez-Bujanda ZA**, Chaimowitz MG, Armstrong TD, Foote JB, Emens LA, and Drake CG (2020) Robust Antigen-Specific CD8 T Cell Tolerance to a Model Prostate Cancer Neoantigen. OncoImmunology 9:1 DOI: 10.1080/2162402X.2020.1809926.
3. Hawley JE, Pan S, Figg WD, **Lopez-Bujanda ZA**, Strope JD, Aggen DH, Dallos MC, Lim EA, Stein MN, Hu J, and Drake CG (2020) Association between immunosuppressive cytokines and PSA progression in biochemically recurrent prostate cancer treated with hormonal therapy. Prostate 4:336-344 DOI: 10.1002/pros.23948.
4. Gonda TA, Fang J, Salas M, Do C, Hsu E, Zhukovskaya A, Siegel A, Takahashi R, **Lopez-Bujanda ZA**, Drake CG, Manji GA, Wang TC, Olive KP, and Tycko B (2020) A DNA hypomethylating drug alters the tumor microenvironment and improves the effectiveness of immune checkpoint inhibitors in a mouse model of pancreatic cancer. Cancer Res DOI: 10.1158/0008-5472.CAN-20-0285.
5. Aggen DH, Ager CR, Obradovic AZ, Chowdhury N, Ghasemzadeh A, Mao W, Chaimowitz MG, **Lopez-Bujanda ZA**, Spina CS, Hawley JE, Dallos M, Zhang C, Wang V, Li H, Guo XV, and Drake CG (2020) Blocking Interleukin-1 Beta Promotes Tumor Regression and Remodeling of the Myeloid Compartment in a Renal Cell Carcinoma Model: Multi-Dimensional Analyses. Clin Cancer Res. In press.
6. LeMagnen C, Virk R, Dutta A, Kim JY, Panja S, **Lopez-Bujanda ZA**, Califano A, Drake CG, Mitrofanova A, and Abate-Shen C (2018) Cooperation of Loss NKX3.1 and Inflammation in Prostate Cancer Initiation. Disease Models & Mechanisms 11:dmm035139 DOI: 10.1242/dmm.035139.

7. Shen YC, Ghasemzadeh A, Kochel CM, Nirschl TR, Francica BJ, **Lopez-Bujanda ZA**, Carrera-Haro MA, Tam A, Anders RA, Selby MJ, Korman AJ, and Drake CG (2018) Combining Intratumoral Treg Depletion with Androgen Deprivation Therapy (ADT): Preclinical Activity in the Myc-CaP Model. Prostate Cancer Prostatic Dis 1:113-125 DOI: 10.1038/s41391-017-0013-x.
8. **Lopez-Bujanda ZA** and Drake CG (2017) Myeloid-derived Cells in Prostate Cancer Progression: Phenotype and Prospective Therapies. J of Leukoc Biol 2:393-406 DOI: 10.1189/jlb.5VMR1116-491RR.
9. Muroyama Y, Nirschl TR, Kochel CM, **Lopez-Bujanda ZA**, Theodros D, Mao W, Carrera-Haro MA, Ghasemzadeh A, Marciscano AE, Velarde E, Tam AJ, Thoburn CJ, Uddin M, Meeker AK, Anders RA, Pardoll DM, and Drake CG (2017) Stereotactic Radiotherapy Increases Functionally Suppressive Regulatory T Cells in the Tumor Microenvironment. Cancer Immunology Res 11:992-1004 DOI: 10.1158/2326-6066.
10. Visvanathan K, Fackler MJ, Zhang Z, **Lopez-Bujanda ZA**, Jeter SC, Sokoll LJ, Garrett-Mayer E, Cope LM, Umbricht CB, Euhus DM, Forero A, Storniolo AM, Nanda R, Lin NU, Carey LA, Ingle JN, Sukumar S, and Wolff AC (2017) Monitoring of Serum DNA Methylation as an Early Independent Marker of Response and Survival in Metastatic Breast Cancer: TBCRC 005 Prospective Biomarker Study. J Clin Oncol 7:751-758 doi: 10.1200/JCO.2015.66.2080.
11. Stearns V, Fackler MJ, Hafeez S, **Lopez-Bujanda ZA**, Chatterton RT, Jacobs LK, Khouri NF, Ivancic D, Kenney K, Shehata C, Jeter SC, Wolfman JA, Zalles CM, Huang P, Khan SA, and Sukumar S (2016) Gene Methylation and Cytological Atypia in Random Fine Needle Aspirates for Assessment of Breast Cancer Risk. Cancer Prev Res DOI: 10.1158/1940-6207.CAPR-15-0377.
12. Ávila-Moreno F, Armas López L, Alvarez-Moran AM, **Lopez-Bujanda ZA**, Ortiz-Quintero B, Hidalgo-Miranda A, Urrea-Ramirez F, Rivera-Rosales RM, Vazquez-Manriquez E, Peña-Mirabal E, Morales-Gomez J, Vazquez-Minero JC, Tellez-Becerra JL, Ramirez-Mendoza R, Avalos-Bracho A, de Alba EG, Vazquez-Santillan K, Maldonado-Lagunas V, Santillan-Doherty P, Peña-Sanchez P, and Zuñiga-Ramos J (2014) Overexpression of MEOX2 and TWIST1 is Associated with H3K27me3 Levels and Determines Lung Cancer Chemoresistance and Prognosis. PLoS One 12:e114104 DOI: 10.1371/journal.pone.0114104.
13. Cope LM, Fackler MJ, **Lopez-Bujanda ZA**, Wolff AC, Visvanathan K, Gray JW, Sukumar S, and Umbricht CB (2014) Do Breast Cancer Cell Lines Provide a Relevant Model of the Patient Tumor Methylome? PLoS One 8:e105545 DOI: 10.1371/journal.pone.0105545.
14. Fackler MJ, **Lopez-Bujanda ZA**, Umbricht CB, Teo WW, Cho S, Zhang Z, Visvanathan K, Jeter S, Argani P, Wang C, Lyman JP, de Brot M, Ingle JN, Boughey J, McGuire K, King TA, Carey LA, Cope L, Wolff AC, and Sukumar S (2014) Novel Methylated Biomarkers and a Robust Assay to Detect Circulating Tumor DNA in Metastatic Breast Cancer. Cancer Res 8:2160-2170 DOI: 10.1158/0008-5472.CAN-13-3392.
15. Choudhury S, Almendro V, Merino VF, Wu Z, Maruyama R, Su Y, Martins FC, Fackler MJ, Bessarabova M, Kowalczyk A, Conway T, Beresford-Smith B, Macintyre G, Cheng YK, **Lopez-Bujanda ZA**, Kaspi A, Hu R, Robens J, Nikolskaya T, Haakensen VD, Schnitt SJ, Argani P, Ethington G, Panos L, Grant M, Clark J, Herlihy W, Lin SJ, Chew G, Thompson EW, Greene-Colozzi A, Richardson AL, Rosson GD, Pike M, Garber JE, Nikolsky Y, Blum JL, Au

A, Hwang ES, Tamimi RM, Michor F, Haviv I, Liu XS, Sukumar S, and Polyak K (2013) Molecular Profiling of Human Mammary Gland Links Breast Cancer Risk to a p27(+) Cell Population with Progenitor Characteristics. Cell Stem Cell 1:117-130 DOI: 10.1016/j.stem.2013.05.004.

16. Martínez ME, Gutierrez-Millan LE, Bondy M, Daneri-Navarro A, Meza-Montenegro MM, Anduro-Corona I, Aramburo-Rubio MI, Balderas-Peña LMA, Barragan-Ruiz JA, Brewster A, Caire-Juvera G, Castro-Cervantes JM, Chavez-Zamudio MA, Cruz G, Del Toro-Arreola A, Edgerton ME, Flores-Marquez MR, Franco-Topete RA, Garcia H, Gutierrez-Rubio SA, Hahn K, Jimenez-Perez LM, Komenaka IK, **Lopez-Bujanda ZA**, Lu D, Morgan-Villela G, Murray JL, Nodora JN, Oceguera-Villanueva A, Ortiz-Martinez MA, Perez Michel L, Quintero-Ramos A, Sahin A, Shim JY, Stewart M, Vazquez-Camacho G, Wertheim B, Zenuk R, and Thompson P (2010) Comparative Study of Breast Cancer in Mexican and Mexican-American Women. Health 2:1040-1048 DOI: 10.4236/health.2010.29153.

Publications, chapters and other non-peer reviewed

1. **Lopez-Bujanda ZA**, Haffner MC, Chaimowitz MG, Chowdhury N, Venturini NJ, Obradovic AZ, Hansen C, Jackow J, Sfanos KS, Bieberich CJ, Hurley PJ, Selby MJ, Korman AJ, Christiano AM, De Marzo AM, and Drake CG (2019) Castration-mediated IL-8 Promotes Myeloid Infiltration and Prostate Cancer Progression. BioRxiv DOI: 10.1101/651083.

Posters, abstracts, etc

1. **Lopez-Bujanda ZA,** Obradovic A, Nirschl TR, O'Donnell T, Laserson U, Macedo-Gonzales RJ, Reshef R, Yuan T, Soni MK, Antonarakis ES, Larman HB, Muranski P, and Drake CG (2020*) A Novel Prostate-Restricted Tumor-Associated Antigen: A Potential Therapeutic Target. Society for Immunotherapy of Cancer (SITC) 34th Annual Meeting, November, 2020. *Accepted.
2. **Lopez-Bujanda ZA,** Chaimowitz MG, Obradovic A, Hawley J, and Drake CG (2020*) Tumor Necrosis Factor Alpha As a Mediator of Enzalutamide Resistance in Prostate Cancer. Annual Prostate Cancer Foundation (PCF) Scientific Retreat, October, 2020.
3. **Lopez-Bujanda ZA**, Chaimowitz MG, Haffner MC, Chowdhury N, Hurley PJ, Christiano AM, and Drake CG (2019) Androgen regulated IL-8 expression in prostate cancer: Insights into tumor cell mediated immunosuppression. Proceedings: AACR Annual Meeting 2019 DOI: 10.1158/1538-7445.AM2019-1510.
4. Spina CS, **Lopez-Bujanda ZA**, Mao W, Chaimowitz MG, Chowdhury N, Aggen DH, and Drake CG (2019) Radiation induces a dose-dependent increase in immunosuppressive myeloid cells in solid tumors. Mini Oral Sessions: International Journal of Radiation Oncology DOI: https://doi.org/10.1016/j.ijrobp.2019.06.101.
5. Hawley J, Pan S, Figg WD, **Lopez-Bujanda ZA**, Strope J, Fojo AT, Dallos M, Aggen DH, Lim EA, Stein MN, Hu J, and Drake CG (2019) Correlation between innate cytokine levels and progression in men with biochemically recurrent prostate cancer treated with intermittent hormonal therapy. Journal of Clinical Oncology DOI: 10.1200/JCO.2019.37.15_suppl.e16554.
6. Dallos M, Obradovic A, Chowdhury N, **Lopez-Bujanda ZA**, Aggen DH,

Hawley J, Rathkopf DE, and Drake CG (2019) Human prostate cancer immune phenotypes after androgen deprivation therapy. Journal of Clinical Oncology DOI: 10.1200/JCO.2019.37.15_suppl.5083.

7. Shen Y, Kochel C, Francica BJ, Alme A, Nirschl C, Nirschl T, **Lopez-Bujanda ZA**, Carrera-Haro MA, Selby M, Kormanand A, and Drake CG (2015) Combining androgen deprivation with immune checkpoint blockade delays the development of castration-resistance in a murine model of prostate cancer. Proceedings: AACR Annual Meeting 2015 DOI: 10.1158/1538-7445.AM2015-267.
8. Fackler MJ, **Lopez-Bujanda ZA**, Umbricht C, Teo WW, Zhang Z, Visvanathan K, Jeter S, Argani P, Wang C, Ingle JN, Boughey J, McGuire K, King TA, Carey LA, Cope LA, Wolff AC, and Sukumar S (2013) cMethDNA is a quantitative circulating methylated DNA assay for detection of metastatic breast cancer and for monitoring response to therapy. Thirty-Sixth Annual CTRC-AACR San Antonio Breast Cancer Symposium DOI: 10.1158/0008-5472.SABCS13-P2-06-01.
9. Sukumar S, Fackler MJ, **Lopez-Bujanda ZA**, Teo WW, Umbricht C, Jeter S, Visvanathan K, and Wolff AC (2012) Accurate identification of metastatic breast cancer using methylated gene markers in circulating free DNA in peripheral blood. Thirty-Fifth Annual CTRC-AACR San Antonio Breast Cancer Symposium DOI: 10.1158/0008-5472.SABCS12-P2-02-01.

Invited talks at local, national, and international meetings

2020	"ADT-mediated Intra-Tumoral Myeloid Infiltration Promotes Resistance to Immune Checkpoint Blockade in Prostate Cancer" talk at the Advances in Cancer Immunotherapy eSymposia Meeting.	Virtual Keystone
2019	"ADT-mediated IL-8 Promotes Myeloid Infiltration and Prostate Cancer Progression" talk at the SITC 34th Annual Meeting.	Society for Immunotherapy of Cancer
2019	"The Effect of Inflammatory Cytokines on Prostate Cancer Progression" talk at Prostate Cancer Meeting.	Columbia University
2018	"Decoding the TME of Castrate-Resistant Prostate Cancer: A Novel Immunotherapeutic Approach Targeting PMN-MDSCs" talk at the Center Meeting, Columbia Center for Translational Immunology (CCTI).	Columbia University Medical Center
2018	"Targeting PMN-MDSCs and TAMs in a Preclinical Castrate-Resistant Prostate Cancer Model: A Novel Immunotherapeutic Approach" talk at TRCCC Meeting.	Translational Research Cancer Center Consortium
2017	"Murine Models to Study Castrate-Resistant Luminal Epithelial Cells in Prostate" talk at Prostate Cancer Meeting.	Columbia University
2016	"Antigen Screening for the Treatment of Castrate-Resistant Prostate Cancer" talk at Translational	Johns Hopkins School of Medicine

Research in Progress Meeting. Bloomberg~Kimmel Institute for Cancer Immunotherapy.

2014 "Antigen Screening for the Treatment of Castration-Resistant Prostate Cancer (CRPC)" talk at Pathology Grand Rounds. Johns Hopkins School of Medicine

Inventions, Patents, Copyrights

2020 Targeting of TGM4 to treat prostate cancer.
Inventors: Charles G. Drake and **Zoila Areli Lopez Bujanda**.
IR CU21049

2019 Treatment of Prostate Cancer by Androgen Ablation and IL-8 Blockade.
Inventors: Charles G. Drake and **Zoila Areli Lopez Bujanda**.
IR CU19210

2013 A Quantitative Multiplex Methylation Specific PCR Method-cMethDNA, Reagents, and Its Use.
Inventors: Saraswati Sukumar, Mary Jo Fackler, Wei Wen Teo, and **Zoila Areli Lopez Bujanda**.
Publication No: WO/2013/177265

Service and leadership

2018 Mentor to Summer Student Nicholas Venturini — Columbia University

2014 Teaching Assistant for the Pathology for Graduate Students course — Johns Hopkins School of Medicine